

**Application of multivariate statistics and Geographic  
Information Systems (GIS) to map groundwater  
quality in the Beaufort West area, Western Cape,  
South Africa**

**Henok Goitom Solomon**

A thesis submitted in fulfillment of the requirement for the degree of



**Environmental and Water Science**

Department of Earth Sciences, Faculty of Natural Science, University of the Western  
Cape.

**Supervisor: <sup>1</sup>Dr. Abdi Mohamoud Siad**

<sup>1</sup>. University of the Western Cape, Department of Earth Sciences, P/Bag X17, Modderdam  
Road, Bellville, 7535, South Africa

November 2013

# **Application of multivariate statistics and Geographic Information Systems (GIS) to map groundwater quality in the Beaufort West area, Western Cape, South Africa**

## **Key words**

Beaufort West

Groundwater

Fractured rock aquifers

Teekloof

Abrahamskraal

Calcrete

Geographic Information Systems (GIS)

Spatial Analysis

Hydrogeochemistry

Factor Analysis

Cluster Analysis

Discriminant Analysis

Water Quality



## Abstract

### **Application of multivariate statistics and Geographic Information Systems (GIS) to map groundwater quality in the Beaufort West area, Western Cape, South Africa**

H.G. Solomon

MSc Thesis, Department of Earth Sciences, University of the Western Cape

Groundwater in arid and semi-arid areas like the Karoo region of South Africa is an important source of domestic, agricultural and industrial source of fresh water. As a scarce resource, it requires extensive quality control and protection through innovative methods and efficient strategies. The town of Beaufort West and its vicinity use groundwater as a major source of municipal and private water supply. Forty nine groundwater samples were collected from spatially referenced boreholes located in and around the town of Beaufort West and were analyzed for EC, pH, TDS, TH, SAR, TA,  $\text{Ca}^{2+}$ ,  $\text{Mg}^{2+}$ ,  $\text{Na}^+$ ,  $\text{K}^+$ ,  $\text{HCO}_3^-$ ,  $\text{Cl}^-$ ,  $\text{NO}_3^-$  and  $\text{SO}_4^{2-}$  according to SANS 241 standards and tested for ionic balance. The groundwater of the study area was characterized using WHO and South African drinking water quality standards as well as TDS and Salinity hazard classifications. These comparisons and classifications characterized the groundwater of the study area as hard to very hard, with low to medium salinity hazard. These results are in accordance with the dominance of the ions  $\text{Ca}^{2+}$ ,  $\text{Na}^+$ ,  $\text{HCO}_3^-$  and  $\text{Cl}^-$  in the groundwater samples. Linear relationships between the hydrochemical variables were analysed through correlation and multiple regression analysis to relate the groundwater quality to the underlying hydrogeochemical processes. These linear relationships explained the contribution of the measured variables towards the salinity, hardness and anthropogenic contamination of the groundwater. The groundwater of the study area was also assessed using conventional trilinear diagrams and scatter plots to interpret the water quality and determine the major ion chemistry. The conventional methods highlighted the sources of the hydrochemical variables through analysis and interpretation of rock-water interaction and evaporations processes. To supplement

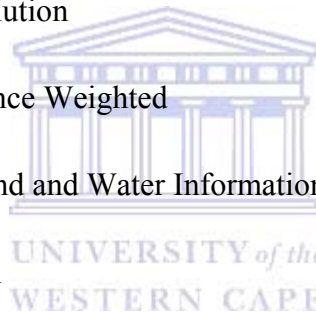
these conventional methods and reveal hidden hydrogeochemical phenomenon, multivariate statistical analyses were employed. Factor analysis reduced the hydrochemical variables into three factors (Hardness, Alkalinity and Landuse) that characterize the groundwater quality in relation to the source of its hydrochemistry. Furthermore, combination of Cluster (CA) and Discriminant analyses (DA) were used to classify the groundwater in to different hydrochemical facies and determine the dominant hydrochemical variables that characterize these facies. The classification results were also compared with the trilinear diagrammatic interpretations to highlight the advantages of these multivariate statistical methods. The CA and DA classifications resulted in to six different hydrochemical facies that are characterized by  $\text{NO}_3^-$ ,  $\text{Na}^+$  and pH. These three hydrochemical variables explain 93.9% of the differences between the water types and highlight the influence of natural hydrogeochemical and anthropogenic processes on the groundwater quality. All the univariate, bivariate, multivariate statistical and conventional hydrogeochemical analyses results were analyzed spatially using ArcGIS 10.0. The spatial analysis employed the Inverse Distance Weighted (IDW) interpolation method to predict spatial distribution of unmeasured areas and reclassification of the interpolation results for classification purposes. The results of the different analyses methods employed in the thesis illustrate that the groundwater in the study area is generally hard but permissible in the absence of better alternative water source and useful for irrigation.

November 2013

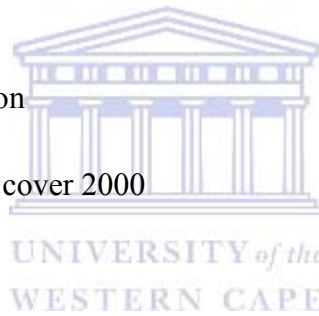
## Abbreviations and Acronyms

$\mu$	Micron
$\mu\text{g/L}$	Micrograms per Liter
$\mu\text{Siemens/cm}$	Micro Siemens per centimeters
$\text{Al}^{3+}$	Aluminum ion
$^{\circ}\text{C}$	degree Celsius
$\text{Ca}^{2+}$	Calcium ion
CA	Cluster Analysis
$\text{CaCO}_3$	Calcium carbonate
$\text{Cl}^-$	Chloride ion
CMAP	Cumulative Mean Annual Precipitation
$\text{CO}_2$	Carbon dioxide
DA	Discriminant Analysis
DEM	Digital Elevation Model
DWAF	Department of Water Affairs and Forestry
DWA	Department of Water Affairs
EC	Electrical Conductivity
EPA	Environmental Protection Agency (USA)
ESRI	Environmental Sciences Research Institute
$\text{F}^-$	Fluoride ion

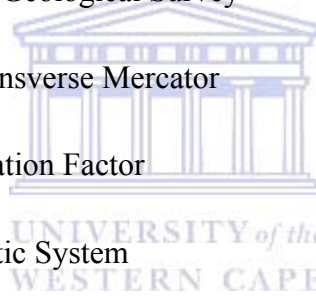
FA	Factor Analysis
GEOSS	Geohydrological and Spatial Solutions
GISCOE	GIS Centre of Excellence
GPS	Global Positioning System
GRAII	Groundwater Resources Assessment II
HCA	Hierarchical Cluster Analysis
HCl	Hydrogen chloride solution
HCO <sub>3</sub> <sup>-</sup>	Bicarbonate ion
HNO <sub>3</sub>	Nitric acid solution
IDW	Inverse Distance Weighted
ILWIS	Integrated Land and Water Information System software
K <sup>+</sup>	Potassium ion
Km	Kilo meters
L/min	Liters per minute
L/s	Litres per second
m <sup>2</sup> /day	Squared meter per day
m	Meter
mamsl	Meters above mean sea level
MAP	Mean Annual Precipitation
MAPE	Mean Annual Potential Evaporation



MCL	Minimum Contamination Level
MDL	Minimum Detection Limit
meq/L	Milli equivalents per Litre
Mg <sup>2+</sup>	Magnesium ion
mg/L	Milligrams per Litre
ml/min	Millilitres per minute
mS/m	MilliSiemens per meter
mV	Millivolt
Na <sup>+</sup>	Sodium ion
NH <sub>4</sub> <sup>+</sup>	Ammonium ion
Nlc2000	National land cover 2000
NO <sub>3</sub> <sup>-</sup>	Nitrate ion
R <sup>2</sup>	Coefficient of determination
R	Correlation coefficient
RMSPE	Root Mean Square Prediction Error
S	Storativity
SANS	South African National Standard (safety)
SAR	Sodium Adsorption Ratio
SAWQG	South African Water Quality Guidelines: Domestic Use
SED	Squared Euclidean Distance



SO <sub>4</sub> <sup>2-</sup>	Sulphate ion
SRTM3	Shuttle Radar Topography Mission 30 m resolution
T	Transmissivity
TA	Total alkalinity
TDS	Total Dissolved Solids
TH	Total Hardness
TZ <sup>+</sup>	Total Cations
USDA	United States Department of Agriculture
USGS	United States Geological Survey
UTM	Universal Transverse Mercator
VIF	Variance Inflation Factor
WGS	World Geodetic System
WHO	World Health Organization
WRC	Water Research Commission



## Declaration

I declare that “Application of Multivariate Statistics and Geographic Information Systems (GIS) to Map Groundwater Quality in the Beaufort West Area, Western Cape, South Africa” is my own work, that it has not been submitted before for any degree or examination in any other university, and that all the sources I have used or quoted have been indicated and acknowledged as complete references.

Henok Goitom Solomon

November 2013



Signed: .....  .....

## Acknowledgements

I would like to acknowledge the NRF for funding the research in its first stage, Mr Louw Smit and the Municipality of Beaufort West for providing crucial data of the study area, and Mr Julian Conrad from GEOSS (custodians of the data) for assisting in data retrieval.

Furthermore, I would like to express my gratitude to the people who supported me academically and financially; my family, friends and staff of the Department of Earth Sciences in general and my mentor and supervisor Dr. Abdi M. Siad in particular. I would also like to thank Prof. Lorna Holtman (Division for postgraduate studies) for her support throughout my studies and above all God Almighty, without whom none of this would have been possible.



*‘The thesis is dedicated to my parents  
Mr. Goitom Solomon Haile and Mrs.  
Belainesh Ghebremichael Hailu’*

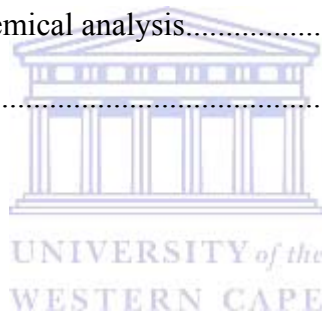


# Table of Contents

Key words .....	ii
Abstract .....	iii
Abbreviations and Acronyms .....	v
Declaration .....	ix
Acknowledgements .....	x
Table of Contents .....	xii
Table of Figures .....	xv
List of Tables .....	xviii
Chapter I .....	1
1. Purpose and scope .....	1
1.1. Research problem .....	2
1.2. Aim and objectives .....	2
<i>Aim</i> .....	2
<i>Objectives</i> .....	3
2. Introduction .....	3
3. Study area background .....	6
4. Regional and local geology .....	9
5. Hydrogeology .....	13
5.1. Study area aquifer types .....	15
5.2. Study area flow dynamics .....	17
6. Hydrogeochemistry .....	20
6.1. Carbonate chemistry .....	22
6.2. Adsorption and ion exchange .....	24



Chapter II.....	26
Methodology.....	26
1. Groundwater sampling, data management and analysis.....	26
1.1. Sampling method.....	26
1.2. Sample data preparation.....	28
2. Univariate and bivariate statistics.....	30
2.1. Descriptive statistics.....	30
2.2. Correlation analysis.....	31
2.3. Multiple regression analysis.....	32
2.3.1. <i>Stepwise multiple regression analysis</i> .....	34
3. Classical hydrogeochemical analysis.....	34
4. Multivariate statistics.....	36
4.1. Factor analysis.....	38
4.2. Cluster analysis.....	41
4.3. Discriminant analysis.....	43
4.3.1. <i>Linear discriminant analysis</i> .....	44
4.3.2. <i>Stepwise discriminant analysis</i> .....	45
5. Spatial analysis.....	45
5.1. Spatial data preparation.....	45
5.2. Spatial data presentation.....	47
Chapter III.....	49
Results and Discussion.....	49
1. Univariate and bivariate statistics.....	49
1.1. Correlation analysis.....	59



1.2.	Regression analysis	60
2.	Hydrogeochemistry.....	62
2.1.	Major ion chemistry	68
2.2.	Spatial distribution of ions	77
3.	Multivariate statistics.....	85
3.1.	Factor analysis	85
3.2.	Cluster and discriminant analysis	91
<b>3.2.1.</b>	<b><i>Analysis 1: Set A</i></b>	92
<b>3.2.2.</b>	<b><i>Analysis 2: Set B</i></b>	96
<b>3.2.3.</b>	<b><i>Analysis 3: Set B</i></b>	101
<b>3.2.4.</b>	<b><i>Analysis 4: Set B</i></b>	103
Chapter IV.....		108
Conclusion and recommendation.....		108
1.	Summary and conclusion.....	108
2.	Recommendation.....	114
List of References.....		115
Appendices.....		127
Appendix A: Laboratory chemical analysis results		127
Appendix B: Hydrogeochemical data collected from the study area		129
Appendix C: Calculated hydrogeochemical data of the study area		131

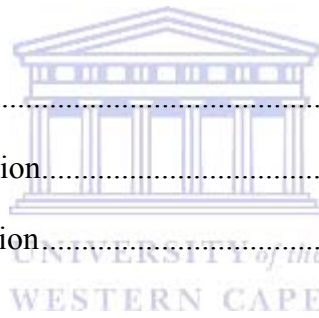


## Table of Figures

Figure 1.1 Borehole location distributions along the six catchment areas: an adaptation of the Water Resources of South Africa 2005 (Middleton & Bailey, 2008). .....	8
Figure 1.2 Schematic north-south cross-section of the Main Karoo Basin (Johnson et al., 2006). .....	9
Figure 1.3 Geological map representation of the study area: an adaptation of 3222 Beaufort West Map (GISCOE, 2005). .....	13
Figure 1.4 Groundwater flow direction and compartments (Rose, 2008). .....	17
Figure 1.5 Groundwater contours with 5 m intervals (Rose, 2008). .....	19
Figure 3.1 Cation (a) $\text{Ca}^{2+}$ , (b) $\text{Mg}^{2+}$ , (c) $\text{Na}^+$ and (d) $\text{K}^+$ concentration classification of the groundwater samples based on WHO (1993) drinking water guidelines: Inverse Distance Weighted Interpolation representation. ....	54
Figure 3.2 Anion (a) $\text{Cl}^-$ , (b) $\text{SO}_4^{2-}$ and (c) $\text{NO}_3^-$ concentration classification of the groundwater samples based on WHO (1993) drinking water guidelines: Inverse Distance Weighted Interpolation representation. ....	55
Figure 3.3 TDS level classification of the groundwater samples based on WHO (1993) drinking water guidelines. ....	56
Figure 3.4 General trilinear diagrammatic classifications of hydrochemical facies. .	63
Figure 3.5 Trilinear diagrammatic classifications of study area hydrochemical facies. ....	64
Figure 3.6 Spatial distribution of the different hydrochemical facies in the study area. ....	66
Figure 3.7 Rock-water interaction and resultant groundwater types (Elango & Kannan, 2007). ....	68
Figure 3.8 Rock-water interaction diagrams (Gibbs, 1970). ....	69
Figure 3.9 Relationships between $\text{Ca}^{2+}$ , $\text{Mg}^{2+}$ , $\text{SO}_4^{2-}$ and $\text{HCO}_3^-$ . ....	70

Figure 3.10 Relationship between total cations, $\text{Na}^+\text{K}^+$ and $\text{Ca}^{2+}\text{Mg}^{2+}$ .	73
Figure 3.11 Ion exchange scatter diagram.	74
Figure 3.12 Relationships between $\text{Na}^+$ and $\text{Cl}^-$ .	75
Figure 3.13 Relationships between EC and $\text{Na}^+/\text{Cl}^-$ .	76
Figure 3.14 Effect of land use on groundwater chemistry.	77
Figure 3.15 Spatial distribution of major ions (a) $\text{Ca}^{2+}$ , (b) $\text{Mg}^{2+}$ and (c) $\text{Na}^+$ against catchment and lithological background: Inverse Distance Weighted Interpolation representation.	78
Figure 3.16 Spatial distribution of major ions (a) $\text{Cl}^-$ and (b) $\text{SO}_4^{2-}$ against catchment and lithological background: Inverse Distance Weighted Interpolation representation.	80
Fig 3.17 Spatial distribution of $\text{HCO}_3^-$ against catchment and lithological background: Inverse Distance Weighted Interpolation representation.	81
Fig 3.18 Spatial distribution of $\text{K}^+$ against catchment and land cover background: Inverse Distance Weighted Interpolation representation.	83
Fig 3.19 Spatial distribution of $\text{NO}_3^-$ against catchment and lithological background: Inverse Distance Weighted Interpolation representation.	84
Fig 3.20 Spatial distribution of the Hardness Factor scores against catchment and lithological background: Inverse Distance Weighted Interpolation representation.	88
Fig 3.21 Spatial distribution of the Alkalinity Factor scores against catchment and lithological background: Inverse Distance Weighted Interpolation representation.	89
Figure 3.22 Spatial distribution of Anthropogenic Factor scores against catchment and land cover background: Inverse Distance Weighted Interpolation representation.	90
Figure 3.23 Water type groups cluster of the groundwater samples using Set A variables (red line indicates level of similarity or distance between groups).	93

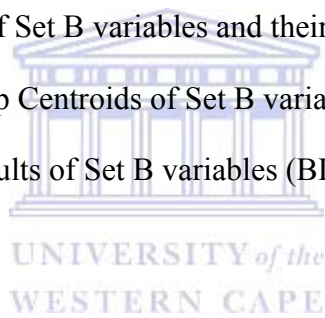
Figure 3.24 Groundwater sample groups (CA1, CA2 and CA3) vs. discriminant functions (Set A variables). .....	95
Figure 3.25 Water type groups cluster of the groundwater samples using Set B variables: a) First attempt (BI) b) Further classification of CB1I in to 4 groups (BII). Red line indicates level of similarity or distance between groups). .....	97
Figure 3.26 Groundwater sample groups (CB1I, CB2I and CB3I) vs. discriminant functions of Set B variables (BI). .....	100
Figure 3.27 Groundwater sample groups (CB1II, CB2II, CB3II and CB4II) vs. discriminant functions of Set B variables (BII). .....	103
Figure 3.28 Groundwater sample groups (CB1III, CB2III, CB3III, CB4III, CB5III and CB6III) vs. discriminant functions of Set B variables (BIII). .....	107
Figure A.1 Groundwater sample analysis result: Report WT1904/2008. ....	127
Figure A.2 Water sample analysis result: Report NR7969/2009. ....	128



## List of Tables

Table 1.1 Summary of T and S values in the study area (Rose, 2008).....	16
Table 3.1 Groundwater physical and chemical quality descriptive statistics* with SAWQG (DWAF, 1996) Limits.....	51
Table 3.2 Major cation mean concentrations percentages (meq/L).....	51
Table 3.3 Major anions mean concentrations percentages (meq/L).....	52
Table 3.4 Comparison of the groundwater samples from Beaufort West area with WHO (1993) drinking water standards.....	52
Table 3.5 Classification of water based on TDS (Davis & DeWiest, 1966) .....	56
Table 3.6 Classification of water based on TDS (Freeze & Cherry, 1979).....	56
Table 3.7 Classification of water based on hardness (Sawyer & McCarty, 1967)....	57
Table 3.8 Classification of water based on EC (US salinity Laboratory, 1954).....	57
Table 3.9 Classification of water based on percentage Na <sup>+</sup> (US salinity Laboratory, 1954) .....	58
Table 3.10 Correlation matrix (Pearson) of the groundwater sample parameters (N= 49). All values are in mg/L unless indicated otherwise.....	60
Table 3.11 Multiple linear regression analysis result of TH, EC and TDS* .....	62
Table 3.12 Multiple linear regression analysis result of the ions* .....	62
Table 3.13 Descriptive statistics of the hydrochemical facies.....	67
Table 3.14 Descriptive Statistics of Ca <sup>2+</sup> /Mg <sup>2+</sup> ratio.....	72
Table 3.15 Descriptive Statistics of equivalent Ca <sup>2+</sup> +Mg <sup>2+</sup> to HCO <sub>3</sub> <sup>-</sup> ratio.....	73
Table 3.16 Descriptive Statistics of equivalent Ca <sup>2+</sup> +Mg <sup>2+</sup> to TZ <sup>+</sup> ratio .....	73
Table 3.17 Factor analysis results: Total variance.....	86
Table 3.18 Factor analysis result: Rotated Component Matrix .....	87

Table 3.19 Structure matrix of Set A variables and their functions .....	94
Table 3.20 Functions at Group Centroids (Set A variables).....	94
Table 3.21 Classification Results (Set A variables) <sup>a</sup> .....	94
Table 3.22 Descriptive statistics of the three water types (A)* .....	96
Table 3.23 Structure matrix of Set B variables and their functions (BI) .....	99
Table 3.24 Functions at Group Centroids of Set B variables (BI).....	99
Table 3.25 Classification Results of Set B variables (BI) <sup>a</sup> .....	100
Table 3.26 Structure matrix of Set B variables and their functions (BII).....	101
Table 3.27 Functions at Group Centroids of Set B variables (BII) .....	102
Table 3.28 Classification Results of Set B variables (BII) <sup>a</sup> .....	102
Table 3.29 Structure matrix of Set B variables and their functions (BIII) .....	104
Table 3.30 Functions at Group Centroids of Set B variables (BIII).....	105
Table 3.31 Classification Results of Set B variables (BIII) <sup>a</sup> .....	106



# Chapter I

## 1. Purpose and scope

Different processes such as aquifer lithology, through water interaction with the chemical constituents of the hosting rock, and anthropogenic processes such as urban and agricultural activities affect groundwater quality. As a scarce resource, it requires a continuous monitoring through quality assessments and management for sustainable use and contamination protection. The thesis investigates the assessment of the groundwater quality in the Beaufort West area using multivariate statistical and spatial analyses methods.

The town of Beaufort West and the different farms in its vicinity obtain their water from both surface water and groundwater. Groundwater quality assessment of the study area can benefit resource managers in protecting and managing it for sustainable municipal and agricultural water supply. To date extensive hydrogeological work has been conducted by the Beaufort West Municipality and DWAF starting in the 1970's due to the heavy reliance of the area on groundwater, scarce rainfall (about 230 mm per annum), drought and uranium exploration (Chevalier et al., 2001; Chevalier & Woodford, 1999; Rose, 2008; Rose & Conrad, 2007; Turner, 2008; van Wyk & Witthueser, 2011; Woodford & Chevalier, 2002). These studies used mostly the conventional hydrogeochemical analysis and interpretation methods and no study of the groundwater in the study area has been conducted using multivariate statistical and spatial analyses methods, hence the need for the current study.

The assessment of the quality of groundwater in the Beaufort West area has important implications in the groundwater's potential as a resource and can indicate where negative impacts may be mitigated and efficacy of water conservation programs can be evaluated. Identification of possible contaminations and potability of the groundwater can be used in aiding site selection for desalination facilities and wastewater treatment plants, based on expected groundwater quality and recovery.

Knowledge of the groundwater quality of the study area can be useful for

- Implementation of a Water Conservation and Water Demand Management Strategy,
- Integration of emergency schemes and re-use of water and
- Further incremental groundwater development to be undertaken by the local municipality.

Therefore, the thesis attempts to assess the groundwater quality using different methods such as Factor, Cluster, Discriminant and Spatial analyses of the hydrochemical data, compare it with international and national standards and make suggestions.

## **1.1. Research problem**

Groundwater in arid and semi-arid areas is an important domestic, agricultural and industrial source of fresh water. The dependency of such socio-economic activities on a scarce resource like groundwater requires constant monitoring of its quality. The groundwater quality in arid and semi-arid regions like the Karoo region of South Africa has been assessed through the use of classical hydrogeochemical classification methods such as trilinear diagrams and multivariate statistical techniques (Adams, 2001; Adhikary et al., 2009; Cloutier et al., 2008; Gomo & Vermeulen, 2013; Love et al., 2004; Van Tonder & Hodgson, 1986) as well as spatial techniques (Nhleko & Dondo, 2008). In the case of the Beaufort West area, there is not much documented work in the integration of multivariate statistical and spatial analysis methods to assess groundwater quality.

## **1.2 Aim and objectives**

### **Aim**

The overall aim of the thesis is to assess groundwater quality of the study area using multivariate statistical and spatial analyses techniques in order to understand the dominant processes that affect its quality and suitability for drinking and irrigation purposes.

## Objectives

To achieve the above aim, the following objectives have been identified:

- Characterization and classification of groundwater quality of the study area using conventional hydrogeochemical classification and interpretation methods,
- Univariate and bivariate statistical analyses of the groundwater quality,
- Characterization and classification of groundwater quality of the study area using multivariate statistics,
- Comparison of trilinear diagram and multivariate statistical interpretation methods,
- Mapping the spatial distribution of borehole locations, ionic concentrations and statistical analysis results of the groundwater quality using ArcGIS 10.

The proceeding sections will discuss and outline the introduction, study area background information, literature and methods employed in the thesis, results, their detailed explanation, and the conclusions and recommendations arrived from the results.

## 2. Introduction

Groundwater has been an important resource to municipalities and rural areas of the arid and semi-arid regions of South Africa where surface water is scarce. As an important part of the total fresh water resources in South Africa, groundwater has the potential to contribute to the growth and development of communities. The thesis focuses on the town of Beaufort West and its immediate vicinity, as the study area, in assessing the quality of the groundwater. The town is located in the Karoo basin of South Africa underlain by the fractured Karoo formations and is heavily dependent on its groundwater resources for domestic, agricultural and industrial activities. Studying groundwater characteristics of such areas is of utmost importance in the management of this resource. The study of groundwater quality requires hydrogeological investigation to interpret the hydrogeological systems and prepare hydrochemical maps. Such maps could be used to describe the spatial and stratigraphic distribution of groundwater chemical constituents and their relationship to the prevailing hydrogeological

parameters.

The description of the constituents and their relationship to the hydrogeological parameters helps to identify probable chemical reactions, the mineralogical controls, source of contaminants and source and flow of the groundwater itself. The identification of such factors would help to explain the source of the chemical constituents, their concentration and distribution as well as the hydrochemical heterogeneity of the groundwater. To get a better understanding of the groundwater quality one would start with a proper study of an area or aquifer of interest, the geological and hydrogeological conditions and design of sample collection, which would culminate in understanding the functioning of the hydrogeological system. According to Weaver et al. (2007), groundwater sampling is conducted for the following reasons:

- Assess groundwater quality for fitness of use
- Understanding the hydrogeology of an aquifer of interest and
- Investigating groundwater pollution

The thesis undertakes these reasons as important components of the objectives and attempts to assess the groundwater quality of the study area.

Different consulting firms and the Department of Water Affairs, with a primary focus on water supply for the local community, have conducted many hydrogeological investigations of the study area (Rose, 2008; Rose & Conrad, 2007; van Wyk & Witthueser, 2011). Based on the information generated from some of these investigations the thesis assess the groundwater quality using multivariate statistical methods and spatial analysis.

The study of hydrogeochemical evolution in fractured rock aquifers requires manipulation of a wide range of data of diverse origin. The hydrochemical parameters indicate the diversity of the groundwater chemistry and orientation of the possible processes that take place through the aquifer. A series of geochemical variables and their associations must also be considered which determine the chemical evolution of the groundwater (Sánchez-Martos et al., 2001).

The main objective of the thesis is the study of the groundwater quality of the fractured

rock aquifers in the Beaufort West area using methods that consider the hydrochemical characteristics of the water in these aquifers. Thus, the thesis attempts to assess the quality of groundwater based on spatially referenced borehole samples from the area. An attempt is made to represent groundwater quality through statistical analysis and assess the spatial distribution using Geographic Information Systems (GIS) map representation.

Statistical methods such as univariate (mean, Standard deviation, minimum and maximum), bivariate (regression and correlation analyses) and multivariate (factor, cluster and discriminant analyses) are used to characterize the hydrogeochemistry of the groundwater in order to understand the dominant processes that affect its quality and assess its suitability for drinking and irrigation purposes.

Correlation Analysis (CA) is a statistical method that is useful for interpreting and relating groundwater quality data to specific hydrogeological processes. This method is rather useful in characterizing and obtaining information of the groundwater system at a glance compared to going through complex methods and procedures (Adhikary et al., 2009). In CA, the degree of linear association between any two-groundwater quality parameters is measured by a value called correlation coefficient ( $r$ ).

Linear regression is the next logical step in a bivariate hydrochemical analysis. It is used to predict the value of a variable (dependent) based on the value of another variable (independent). This method is useful in identifying relationships with the different measured hydrochemical variables and predicting one from a set of other variable. A typical example is the prediction of TDS (mg/L) from EC (mS/m). Hydrogeochemical investigations involve multiple variables and more than one of these variables can be predicted using multiple variables. Such multivariate environment thus necessitates the use of another method known as Multiple Regression Analysis.

Based on the correlation analysis results, Factor Analysis can significantly explain observed relations among several variables in terms of simpler relations that provide insight into the underlying structure of the variables (Matalas & Reihner, 1967). These simpler relations are expressed in terms of a new set of variables, called factors.

Cluster and discriminant analyses provide an insight in to the different

hydrogeochemical processes that affect the groundwater chemistry based on the explanation of the relationships between the variables (Factor analysis) or independently. These methods, in conjunction with standard geological and hydrogeological analyses, provide a consistent and reliable method for delineating physical and chemical trends in hydrogeological units. It distinguishes members of one group from the members of other groups and represents them in a graphical form called dendrogram, which makes the data interpretation easy and understandable. In CA, there is no prior knowledge about which sample belongs to which cluster.

The results of the conventional hydrogeochemical and multivariate statistical analyses are further analysed using Geographic Information Systems (GIS) to describe their spatial and stratigraphic distribution. GIS as a tool is becoming an important means of understanding and analysing water and related resources management in the world. Such a system is useful in collecting and organizing data about these resources and understanding their spatial relationships. GIS is an effective tool for assessment of groundwater quality, land cover and geological mapping that are essential for monitoring environmental changes and contamination detection.

Analysis, using the Spatial Analyst Tool of ArcGIS 10, of the hydrochemical facies, classifications derived from the major ions analysis and multivariate statistical analyses enables the assessment of their spatial distribution throughout the aquifer by producing groundwater quality maps in a reduced multivariate space.

The ultimate aim of the thesis is to identify the principal processes that affect the groundwater quality of the study area and represent its spatial distribution.

### **3. Study area background**

The study area is located in the Karoo Basin of South Africa, in and around the town of Beaufort West, about 460 Kilometres to the northeast of Cape Town and lies in the coordinate range of 32°11'22" S & 32°43'39" S latitude and 22°23'50" E & 23°10'30" E longitude. The town of Beaufort West is the economic, political and administrative centre of the Central Karoo and lies at about 930 metres above sea level (Spies & Du Plessis, 1976). The area receives its rain mostly during the summer season

due to a high pressure system that dominates the inflow of moisture filled air into the escarpments (Tyson & Preston-Whyte, 2000). Average precipitation in the vicinity of Beaufort West is 235 mm per annum (Kotze et al., 1997; Schultze, 1997) while the Mean Annual Potential Evaporation(MAPE) generally exceeds 2400 mm per annum which results in a rainfall deficit (MAP-MAPE) that varies between -2463 and 1230 mm per annum (Woodford & Chevalier, 2002). The northern part of the study area is mainly plateau of the Nuweveld Mountains that rise up to 1450 mamsl and is covered mainly by erosion resistant dolerite intrusions that play a major role in controlling the geomorphology and groundwater recharge (Figure 1.3). The town of Beaufort West lies at the base of the escarpment (Figure 1.1). According to Rose (2008), the town has four municipal well fields viz. Brandwag (in the northeast), Tweeling, Lemoenfontein and Town well fields. The Town well field supplies the majority of groundwater to the town and the volume of water from this well field amount to about 50% of the total groundwater supply (Rose, 2008). Besides, the town uses surface water from the Gamka Dam and the ratio of groundwater to surface water usage is about 1:1 (UMVOTO, 2010). The town has a Sewarage plant in the south and the output of the sewerage plant is generally used for irrigation of golf estates. A reconciliation strategy report for Beaufort West (UMVOTO, 2010) indicated that the current wastewater treatment plant is contaminating the groundwater used for municipal supply through leakage and unlined ponds. The report suggested to purify the groundwater from this area through reverse osmosis. According to the Beaufort West Local Municipality (2013) website the raw sewage received annually at the sewage farm, comprises 33.5 % of the water provided for the local municipality. The purified sewage water (~ 50.79%) is then used for irrigation of sports fields (UMVOTO, 2010) as well as the Flagship Project for the irrigation of lucerne.

The borehole locations in the study area are within six Quaternary Catchments (L11F, L11G, J21A, J21B, L12B, and J21C) and two Water Management Areas (Gouritz and Fish to Tsitsikamma) (Figure 1.1). The Quaternary catchment J21A contains most of the borehole locations while the rest of the boreholes are spread among the remaining catchments.

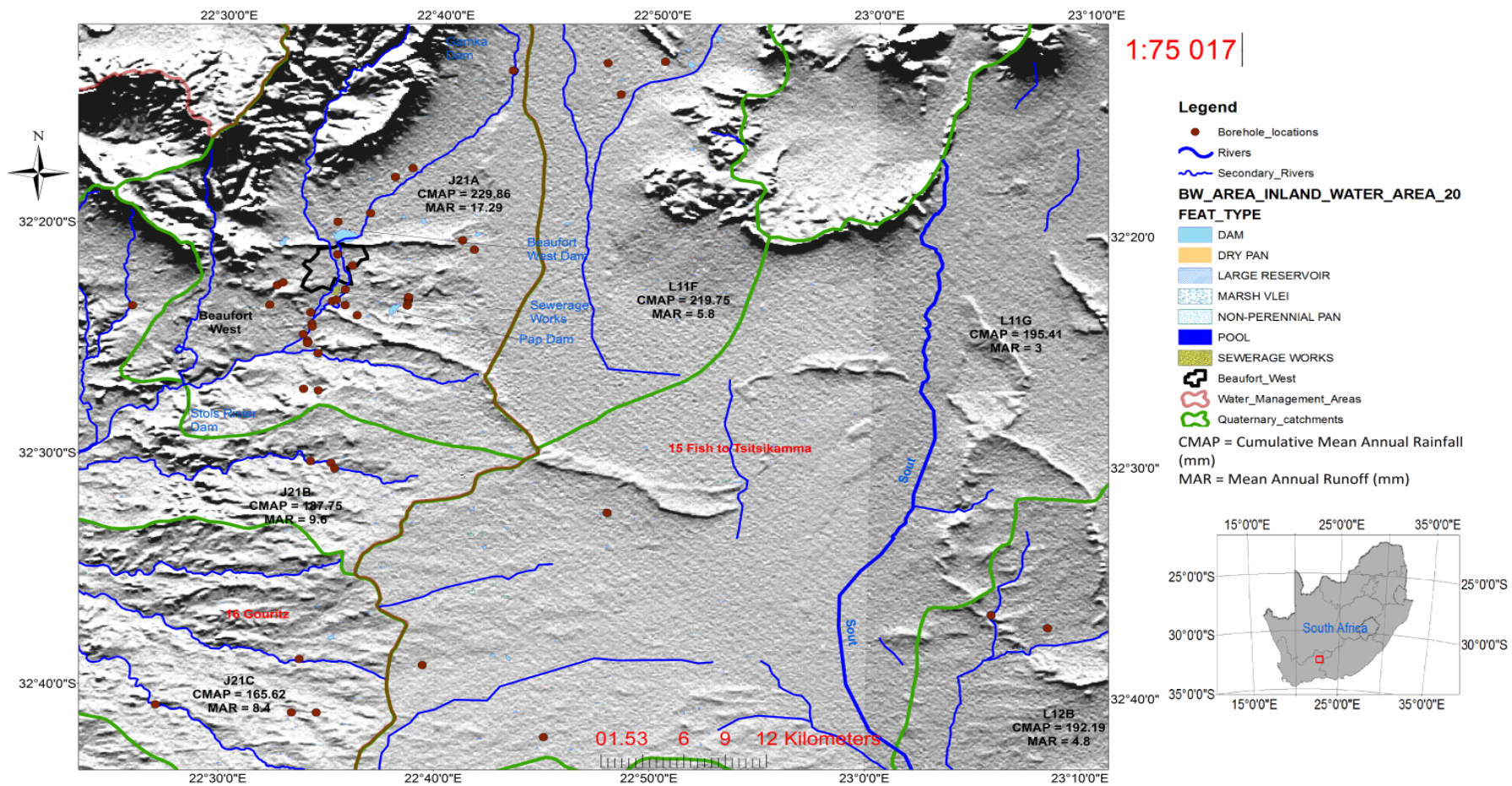


Figure 1.1 Borehole location distributions along the six catchment areas: an adaptation of the Water Resources of South Africa 2005 (Middleton & Bailey, 2008).

The Cumulative Mean Annual Precipitation (CMAP) of these catchments range from 165.62 mm to 229.86 mm while the Mean Annual Runoff ranges from 3.0 mm to 17.3 mm (Middleton & Bailey, 2008).

According to the Groundwater Resources Assessment (GRAII) report, quaternary catchment J21A has a mean recharge value of 1.76% while quaternary catchment L11F has a mean recharge value of 2.315% of the total rainfall. This is equivalent to approximately 3.46 Mm<sup>3</sup> and 3.79 Mm<sup>3</sup> for these two quaternary catchments, respectively (DWAF, 2005).

#### 4. Regional and local geology

The Karoo Basin is a Late Carboniferous-Middle Jurassic retroarc foreland fill, developed in front of the Cape Fold Belt (CFB) in relation to subduction of the palaeo-Pacific plate underneath the Gondwana plate (Catuneanu et al., 1998). The sedimentary rocks of the Karoo Sequence reflect the progressively changing depositional environment of a combined total thickness of about 12 Km of sedimentary strata, which are capped by a 1.4 Km thick unit of basaltic lava (Figure 1.2) (Woodford & Chevalier, 2002).

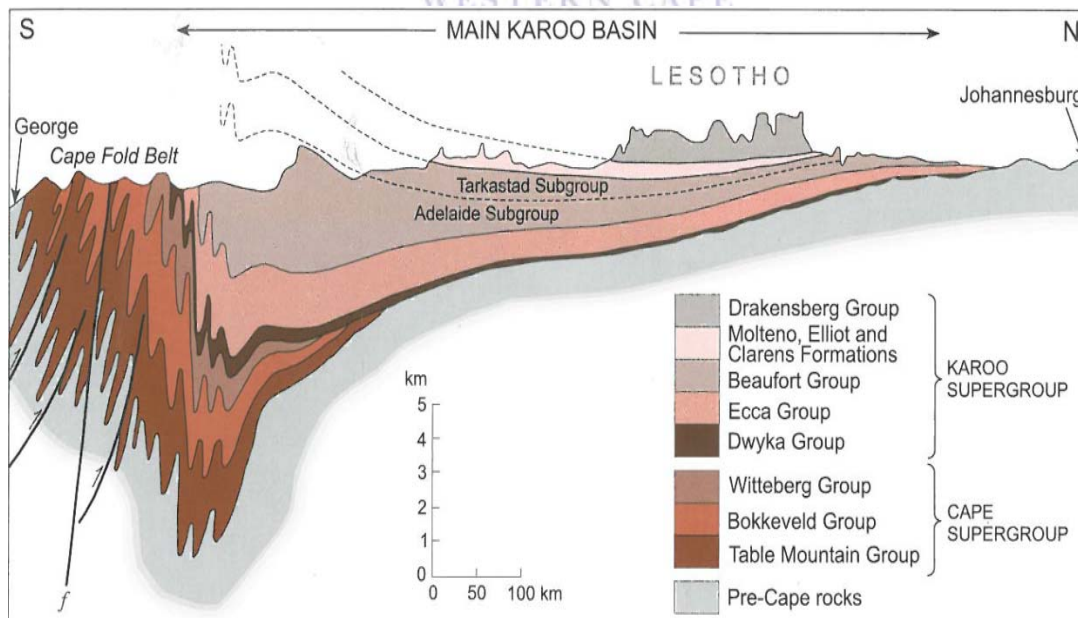


Figure 1.2 Schematic north-south cross-section of the Main Karoo Basin (Johnson et al., 2006).

The sequence consists of the Dwyka group (Tillite, a 700 m thick diamictite), Ecca group (rhythmitite of about 2000 – 3000 m thickness), Beaufort group (composing of the Adelaide and Tarkastad subgroups), Stormberg group and the Drakensberg group (up to 1200 m of basalt with some pyroclastic intercalations near the base) (Johnson, 1976).

The Beaufort Group of the Karoo Sequence is subdivided into the lower Adelaide and upper Tarkastad Subgroups. Cole and Labuschagne (1985) described the lower Adelaide Subgroup that is found in the southwestern Karoo as having its sandstone interbedded with mudstone and siltstone, where the sedimentary sequence forms several upward-fining megacycles of up to 400 metres thick megacycles. The authors also illustrated that each of these megacycles consists of several sandstones in the lower portion and a mudstone-dominated sequence in the upper portion. From bottom to top, the sandstone-rich parts of the upper three megacycles are known as the Moordenaars sandstone, Poortjie Member and Oukloof sandstone.

Cole and Labuschagne (1985) described the lower Adelaide Subgroup's lithofacies as follows: Several lithofacies can be recognized and the sandstone has all the characteristics of a fluvial depositional environment, is invariably immature, and is in fact a type of lithofeldspathic greywacke, containing quartz, feldspar and rock fragments set in a fine-grained matrix. A considerable amount of calcite can be present, particularly in some of the mineralized sandstones, along with organic material and minor amounts of disseminated sulphides. The feldspar present in these sandstones consists of plagioclase and orthoclase in variable amounts. In unmineralized sandstone, orthoclase is in the order of 5% and plagioclase about 20%, whereas in mineralized sandstone, the amount decreases to 2% or 3% for both feldspars. Two main periods of carbonate replacement took place: the first phase being a manganese-rich variety with minor calcium, whereas the later phase is almost pure calcite. The carbonate content in mineralized sandstone varies from 2% to 30% and an increase of carbonate takes place at the expense of plagioclase. (p. 265)

The Late Permian Lower Beaufort Group, which comprises the two successive formations, characterizes the geology of the study area predominantly: the Mid Permian

Abrahamskraal Formation and the conformably overlying Late Permian Teekloof Formation (Rubidge, 1995) and Jurassic dolerite dykes and sills. According to Chevalier et al. (2001), these dykes and sills were intruded into the sediments of the Karoo Supergroup during a period of extensive magmatic activity that took place over almost the entire Southern African subcontinent during one of the phases in the Gondwanaland break-up. These intrusions resulted in a network of dolerite dykes, sills and inclined sheets as shown in Figure 1.3.

Johnson et al. (2006) described the older Abrahamskraal (~ 2500 m thick) and younger Teekloof Formations (~ 1000 m thick) as composed of alternating bluish-grey, greenish-grey or greyish-red mudrocks and grey, very fine to medium-grained, lithofeldspathic sandstones (Figure 1.3). The authors also illustrated that the sandstone generally constitutes 20-30% of the total thickness, but in certain areas may be as little as 10% while some sandstone-rich intervals may in places contain up to 60% sandstone. According to Chevalier et al. (2001), the sandstone units were formed by lateral migration of meandering rivers, whereas the mudstone units were formed by deposition in a flood plain and lacustrine environment.

Patrick et al. (2010) described the Abrahamskraal Formation (Pa in Figure 1.3) as a very thick (~ 2.4 km) succession of fluvial deposits laid down in the Main Karoo Basin by meandering rivers on an extensive, low-relief floodplain during the Mid Permian Period, some 266-260 million years ago. In these sediments brown-weathering limestone (palaeocaliche) layers are up to 1.5 m thick and extend up to 2 km. A number of greenish grey, cherty layers a few cm to two metres thick and extending a few tens of kilometres in some cases are also present in this formation. Most are massive, but ripple lamination, bioturbation and ripple marks are not uncommon.

It appears that at least some of these layers represent reworked, silicified volcanic ash (Johnson et al., 1997).

Johnson et al. (2006) described the Teekloof Formation as being characterized by a greater relative abundance of red mudstone compared to the underlying units, but in practice, the boundaries are linked to specific sandstone-rich marker units (members).

Thus, the authors indicated that the arenaceous Poortjie Member constitutes the base of the Teekloof Formation.

Patrick et al. (2010) described the Teekloof Formation (Pt in Figure 1.3) as follows: The formation has a generally higher proportion of sandstones and reddish mudrocks are more abundant compared to the underlying Abrahamskraal Formation. This formation is characterized by multi-storied sandstones that are common in the basal arenaceous Poortjie Member and thin impersistent lenses of pinkish “cherts” that are probably altered volcanic ashes. The presence of fine-grained pedogenic (soil) limestone or calcrete as nodules and more banks that are continuous indicates that semi-arid, highly seasonal climates prevailed in the Late Permian Karoo. This is also indicated by the frequent occurrence of sand-infilled mudcracks and silicified gypsum “desert roses”. The interbedded mudrock horizons of contrasting colours indicate fluctuating water tables and redox processes in the alluvial plain soil and subsoil. The reddish brown to purplish mudrocks were probably developed during drier, more oxidising conditions associated with lowered water tables, while the greenish-grey mudrocks reflect reducing conditions in waterlogged soils during periods of raised water tables.

Calcrete (Caenozoic) and hardpan deposits (low lying areas) which are possible results of secondary weathering of the Karoo sediments cover the rest of the study area (Figure 1.3). These weathered deposits include pedocretes (e.g. calcrete or soil limestones), colluvial slope deposits (sandstone scree, downwasted gravels etc.), sheet wash, river channel alluvium and terrace gravels, as well as spring and pan sediments (Patrick et al., 2010). Larger tracts of alluvium overlying the Beaufort Group bedrock are indicated in yellow on the geological map and as Alluvial in the legend of Figure 1.3.

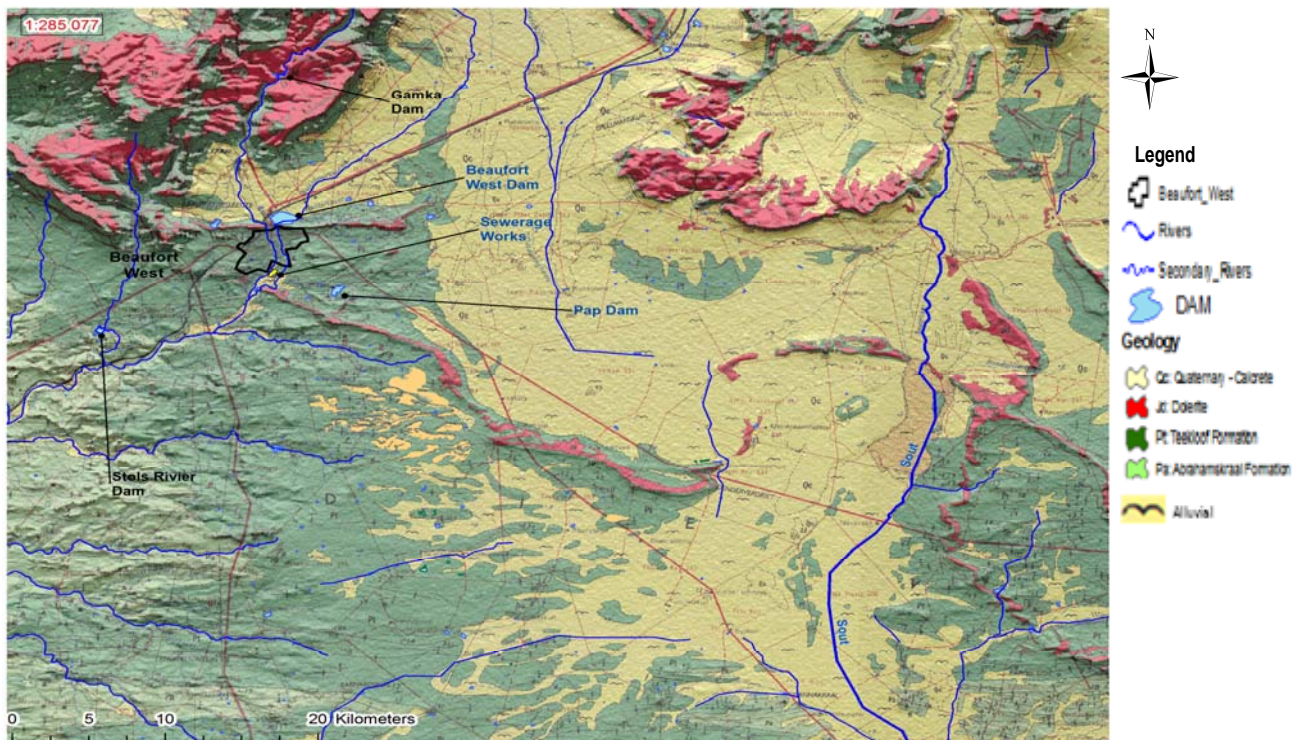


Figure 1.3 Geological map representation of the study area: an adaptation of 3222 Beaufort West Map (GISCOE, 2005).

## 5. Hydrogeology

The study area is extensively covered by alluvium that sits on top of the bedrock. These bedrocks comprise mudstones, siltstones and sandstones of the Beaufort group with gentle amplitude folding and dip rarely exceeding few degrees. There are isolated dolerite intrusions (dykes and rings) with gentle southerly slope and fracturing of the bedrocks (Figure 1.3).

According to Cook's (2003) description of fractured aquifers, they comprise a network of fractures that cut through a rock matrix and their characterization requires information on the nature of both the fractures and the rock matrix. Fetter (2001) asserted that the classification of fractures requires a complex examination of specific dimensions such as the length, width and aperture of the fracture and stresses the role that heterogeneity, in the saturated media, plays in affecting hydraulic properties within a certain area.

In the past three decades, understanding solute transport in fractures has been a major hydrogeological focus area because of two fundamental problems associated with such aquifers (Bodin et al., 2003):

- The selection of repository sites for radioactive waste in deep geological formations
- Groundwater pollution in fractured reservoirs

Therefore, understanding the dominant processes governing solute flow within fractured rocks is of the utmost importance in assessment of groundwater quality. Smith et al. (2001) assumed the processes to be:

- Advection and dispersion within the water conducting features and
- Retardation due to matrix diffusion into the rock matrix and sorption onto mineral surfaces

Botha et al. (1998) described Karoo fractured rocks as multi-layered, highly heterogeneous and isotropic with relatively low and variable permeability.

Fractured rock aquifers (secondary aquifers) cover most of the surface area around Beaufort West, although a combination of intergranular and fractured rock aquifers also exist as a result of alluvium and /or deeply weathered Beaufort sediments overlying the fresher Beaufort sediments (DWAF, 2002). Generally, the Beaufort Group sediments have low primary porosities, but the secondary porosity is well developed and is associated with weathering, minor folding, fracturing, faulting and jointing. As a result the secondary hydrogeological properties of the rocks, such as the degree, density, continuity and interconnection of fracturing control the occurrence, storage and movement of groundwater (Kotze et al., 1997). Most secondary aquifers are of the dual porosity type (Cook, 2003). Kovalevsky et al. (2004) suitably described the double porosity concept of fractured rocks as consisting of matrix blocks with a primary porosity and low hydraulic conductivity, separated by fractures with a low storage capacity but a high hydraulic conductivity. This has great implication on the movement of contaminants and dissolved chemical species. Hence, with time an apparent decrease in solute velocity prevails due to diffusion into the matrix (Cook, 2003).

High groundwater potential exists at the dolerite/sediment contact zones, the mudstone/sandstone contact zone, as well as in the fractured sandstone, especially where the proportion of mudstone to sandstone is small. Gomo et al. (2013) highlighted that the contact area between these impermeable dolerite intrusions and unconsolidated sediments has great potential to form preferential flow paths for both the groundwater and its constituents. The alluvium in turn acts as storage reservoirs for recharged water from rain events and recharges the underlying formations.

The fractured aquifer of the study area has been extensively studied over the past two decades and Woodford & Chevalier (2002) have provided the most comprehensive compilation of the hydrogeology of the Karoo basin. The compilation includes extensive lineament mapping of the study area that creates a better understanding of the structural controls on groundwater flow within the area. According to Cook (2003), boreholes cited on lineaments usually have higher yields. Kotze et al. (1997) further illustrated that fractured rock aquifers tend to produce higher yielding boreholes in excess of 5 L/s, whereas those with dual porosities tend to produce boreholes with yields of between 0.1 - 0.5 L/s.

### **5.1. Study area aquifer types**

The aquifer system of the study area has been investigated and characterized by several studies (Kotze et al., 1997; Nhleko & Dondo, 2008; Rose, 2008; Rose & Conrad, 2007).

Nhleko and Dondo (2008) divided the Beaufort west area into three aquifer systems based on aquifer mapping as follows: The top aquifer, extended to a depth of 10 m is characterised by weathered intergranular material consisting of primary sandstone, mudstone, siltstone and dolerite. It is postulated that this aquifer is recharged directly by precipitation, surface water sources such as rivers and pans where connectivity exists. The authors stressed that the sustainability of this aquifer remains questionable due its low storage capacity. The middle fractured-rock aquifer is characterized mainly by thick sandstone and mudstone with associated dolerite intrusions. The aquifer occurs at a depth of 50 m and is regarded as the most extensive aquifer in the study area. Recharge occurs along bedding planes as well as from runoff and leakage

albeit at a much slower rate. Due to the large-scale connectivity of fractures, the aquifer is highly transmissive. A deeper aquifer exists at a depth of around 80-90 m, and due to dolerite intrusions, the surrounding sandstones are heavily fractured.

Rose (2008) collected pump test data of the study area from variety of sources to compile a regional map of transmissivity and storativity. Table 1.1 gives the average horizontal transmissivity and storativity values subareas of the study area. Because limited data exist to the south of Beaufort west, the information is restricted mainly to the municipal well fields situated to the north of the town. This reflects areas most extensively explored over the past twenty years (Rose, 2008).

**Table 1.1 Summary of T and S values in the study area (Rose, 2008)**

Subarea	Transmissivity (T in m <sup>2</sup> /day)	Storativity (S dimensionless)
Brandwag east	>200	0.01 - 0.001
Brandwag west	<200	0.0001 - 0.00001
De Hoop	30 – 300	0.001 - 0.00001
Platdoorns	From <10 to >200	0.00001
Lemoenfontein	100 - 250	0.0001-0.00001
Town well	From 40 to >400	0.001 - 0.0001
Droerivier	<10	0.001 - 0.0001
Hansrivier	>300	0.001 - 0.0001
Sunnyside	100 – 360	0.00001 - 0.000001

According to Rose (2008) there is a strong correlation between borehole yields and transmissivities, whereby areas with high transmissivities > 100 m<sup>2</sup>/day is generally associated with borehole yields greater than 5 L/s. The influence of dolerite dykes on the yields of boreholes can be seen by the large amount of boreholes drilled in close proximity to these geological structures (Kotze et al., 1997). Pumping test data from boreholes collected by Rose and Conrad (2007) indicated that boreholes drilled on the farm Hansrivier (southeast of Beaufort West) on a contact zone between the dolerite dyke and fractured Teekloof formation produced sustainable yields in excess of 10 L/s.

## 5.2. Study area flow dynamics

A regional scale groundwater contour map (Figure 1.5) produced by Rose (2008) has shown the regional groundwater flow pattern of the study area as a generally north to south flow (Figure 1.4). The piezometric heads vary from > 1500 mamsl in the north coinciding with the Nuweveld Mountains to about 800 mamsl in the south coinciding with the flat lying plains. Note that the author sourced only 4 points with piezometric head information above 1300 mamsl, which are all situated in the mountainous areas in the north. However, the author argued the spatial distribution of the boreholes in the flatter area is sufficient to confirm the regional groundwater flow paths to be from north to south. It must also be noted that the current study area is twice the size of the area covered by Rose (2008) and about 30% of the boreholes which are in the southern part of the study area are not included.

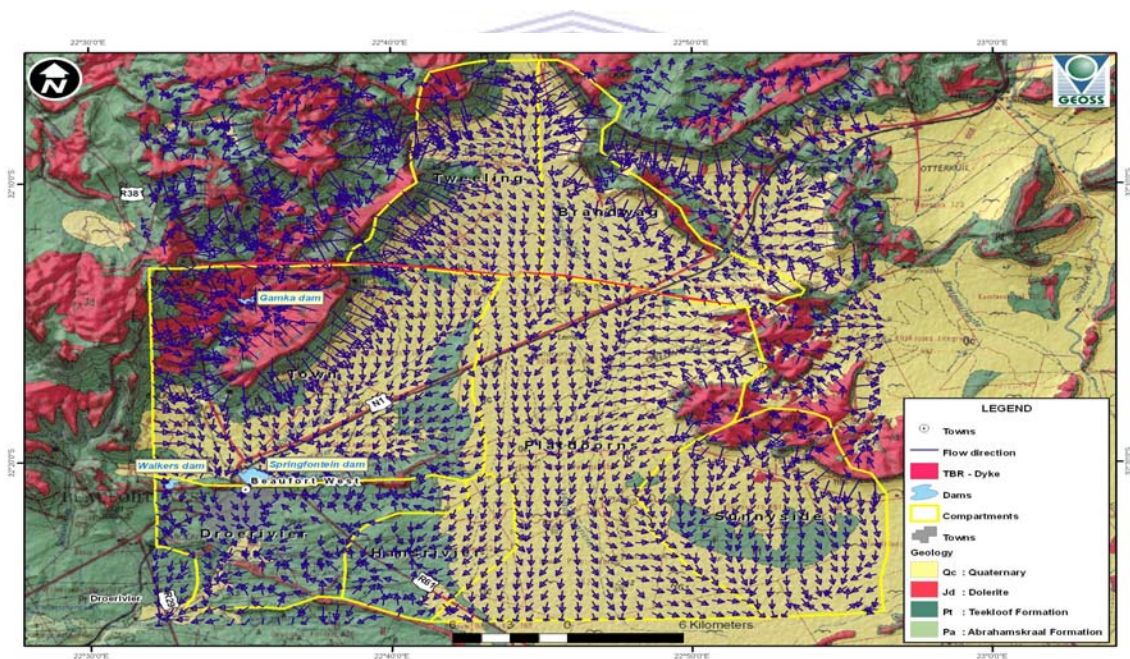


Figure 1.4 Groundwater flow direction and compartments (Rose, 2008).

Based on these groundwater flow paths several groundwater compartments of the study area were identified by Rose (2008). These compartments are

- Droerivier compartment
- Hansrivier compartment

- Platdoorns compartment
- Brandwag compartment
- Tweeling compartment and
- Town compartment.

Based on Rose's (2008) description of the compartments some of them are discussed below.

The Droerivier compartment is situated south of the town of Beaufort West. It contains most of the sampling locations, the wastewater treatment plant and the town of Beaufort West. The Teekloof Formation with some calcareous quaternary deposits and the northern part of the NW-SE trending dolerite dyke characterizes the compartment (Figure 1.5). The W-E trending Town dyke acts as the northern boundary of this compartment separating the town and the Beaufort West dam. Rose (2008) described the groundwater flow based on the groundwater level contours (Figure 1.5) as groundwater draining from the north and northeast towards the southwest. The author emphasised that the Gamka River is likely to be the main driving force behind the groundwater flow. Based on the EC values of the groundwater samples, the water in this compartment is relatively fresher except for the boreholes located on the calcrete deposits.

The Hansrivier compartment is situated east of the Droerivier compartment. It is separated from the Droerivier compartment by a small N-S trending dyke (the Hansrivier dyke) on the farm Hansrivier. It contains few boreholes and is characterized by a mix of the Teekloof Formation and Calcrete deposits. The NW-SE trending dyke in the study area is the southern boundary of this compartment (Figure 1.5). Rose (2008) showed using magnetic data that the Hansrivier dyke is not laterally extensive to the north and it is likely that some mixing occur with the fresher Droerivier compartment in the north of this compartment. The Hansrivier compartment drains from the north, east and southeast towards the west up to the Hansrivier dyke (Figure 1.4).

The Town compartment is situated to the north of the town of Beaufort West and has the W-E trending Town dyke as its southernmost boundary (Figure 1.5).

Rose (2008) indicated that some groundwater flow across this dyke towards the Droerivier compartment is expected. This compartment has few boreholes and includes the town of Beaufort West and Gamka dams. Mostly the calcrete alluvium and the Nuweveld dolerite caps in the northwest characterize it. Nuweveld Mountains in the north and west provide the main recharge area. Rose (2008) indicated that the extent of the capture zone could extend for kilometres into the Nuweveld Mountain; hence, the northernmost boundary of this compartment is not well defined. Groundwater generally flows from the north and northeast towards the southwest (town) (Figure 1.4). The groundwater quality in this compartment, especially for boreholes close to the main recharge area is good ( $EC < 150$  mS/m). According to Rose (2008), declining water levels are also known to recover quickly after rainfall events, which further indicate good active recharge in this area. The author also highlighted that groundwater quality in the eastern side of this compartment has slightly higher EC (70–300 mS/m), but could indicate greater travel distances from the recharge area.

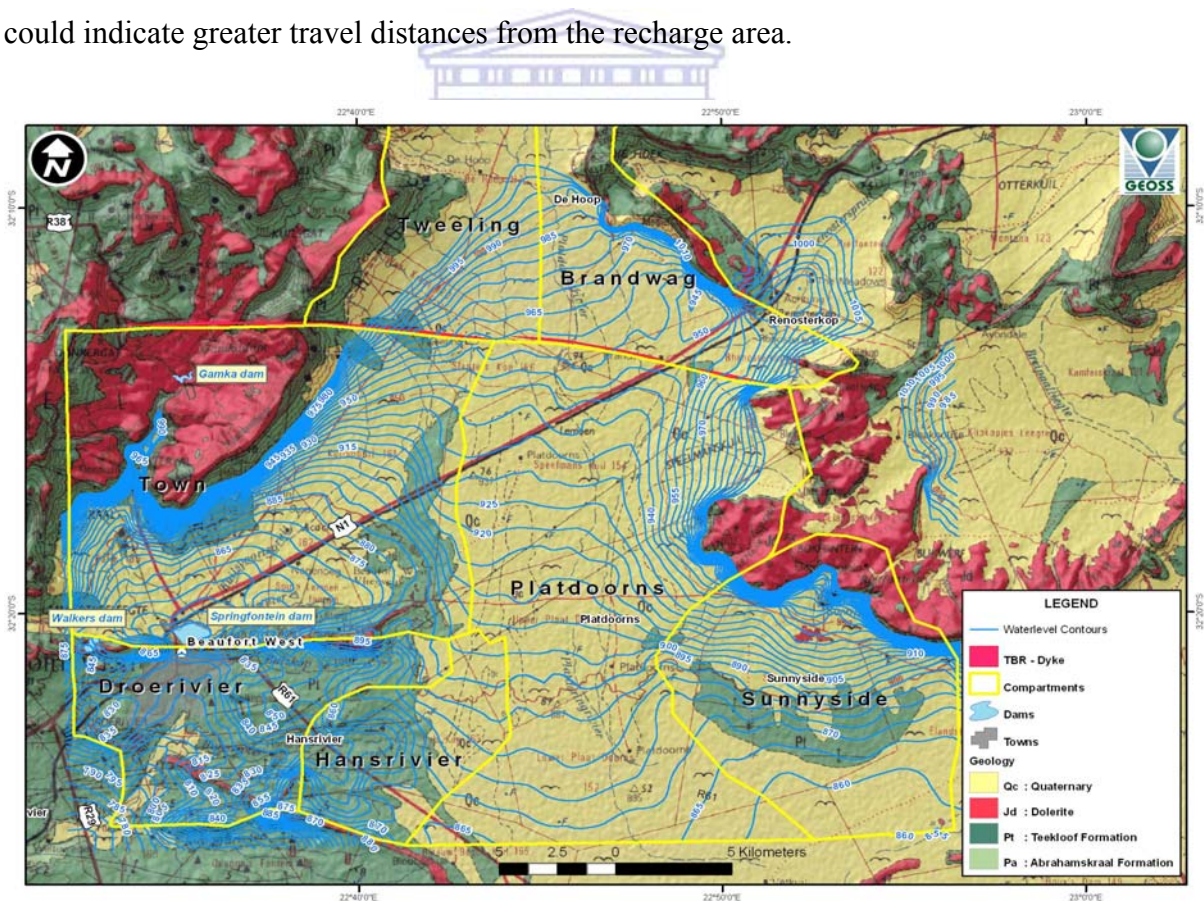


Figure 1.5 Groundwater contours with 5 m intervals (Rose, 2008).

## 6. Hydrogeochemistry

The interpretation of the distribution of hydrochemical parameters in groundwater helps in understanding the principal hydrological and hydrochemical processes. Such interpretations can be very useful in assessing the quality of the water for drinking and irrigation purposes (Hiscock, 2005).

Water, as a polar molecule is an effective solvent and dissolves variety of salts, some types of organic matter and ions from rock matrix and soil surfaces through the process of hydration. Such unique property makes water in aquifers interact with the geological formations and soils that it passes through and produces a wide variety of dissolved organic and inorganic constituents. These dissolved constituents found in groundwater characterize the quality of the water for the specific intended use. The composition of groundwater is also affected by other important factors such as rainfall composition, atmospheric dry deposition (oceanic salts in rain water) in recharge areas, evapotranspiration, differential uptake by biological processes in the soil zone and seawater mixing in the case of coastal areas (Hiscock, 2005). Sewage from urban settlements and fertilizer chemicals used in agricultural activities also affect groundwater composition. Groundwater tends to have much higher concentrations of dissolved constituents than surface water. This is also generally true when comparing deep groundwater to shallow or young groundwater due to the longer residence time and contact with the rock matrix.

Groundwater composition generally comprises the six major ions:  $\text{Na}^+$ ,  $\text{Ca}^{2+}$ ,  $\text{Mg}^{2+}$ ,  $\text{Cl}^-$ ,  $\text{SO}_4^{2-}$  and  $\text{HCO}_3^-$ ; minor ions, trace constituents and dissolved gases. These dissolved constituents are, typically expressed in mg/L for the major ions and  $\mu\text{g/L}$  for trace elements. In the absence of contaminants due to anthropogenic activities, the major ions constitute 90% of the total dissolved solids content in groundwater (Hiscock, 2005). The sum of the concentrations of all the dissolved constituents in groundwater is known as total dissolved solids (TDS), which can be estimated by measuring the electrical conductivity (mS/m). The relationship between TDS and EC is discussed in section 1.2 of chapter 2.

Groundwater chemistry is largely characterized by the mineral composition of the rocks it flows through and is normally explained as a water-rock interaction. Evaporation, concentration and dilution due to precipitation also affect the chemical composition of groundwater. Kumar et al. (2006) stated that hydrogeochemical processes help to understand changes in groundwater quality due to water interaction with the host matrix and anthropogenic influences. The author further explained that groundwater quality depends also on the chemistry of water in recharge area and the geochemical processes that occur in the subsurface. Matthes (1982) also emphasized that these hydrogeochemical processes are responsible for the seasonal and spatial variations in groundwater chemistry.

It is understood that groundwater chemically evolves through its interaction with aquifer minerals, anthropogenic influences and internal mixing among different groundwater flow paths in the subsurface (Domenico, 1972; Toth, 1985; Wallick & Toth, 1976). Therefore, the spatial distribution of hydrochemical species provides information on the direction of groundwater movement. Solute concentrations in the groundwater increase due to spatial variability of recharge because of microtopographic controls (Schuh et al., 1997). Freeze & Cherry (1979) compared groundwater mineralization between recharge and discharge zones and found that the latter tends to have higher mineral concentrations. The authors explained that this could be due to the longer residence time and prolonged contact with the aquifer matrix. Furthermore, the weathering of primary and secondary minerals also contributes cations and silica in the system (Bartarya, 1993). The silica from the lithofeldspathic sandstones of the study area does not react readily with groundwater compared to the carbonate minerals that play an important role in the evolution of the groundwater.

Several studies have been carried out in understanding, identifying and interpreting hydrogeochemical processes around the world's aquifers. In India, Elango and Kannan (2007) discussed in detail the interaction of rocks with groundwater and the control of this interaction on the chemical composition of groundwater. Lakshmanan et al. (2003) also inferred that carbonate weathering and dissolution, silicate weathering and ion exchange processes are responsible for groundwater chemistry in their study area. In Argentina, Martinez and Bocanegra (2002) identified cation exchange processes and

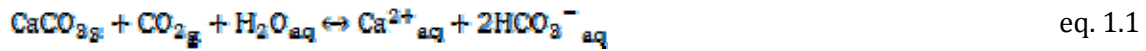
calcite equilibrium as the important hydrogeochemical processes that control groundwater composition of their study area aquifer. In South Africa, Sami (1992) demonstrated that leaching of surficial salts, ion exchange processes and residential time causes hydrogeochemical variations of groundwater in the semi-arid sedimentary basin in the Eastern Cape. Some of the hydrogeochemical processes that affect the groundwater chemistry are discussed in the proceeding sections.

## 6.1. Carbonate chemistry

According to Woodford and Chevalier (2002), quaternary deposits are major characteristics along the main rivers in the Karoo Basin and calcrete occurrence in shallow depth sediments is common phenomenon near river channels in arid to semi-arid climate. These calcrete formations near river channels have been related to shallow water table and high infiltration rate, which contribute to the precipitation of leached carbonate and dolomite minerals (Parsons & Abrahams, 1994). The study area is mostly covered with calcareous quaternary deposits. Dissolution of calcite and dolomite minerals has great potential to influence groundwater chemistry (Gomo et al., 2013). Cardona et al. (2004) highlighted that ion exchange reaction of  $\text{Na}^+$  and  $\text{Ca}^{2+}$  often dominates the geochemical processes in detrital sedimentary aquifers. The geochemistry of carbonates and cation-exchange reactions (both direct and reverse) control the concentration of  $\text{Ca}^{2+}$ ,  $\text{Mg}^{2+}$ ,  $\text{Na}^+$ , and  $\text{HCO}_3^-$ , as well as pH values in groundwater.

The study area lithology is mostly sedimentary rocks (Abrahamskraal and Teekloof formations) and an overlying calcrete alluvium with dolerite intrusions as discussed in section 4 of chapter 1. Carbonates are present in different types of rocks, including most sedimentary rocks and are important in the evolution of groundwater chemistry. Calcite ( $\text{CaCO}_3$ ) is one of the carbonate sources in groundwater. Its dissolution is mainly controlled by dissolved carbon dioxide gas ( $\text{CO}_2$ ) and pH. Appelo and Postma (2010) indicated that the  $\text{CO}_2$  value in the atmosphere is  $0.3 \times 10^{-3}$  atmosphere while the highest concentration in contact with soil water is  $30 \times 10^{-3}$ . The proportion of  $\text{CO}_2$  in the atmosphere would, therefore, be about 0.03% and increases in the soil zone to several per cent of the soil atmosphere due to decay of organic matter.

Carbonate reactions in groundwater starts with the infiltration of groundwater in the soil zone to recharge of the aquifer and react with carbonate minerals. The dissolution mechanism is shown in equation 1.1.



Where

**s** stands for solid (carbonate mineral) state,

**g** for dissolved gas state and

**aq** for aqueous state.

The reaction in equation 1.1 takes place in two steps. The first step is the reaction of dissolved CO<sub>2</sub> gas with water to produce an intermediate weak carbonic acid (H<sub>2</sub>CO<sub>3</sub>) as in equation 1.2. This reaction shows that calcite solubility is controlled by CO<sub>2</sub> and prevails in the subsurface compared to surface (open system) and deep groundwater environments. The dissolution of calcite eventually culminates in the calcite saturation of the groundwater with the depletion of CO<sub>2</sub>. The weak carbonic acid is polyprotic (more than one H<sup>+</sup> ion) and dissociates in two steps as shown in equations 1.3 and 1.4.



Hiscock (2005) indicated that over most of the normal pH range of groundwater (6-9) HCO<sub>3</sub><sup>-</sup> is the dominant carbonate species. The author further asserted that this is the reason for HCO<sub>3</sub><sup>-</sup> being one of the major dissolved inorganic species in groundwater.

Groundwater that is primarily controlled by carbonate reactions has relatively high Ca<sup>2+</sup>

and  $\text{HCO}_3^-$  concentrations, which is typical of the groundwater samples collected from the study area. The presence of dolomite could also result in elevated  $\text{Mg}^{2+}$  concentrations due to the carbonate reactions.

## 6.2. Adsorption and ion exchange

Ions in groundwater have a tendency to be attracted to solid surfaces because of their electrical charge. Solid surfaces in groundwater include ordinary mineral grains (e.g. feldspar or quartz), iron oxides and clay minerals. Both anions and cations take part in ion exchange processes. Such process of attraction of ions to mineral surfaces in groundwater is known as adsorption. A typical adsorption is one known as ion exchange, where ions in the water solution replace ions in the mineral lattice. The process of adsorption coupled with ion exchange reactions in groundwater affect the hydrochemical composition significantly. Major ion exchange reactions in groundwater also affect other ions that are not involved in the reaction through dissolution and precipitation. Carlyle et al. (2004) stated that the attenuation of some pollutants such as  $\text{NH}_4^+$  is mainly through the process of ion exchange while Zhang and Norton (2002) associated ion exchange with changes in hydraulic conductivity of natural materials. pH plays a major role in ion exchange process. Point of zero charge (PCZ) is the pH of a rock forming mineral when it has zero charge. Based on the pH of the groundwater environment different minerals attract ions to their surfaces. Clay minerals, for example, have consistently negatively charged surfaces (except in most acidic solutions) and are particularly effective at adsorbing cations to neutralize their negative charge. Soil organic matter and metal oxides and hydroxides also have measurable cation exchange capacity (CEC).

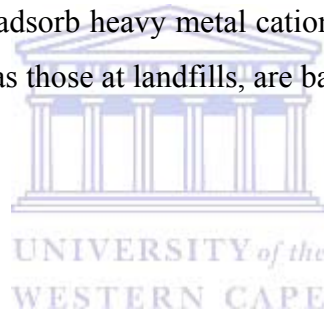
The degree of adsorption of ions by a mineral's surface depends on the surface area and grain size of the mineral. An increase in surface area and decrease in grain size generally increases the adsorption of ions on a mineral's surface. Clay minerals are typical example of such phenomenon. The adsorption process could occur due to either a weak Van der Waals force (a physical process) or a strong chemical bonding of the ions with the mineral surface's crystal lattice. Different ions have different degrees of adsorption depending on their charge density, which is a result of their valence and

hydrated radius in solution. Thus, divalent ions such as  $\text{Ca}^{2+}$  are usually more strongly adsorbed compared to monovalent ions like  $\text{Na}^+$  while trivalent cations tend to replace divalent cations and so on. The process is determined by the interaction of the concentration of the cations in solution and their energy of adsorption at the exchange surface. The general ordering of cation exchangeability for common groundwater ions is shown below.

(Strongly adsorbed)  $\text{Al}^{3+} > \text{Ca}^{2+} > \text{Mg}^{2+} > \text{NH}_4^+ > \text{K}^+ > \text{Na}^+$  (Weakly adsorbed)

Based on the above order  $\text{Ca}^{2+}$  is more abundant as an exchangeable cation than  $\text{Mg}^{2+}$ ,  $\text{K}^+$  or  $\text{Na}^+$ . In the presence of a reservoir of  $\text{Na}^+$  adsorbed onto clay minerals,  $\text{Ca}^{2+}$  and/or  $\text{Mg}^{2+}$  in the groundwater will preferentially attach to the exchange surface and the  $\text{Na}^+$  will be in solution.

Ion exchange plays an important role in trace element cations. Clay minerals bearing rocks and sediments naturally adsorb heavy metal cations from contaminated water and engineered clay barriers, such as those at landfills, are based on this principle.



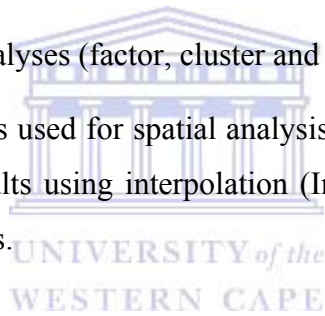
# Chapter II

## Methodology

This chapter will discuss the methodology and literature associated for acquiring, preparing, and interpreting data used for the assessment of the groundwater quality of the study area.

Methods described and discussed in this chapter include:

- Groundwater sampling and data preparation,
- Conventional trilinear diagram water classification,
- Univariate and bivariate statistical analyses (descriptive statistics, correlation and regression analysis),
- Multivariate statistical analyses (factor, cluster and discriminant analysis) and
- The visualization methods used for spatial analysis of the hydrochemical data and statistical analyses results using interpolation (Inverse Distance Weighted) and reclassification methods.



### 1. Groundwater sampling, data management and analysis

#### 1.1. Sampling method

The sampling sites are spread between two water management areas, namely the Fish to Tsitsikamma and Gouritz and six quaternary catchments. The outline of the study area was delineated mainly based on municipal water uses and hydrochemical data availability.

The study area is limited to areas with available hydrochemical data and areas where access was permitted. These areas include the Town well fields in the north and northeast (up to 40 km northeast of town), about 40 km east of the town including the farm Sunnyside and about 30 km south of the town up to the farm Blydskap. The southern part of the study area has large gaps in data since most of these properties were

strictly prohibited from being accessed. For interpolation purposes, such situation is not ideal as it influences the accuracy of the interpolation in the southern areas. However, the areas in the south were included since they include agricultural activities (irrigation and stock watering) as well uranium mining and exploration areas that could affect the groundwater quality.

The groundwater samples were obtained based on the hypothesis that the different chemical concentrations of the constituents will provide information that could be used to assess the quality of the groundwater in the study area. The investigation of these constituents' similarity, variability and interactions between each other and the lithology is expected to give an insight to the quality of the groundwater.

Twenty-four of the borehole water samples were collected during a WRC Hydrocensus project conducted in and around the town of Beaufort West in 2008/09 while the remaining 25-groundwater samples were obtained from GEOSS with the permission of Beaufort West Municipality. Groundwater samples were collected according to SANS 241 (SABS, 2001) from boreholes in and around the town of Beaufort West and were sent for major and trace elements analysis to BemLab (Pty) LTD in Somerset West (Cape Town, South Africa).

Necessary communication was made with the laboratory in order to ascertain which containers, preservatives and reagents were to be used when sampling (Weaver et al, 2007). Wilde et al. (1998) recommended that a 1-litre polyethylene bottle should be rinsed with acid and water samples should be preserved to  $\text{pH} < 2$  using  $\text{HNO}_3$ . Levin (1983) on the other hand stated that sample bottles should be thoroughly rinsed with 10 % HCl solution and then rinsed 2 to 3 times with de-ionised water. Levin (1983) also stated that water samples should be taken as follows:

- 500ml for the determination of  $\text{NO}_3^-$
- 250 ml for the determination of the major components:  $\text{SO}_4^{2-}$ ,  $\text{Cl}^-$ ,  $\text{F}^-$ ,  $\text{Na}^+$ ,  $\text{K}^+$ ,  $\text{Ca}^{2+}$  and  $\text{Mg}^{2+}$

Some parameters (such as pH, EC and Temperature) of groundwater are measured on site for the following reasons (Weaver et al., 2007):

- to check the efficiency of purging
- to obtain reliable values of those determinants that will change in the bottles during transport to the laboratory
- to obtain some values that may be needed to decide on the procedure or sampling sequence immediately during the sampling run

Hence, on site measurements of pH, EC (mS/m) and Temperature ( $^{\circ}\text{C}$ ) were taken for the twenty four groundwater samples and the GEOSS documentation highlighted that the same on site parameters were measured for the remaining twenty five groundwater samples (see Appendix B). The selected boreholes are both municipal and privately owned, fitted with either hand pump or electric motor, and are being used to supply water for municipal (16 boreholes), domestic (5 boreholes) and agricultural (27 boreholes) activities. During the sampling process, the borehole water was run or purged for each sampling location and the containers were rinsed according to literature prior to collection of the sample.

The groundwater samples were immediately transferred to the BemLab (Pty) Ltd laboratory and analysed for various hydrochemical parameters namely, pH (lab), EC,  $\text{Ca}^{2+}$ ,  $\text{Mg}^{2+}$ ,  $\text{Na}^{+}$ ,  $\text{K}^{+}$ ,  $\text{HCO}_3^{-}$ ,  $\text{Cl}^{-}$ ,  $\text{SO}_4^{2-}$ ,  $\text{NO}_3^{-}$  and other trace elements (see Appendix A).

## 1.2. Sample data preparation

The groundwater samples acquired from the Beaufort West Municipality were checked for completeness of major ion data and quality including borehole location coordinates. Only groundwater samples with complete major ion records and acceptable ionic balance were selected for further analysis in addition to the hydrocensus samples (see Appendix C). Electrical balance is used to check the correctness of a given water analysis by calculating the charge balance. A less than a  $\pm 5\%$  difference of anion-cation balance is reasonably acceptable for groundwater samples. Electrical balance could be more than  $\pm 5\%$  due to laboratory analysis error and exclusion of a major

dissolved species (element) from the species used for the ion balance calculation (Appelo & Postma, 2010). All the groundwater samples were checked for electrical neutrality using equation 2.1 (meq/L units) and samples with approximately  $\pm 10\%$  ionic balance difference were considered for further analysis.

$$EN(\%) = \left[ \frac{(\sum \text{Cations} - \sum \text{Anions}) + (\sum \text{Cations} + \sum \text{Anions})}{\sum \text{Cations} + \sum \text{Anions}} \right] \times 100 < \pm 5\%$$

eq. 2.1

The hydrochemical data used in equation 2.1 were  $\text{Ca}^{2+}$ ,  $\text{Mg}^{2+}$ ,  $\text{Na}^+$ ,  $\text{K}^+$ ,  $\text{HCO}_3^-$ ,  $\text{Cl}^-$ ,  $\text{SO}_4^{2-}$  and  $\text{NO}_3^-$ . About 6% of the groundwater samples were found to have an ionic balance between  $\pm 10$  and  $\pm 13.6$  and were included in the analysis with precaution due to the relatively small number of samples (see Appendix C).

$\text{K}^+$  and  $\text{NO}_3^-$  data for some of the groundwater samples with null values were replaced with the minimum detection limits (MDL). TA was calculated using  $\text{HCO}_3^-$  concentration (mg/L) while TH was calculated using  $\text{Ca}^{2+}$  and  $\text{Mg}^{2+}$  concentrations (mg/L) as follows:

$$TA = \text{HCO}_3^- \times 0.8202$$

eq. 2.2

$$TH = 2.5 \times \text{Ca}^{2+} + 4.1 \times \text{Mg}^{2+}$$

eq. 2.3

Total Hardness (mg/L) is normally expressed as the total concentration (mg/L) of  $\text{Ca}^{2+}$  and  $\text{Mg}^{2+}$  in water as equivalent of  $\text{CaCO}_3$ .

The proportion of Sodium ( $\text{Na}^+$ ) to Calcium ( $\text{Ca}^{2+}$ ) and Magnesium ( $\text{Mg}^{2+}$ ) in water solution was calculated as the Sodium Adsorption Ratio (SAR) for all the groundwater samples using equation 2.4 (see Appendix C) (Hiscock, 2005).

$$SAR = \frac{[\text{Na}^+] \left( \frac{\text{meq}}{\text{L}} \right)}{\sqrt{([\text{Ca}^{2+}] \left( \frac{\text{meq}}{\text{L}} \right) + [\text{Mg}^{2+}] \left( \frac{\text{meq}}{\text{L}} \right)) + 2}}$$

eq. 2.4

Total Dissolved Solids (TDS) could be defined as molecular, ionized or micro-granular (colloidal) solids dissolved in water and can pass through a 2-micron sieve. The Minimum Contamination Level (MCL) of TDS according to the EPA is 500 mg/L. Typical TDS of water from mountain springs or aquifers would range between 50 and 170 mg/L while typical tap water's TDS would range between 170 and 400 mg/L. Although it depends on the dissolved constituents, TDS is highly related to Electrical Conductivity (EC) and a factor of 0.67 is widely accepted for calculating TDS as in equation 2.5 (Hiscock, 2005).

$$\text{TDS (mg/L)} \sim (0.5 \text{ to } 0.8) \times \text{EC } (\mu\text{S/cm}) \quad \text{eq. 2.5}$$

Eleven out of forty nine groundwater samples did not have TDS data and the above relationship with EC and Linear Regression Analysis was used to predict the missing values. In this technique, the TDS for the 38 samples were first predicted from their EC values with a reliability of 97.6% and resulted in equation 2.6 that could be used to predict the missing TDS values (see Appendix C).

$$\text{TDS (mg/L)} = (6.501) \times \text{EC (mS/m)} + 92.879 \quad \text{eq. 2.6}$$

Correlation analysis between the predicted and original TDS values for the 38-groundwater samples resulted in a highly positive correlation with an  $r$  value of 0.980.

## 2. Univariate and bivariate statistics

### 2.1. Descriptive statistics

Hydrochemical variables of the groundwater samples were analysed using IBM® SPSS® Statistics 21 (IBM, 2012). This software was utilized for descriptive statistical analysis of the groundwater samples to produce different tables that provide information on the following:

- Descriptive results such as minimum, maximum, mean, standard deviation, range, sum...etc.

- Descriptive statistics used for groundwater type classifications based on TDS, TH, Salinity, WHO (1993) and South African water quality guidelines: domestic use (SAWQG) (DWAF, 1996) drinking water guidelines,
- Measured variable frequencies for comparison purposes

## 2.2. Correlation analysis

Correlation analysis produces pairwise associations from a set of variables and displays them as a matrix. This type of analysis provides information on the strength and direction of association between two variables. In this context, the null hypothesis asserts that the two variables are not correlated, and the alternative hypothesis asserts that the variables are correlated. In the case of the alternative hypothesis, a small P-value is evidence that the null hypothesis is false and the variables are, in fact, correlated (Reimann et al., 2008).

The linear relationship between two variables is measured by the correlation coefficient  $r$ , which is also known as the Pearson product-moment correlation coefficient (Cohen et al., 2013). The value of  $r$  can range from  $-1$  to  $+1$  and is independent of the units of measurement. A value of  $r$  near zero indicates little correlation between variables while a value near  $+1$  or  $-1$  indicates a high level of correlation between the variables (Reimann et al., 2008). This means when two variables have a positive correlation coefficient, an increase in the value of one variable indicates a likely increase in the value of the second variable while a negative correlation would mean the opposite. A scenario where  $r = 0$ , then the two variables are not correlated or do not have an apparent linear relationship although it does not mean that they are statistically independent (Reimann et al., 2008).

When comparing more than two variables simultaneously, multiple linear regression analysis becomes more useful than correlation analysis for evaluating their interdependency. The square of the correlation coefficient ( $r$ ) provides the coefficient of determination value or  $R^2$  for multiple regression analysis and is more readily interpretable than  $r$  as a measure of the degree of association.  $R^2$  provides the proportion of the total variability in the dependent variable that may be ascribed to the effects of

the independent variables.

Correlation Analysis (CA) is very useful for interpreting groundwater quality data and relating them to specific hydrogeological processes. This tool is quite useful in characterizing and obtaining first-hand information of the groundwater system than actually going through complex methods and procedures (Adhikary et al., 2009). CA method along with multiple regression analysis has been used in several hydrogeochemical investigations aiming to assess groundwater quality (Meyer, 1975; Raju, 2006; Saleem et al., 2012).

Fourteen variables viz. EC, SAR, TDS, TH, TA, pH,  $\text{Ca}^{2+}$ ,  $\text{Mg}^{2+}$ ,  $\text{Na}^+$ ,  $\text{K}^+$ ,  $\text{Cl}^-$ ,  $\text{SO}_4^{2-}$ ,  $\text{HCO}_3^-$  and  $\text{NO}_3^-$  from the groundwater samples were analysed for their interrelation using bivariate correlations method with Pearson correlation coefficient and a two-tailed test of significance in IBM® SPSS® Statistics 21 (IBM). In this analysis mg/L unit was used for the ions and the calculated variables such as TDS, TH and TA. mS/m was used as the unit of EC while the square root of meq/L was used as the unit of Sodium Adsorption Ratio (SAR).

### 2.3. Multiple regression analysis

Linear regression is the next logical step in a bivariate hydrochemical analysis. It is used to predict the value of a variable (dependent) based on the value of another variable (independent). This method is useful in identifying relationships with the different measured hydrochemical variables and predicting one from a set of other variables. A typical example is the prediction of TDS (mg/L) from EC (mS/m). Hydrogeochemical investigations involve multiple variables and more than one of these variables can be predicted using multiple variables. Such multivariate environment thus necessitates the use of another method known as Multiple Regression Analysis (MRA).

In regression analysis, it is crucial to test the hydrochemical data using definite criteria in order to achieve valid results (Cohen et al., 2013). These criteria are also known as assumptions in the process of running regression analysis using statistical software IBM® SPSS® Statistics 21 (IBM). In a real-world data, like a hydrogeochemical investigation data, not all hydrochemical datasets would pass these assumptions and this

violation of the criteria could be used for deciding on alternative methods to overcome them.

The first criterion is that the data used for regression analysis must be measured at the interval or ratio level (i.e., they must be continuous). This criterion is easily met with hydrochemical variables analysed in the thesis.

The second criterion is that there needs to be a linear relationship between the hydrochemical variables. Not meeting this criterion would require either transforming the variables or performing a non-linear regression analysis. The linear relationship of the variables was tested using scatter plots and the correlation coefficient  $r$  obtained from the correlation analysis (section 2.2 of this chapter).

The third criterion in performing regression analysis is that there should not be significant outliers. The presence of these outliers can have a negative effect in the prediction of dependent variables and therefore the accuracy of the result. For the current data set, being analysed the Durbin-Watson test for serial correlation of the residuals and casewise diagnostics for the cases meeting the selection criterion were used to detect outliers. The Durbin-Watson test for serial correlation was also used for testing the fourth criterion, which is independence of the observations. The Durbin-Watson value is dependent on the associated data matrix and exact critical values cannot be tabulated for all possible cases. Instead, Durbin and Watson (1971) established upper and lower bounds for the critical values. Typically, tabulated bounds are used to test the hypothesis of zero autocorrelation against the alternative of positive first-order autocorrelation. This is generally because positive autocorrelation is seen much more frequently in practice than negative autocorrelation. The autocorrelation statistic ranges from 0 to 4, with near 0 indicating positive autocorrelation, a value near 2 indicating non-autocorrelation and a value near 4 indicating negative auto-correlation. The Durbin-Watson test for all the predicted variables showed values between 0 and 2 and was in accordance with the correlation analysis results.

The model was also checked to see if it was prone to a multicollinearity effect. The Variance Inflation Factor (VIF) value obtained was close to one and thus there was no evidence of multicollinearity (Hair et al., 1998). The significance was set to  $P \leq 0.05$

and analyses were performed with IBM® SPSS® Statistics 21 (IBM).

### 2.3.1. Stepwise multiple regression analysis

The linear regression procedure adds variables consecutively, starting with the one with the highest partial correlation coefficient. Once an independent variable is in the regression equation, a highly correlated variable assumes decreased significance and has only a minor effect on a multiple correlation coefficient. As other variables are added to the independent variable, the multiple correlation coefficients and the variance explained by the regression equation is computed. The hydrochemical data was checked for normality as it is compulsory for multivariate statistical analysis (Siad, 1991) and was found to have a normal distribution.

Once the data was tested using some of the above criteria or assumptions step-wise linear regression analysis was performed for the dependent variables EC, TH and TDS against the ions  $\text{Ca}^{2+}$ ,  $\text{Mg}^{2+}$ ,  $\text{Na}^+$ ,  $\text{K}^+$ ,  $\text{Cl}^-$ ,  $\text{SO}_4^{2-}$ ,  $\text{HCO}_3^-$  and  $\text{NO}_3^-$ . The cations were also predicted using the anions and vice versa.

## 3. Classical hydrogeochemical analysis

Hydrogeochemical facies are generally studied and compared using different graphical representations such as Stiff (Stiff Jr, 1951), trilinear (Piper, 1944) and Durov (1948) diagrams. These methods are useful for visual inspection of hydrochemical data for identifying specific patterns and trends. The grouping of chemical analysis results using these methods helps in identifying hydrochemical facies and understanding the hydrogeological processes that influence the groundwater chemistry (Hiscock, 2005). Trilinear diagrams are one of the most commonly and extensively used methods in representing and interpreting groundwater quality trends (Back, 1960, 1961, 1966; Back & Hanshaw, 1965; Hanshaw et al., 1971; Rose, 2008; Zaporozec, 1972). These representations have contributed greatly to understanding and interpreting groundwater flow and quality trends. To assess the hydrogeochemistry of the groundwater from the study area, Piper diagram (Piper 1944) graphical representation method from AquaChem 3.7.42 (Calmbach, 1997) was used. The Piper diagram graphical

presentation shows the concentrations of individual groundwater samples that are plotted as percentages of the total cation and/or anion concentrations in meq/L, such that the samples with very different total ionic concentrations can occupy the same position in the diagrams. Seven ions namely  $\text{Ca}^{2+}$ ,  $\text{Mg}^{2+}$ ,  $\text{Na}^+$  plus  $\text{K}^+$ ,  $\text{Cl}^-$ ,  $\text{SO}_4^{2-}$  and  $\text{HCO}_3^-$  were used for this analysis. Such graphical presentation represents the relative abundance of the ions and is composed of two triangles and a diamond field. The two triangles used in this analysis represent meq percentages of three sets of components, totalling 100%. Typically, components of one triangle are cations ( $\text{Ca}^{2+}$ ,  $\text{Mg}^{2+}$  and  $\text{Na}^+$  plus  $\text{K}^+$ ) at each corner while components of the other are anions ( $\text{Cl}^-$ ,  $\text{SO}_4^{2-}$  and  $\text{HCO}_3^-$ ).

With such trilinear diagrams, groundwater samples that plot on a straight line within the central diamond field represent mixing of groundwaters between two end member solutions (e.g. Fresh and saline water). The results of the trilinear diagram graphical representation were compared with Cluster and Discriminant Analyses results to highlight the advantages and shortcomings of this method.

Major ion chemistry of the groundwater chemistry was analysed using scatter plot representations of the relationships that exist between the different groundwater constituents. The influence of rock-water interaction, evaporation and precipitation were determined using Gibbs (1970) plot. Gibbs (1970) reported that the presence of rock-water interaction in groundwater could be identified using TDS (mg/L) vs.  $\text{Na}^+$  / ( $\text{Na}^+$  +  $\text{Ca}^{2+}$ ) and TDS (mg/L) vs.  $\text{Cl}^-$  / ( $\text{Cl}^-$  +  $\text{HCO}_3^-$ ) scatter diagrams. The reactions between groundwater and the minerals of the aquifer it resides and flows through play significant role in its chemistry. These interactions characterize groundwater quality and its genesis (Cederstrom, 1946; Elango & Kannan, 2007).

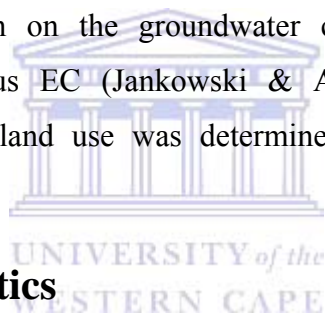
The dominance of carbonate and silicate weathering in rock water interaction was determined using  $\text{Ca}^{2+}$  +  $\text{Mg}^{2+}$  vs.  $\text{HCO}_3^-$  +  $\text{SO}_4^{2-}$  scatter plots (Datta & Tyagi, 1996). Based on the these results, the groundwater samples were further analysed for determination of the dominance of calcite and dolomite as the source of meq/L  $\text{Ca}^{2+}$  and  $\text{HCO}_3^-$  in carbonate weathering using  $\text{Ca}^{2+}$  versus  $\text{HCO}_3^-$  scatter plots as well as  $\text{Ca}^{2+}$  /  $\text{Mg}^{2+}$  molar ratio comparison. (Garrels & Mackenzie, 1971; Holland, 1978; Katz et al., 1997; Mayo & Loucks, 1995).

The sources of  $\text{SO}_4^{2-}$  were determined using  $\text{Ca}^{2+}$  vs.  $\text{SO}_4^{2-}$  scatter plots to determine the contribution of gypsum and/or anhydrite (Das & Kaur, 2001).

The influence of silicate weathering on the groundwater chemistry was determined using scatter plots that depict the relationships between  $\text{Na}^+\text{+K}^+$ ,  $\text{Ca}^{2+}\text{+Mg}^{2+}$  and Total Cations ( $\text{TZ}^+$ ) and the meq/L ratios of these cations to the total cations. (Das and Kaur, 2001; Stallard & Edmond, 1983).

The influence of ion exchange in the rock-water reactions was determined using scatter plots showing the relationships between  $\text{Na}^+\text{-Cl}^-$  and  $\text{Ca}^{2+}\text{+Mg}^{2+}\text{-HCO}_3^- \text{-SO}_4^{2-}$  showing the fixations and/or availability of the cations in solution (Fisher & Mullican, 1997). In conjunction with silicate weathering and ion exchange processes, the dissolution of halite ( $\text{NaCl}$ ) was analysed using  $\text{Na}^+$  vs.  $\text{Cl}^-$  scatter plot to determine its contribution to the  $\text{Na}^+$  concentration (Hem, 1985)

The influence of evaporation on the groundwater chemistry was determined by analysing  $\text{Na}^+\text{/Cl}^-$  ratio versus EC (Jankowski & Acworth, 1997) while surface contamination and effect of land use was determined using  $\text{Cl}^-$  vs.  $\text{SO}_4^{2-}$  scatter diagram.



#### 4. Multivariate statistics

Hem (1970) pointed out that conventional graphical analysis methods such as the trilinear diagrams (Piper, 1994) are limited to two dimensions in analysing and interpreting groundwater chemistry. Groundwater chemistry is a multivariate data involving many variables and multivariate statistical analysis is required for a comprehensive evaluation and interpretation to supplement the conventional methods. Many hidden phenomena and inherent complex groundwater chemistry can be expressed through these statistical methods without losing the original information (Cloutier et al., 2008).

There are numerous graphical methods for the classification and interpretation of hydrochemical data and each of them serves a purpose. Although the Piper (1944) diagram is extensively used throughout the literature, it suffers from some serious drawbacks, namely that percentages of various ions are considered and not the actual

concentrations of the dissolved solids. This shortcoming was overcome by the Durov (1948) double triangle diagram and the Schoeller (1977) diagram (Zaporozec, 1972). Nevertheless, Schoeller diagram method in itself has the problem that limited water analyses can be presented in the diagram while the Durov diagram suffers specific drawbacks and limited number of parameters can be considered (van Tonder & Hodgson, 1986).

Dalton and Upchurch (1978) showed that graphical interpretations (trilinear) of groundwater quality have certain limitations compared to multivariate statistical analysis. These limitations include:

- a) Finite number of variables (chemical constituents) that can be considered. In the case of Piper (1944) diagram only seven to eight variables ( $\text{Ca}^{2+}$ ,  $\text{Mg}^{2+}$ ,  $\text{Na}^{+}+\text{K}^{+}$ ,  $\text{Cl}^{-}$ ,  $\text{SO}_4^{2-}$  and  $\text{HCO}_3^{-}+\text{CO}_3^{2-}$ ) are used.
- b) The variables are generally limited by convention to major ions.  $\text{NO}_3^{-}$  for example is not used in trilinear diagrams.
- c) Spurious relationships may be introduced because of the closed-number computing system these methods use.
- d) In the case of trilinear diagram (Piper, 1944); percentages of the meq/L concentrations of the ions are used in comparison to the raw data concentrations (mg/L) which avoid inherent problems of the closed number system.

Multivariate statistical analysis has been successfully applied in a number of hydrogeochemical studies. Steinhorst & Williams (1985) used this technique in analysing groundwater chemistry data to identify groundwater sources. Several other studies have successfully applied multivariate statistics in hydrogeochemical investigations and interpretations, assessment of regional anthropological impact on groundwater compositions, identifying groundwater interaction with lithology and groundwater classification (Chen et al., 2007; Cloutier et al., 2008; Davis, 1986; Farnham et al., 2002; Lambrakis et al., 2004; Melloul & Collin, 1992; Schot & van der Wal, 1992; Usunoff & Guzmán-Guzmán, 1989; Van Tonder & Hodgson, 1986). These studies show that multivariate statistical analyses significantly help in classifying and

characterizing groundwater as well as identifying the hydrogeological processes that influence groundwater chemistry.

Factor analysis (FA), Cluster analysis (CA) and Discriminant analysis (DA) are typical multivariate data analyses that can be employed for groundwater characterization and classification. Multivariate data analysis involves sequential application of several statistical techniques. For example, cluster analysis (CA) uses unclassified data to reveal groups of observations, while discriminant analysis (DA) uses data matrix that is pre-classified into groups. Multivariate statistical analysis is therefore, a quantitative approach that allows one to classify groundwater samples, study the correlations between their chemical constituents, and evaluate the similarity between the observations sites (Cloutier et al., 2008).

In this section, the utility of multivariate data analysis statistical techniques in characterization and classification of the groundwater chemistry of the study area is demonstrated.

Multivariate statistical analysis of the groundwater samples were processed using factor, cluster and discriminant analysis in IBM® SPSS® Statistics 21 (IBM).

#### **4.1. Factor analysis**

As a multivariate statistical method, Factor Analysis (FA) yields the general relationship between variables, by showing multivariate patterns that may help to classify the original data. It enables the distribution of the resulting factors to be determined (Manly, 1994), and Liu et al., (2003) stated that the hydrogeological interpretation of factors yields insight into the main processes which may govern the distribution of hydrogeochemical variables. FA has been used in several hydrogeochemical studies to interpret groundwater mixing and quality assessments. Dalton and Upchurch (1978) used Factor Analysis to interpret the multiple mixing trends between sulphate and bicarbonate groundwater masses in comparison to single mixing trend observed using trilinear diagrams (Piper, 1994). Lawrence and Upchurch (1982) applied Factor Analysis for identification of recharge areas based on factors that represent different chemical processes in groundwater and their relative areal impact.

Love et al. (2004) used R-mode Factor Analysis to separate different probable sources of contamination in groundwater and used the factor distributions in recommending management interventions. Other studies used FA to classify groundwater facies based on chemical data and identification of groundwater contamination sources (Davis, 1973; Harmon, 1967; Love & Hallbauer, 1998; Olmez et al., 1994; Reghunath et al., 2002; Sneath & Sokal, 1973; Subbarao et al., 1995; Usunoff & Guzmán-Guzmán, 1989). These studies indicated that Factor Analysis could be used to classify groundwater facies in a similar manner to classical graphical techniques and provide an opportunity to investigate the spatial distribution of the water quality based on their factor classification.

The approach used in the thesis is similar to that of Boyacioglu et al. (2005). Factor analysis of the groundwater chemical data (EC, TDS, TH, TA,  $\text{Ca}^{2+}$ ,  $\text{Mg}^{2+}$ ,  $\text{Na}^+$ ,  $\text{K}^+$ ,  $\text{Cl}^-$ ,  $\text{SO}_4^{2-}$ ,  $\text{HCO}_3^-$  and  $\text{NO}_3^-$ ) was done to quantify the contributions of natural chemical weathering processes, ion exchange processes and anthropogenic effects of the measured ion concentrations and other chemical variables. These processes were used as the basis for the hypothesis that the variables considered could be reduced to these factors highlighting the range of natural chemical processes to anthropogenic effects.

In performing Factor Analysis, the first step undertaken was to compute a correlation matrix. This involved the correlation coefficient, which is a measure of interrelation, for all pairs of constituents as mentioned in section 2.2 of this chapter. The second step involved estimation of the factor loadings and the final step was obtaining easy interpretation of factors by factor rotation.

The principal component analysis method was used as the parameter estimation method to transform the set of observed interdependent variables into an orthogonal set of variables called principal components (Matalas & Reihner, 1967). The resulting principal components accounted for the variance of the observed variables in such a way that the first component accounted for as much as possible of the variance and the succeeding components accounted for the residual variance not accounted for by the preceding component in a similar manner.

The initial factor loadings obtained by principal component analysis are, commonly,

unlikely to reveal the underlying structure of the observed variables because of certain mathematical conditions, such as variance and properties of the principal component. To reveal this structure better, the common factor associated with the initial set of loadings were linearly transformed into a new set of common factors, associated with a new set of loadings, by factor rotation (Suk & Lee, 1999). Kaiser's scheme called Varimax rotation was used to yield a set of loadings such that the variance of the square of the loadings becomes the maximum. In this research, the factor scores were obtained using the regression method (Johnson & Wichern, 1992).

The question of "how many factors ought to be rotated" is a common question encountered during Factor Analysis. This question has been one of the criticisms of Factor Analysis (Rummel, 1988). Ideally, the number of factors would be dictated by theory but that is not the case in hydrogeological investigations. Hence, the data was allowed to determine the number of factors. One of the methods of selecting the number of factors is by using their eigenvalues. The common guideline is that only factors whose eigenvalues are greater than one are selected. Afifi and Clarke (1990) stated that this method yields roughly one factor for every 3 to 5 variables and appears to correctly estimate the number of factors if the communalities are high and the number of variables is not too large. Cattell (1978) argued that this method severely underestimates the number of factors in large matrices and promoted the use of the *Scree* method. This method involves creating a Scree plot against the eigenvalues and selecting the point where the slope changes as the cut-off point for determining the number of factors. The groundwater sample data used in the thesis is considered to be a small matrix ( $n = 49$  and 12 variables from each sample) and was found to have a simple structure with all the variables considered having moderate to high loadings on only one of the factors. Thus, the Scree plot produced the same number of factors as that of the eigenvalues ( $\geq 1$ ) based number of factors (Table 3.13).

Another important criticism of Factor Analysis as discussed by Rummel (1988) is that it is arbitrary (different investigators can arrive at different answers using the same data and technique). Nevertheless, Rummel (1988) argued that this is not the case with the commonly used component factor analysis model. He further clarified that a complete factor analysis of a data matrix is mathematically unique, meaning different

investigators using the same research design and factor technique on the same data must arrive, within computation error at the same results. Kline (1994) also argued that rotation to simple structure usually yields replicable factors. He explained that a matrix has simple structure when each variable has moderate to high loadings on only one or two factors and very low loadings on the other factors. Therefore, he concluded that in exploratory Factor Analysis, simple structure and factor replicability is the answer to the problem of indeterminacy and emphasized that an infinity solutions there may be, but the simple structure solution is best.

Factor scores are commonly obtained by two approaches: the weighted least squares method and the regression method. The latter was used in the thesis to compute the factor scores.

## **4.2. Cluster analysis**

Cluster Analysis (CA) is a method that provides a means of classifying a given set of variables into groups (clusters), based on similarity or closeness measures. The basic aim of CA is classifying variables like sampling sites or groundwater quality parameters into mutually exclusive groups based on their similarity or dissimilarity trend. According to Suk and Lee (1999), this method, in conjunction with standard geological and hydrogeological analyses, provides a consistent and reliable method for delineating physical and chemical trends in hydrogeological units. It distinguishes members of one group from the members of other groups and represents them in a graphical form called dendrogram, which makes the data interpretation easy and understandable. In CA, there is no prior knowledge about which sample belongs to which cluster. It must be noted that this technique does not provide any explanation by itself as to why the clusters exist but reveals association and structure in the data. These associations, though not previously evident, would be sensible and useful when discovered through CA. The grouping or clusters are defined through an analysis of the data. The classification approach used in the thesis is similar to that of Ragno et al. (2007), but used instead the Ward's method (Ward, 1963), which is described as the best performing hierarchical clustering as opposed to other clustering methods when dealing with hydrogeochemical data (Templ et al., 2008). The groundwater hydrochemical data were standardized

(mean of 1) prior to clustering, which allows one to compare different variables (e.g. EC and  $\text{Ca}^{2+}$ ) expressed in different units of measurement, and the Ward Linkage was used as the hierarchic agglomerative cluster algorithm. Ward's method (Ward, 1963) is an efficient linkage and uses an analysis of variance approach to evaluate the distances between clusters. In this technique, cluster membership is assessed by calculating the total sum of squared deviations from the mean of a cluster. The distance or similarity measure was performed by adopting the Squared Euclidean Distance (SED), which helps determine the optimum number of clusters. This measure of similarity is used more often, compared to simple Euclidean distance in order to place progressively greater weight on objects that are further apart.

Cluster Analysis has been used in several studies to characterize groundwater hydrochemical systems. Suk and Lee (1999) used Cluster Analysis in combination with factor score in characterizing groundwater hydrochemical system based on the dominant hydrochemical processes in their study area. The authors highlighted the use of factor scores compared to the hydrochemical data to avoid classification error due to data error (outliers) or multicollinearity. Colby (1993) also used Cluster Analysis as a means of objectively analysing a large number of physical and chemical variables simultaneously in order to identify distribution zones with similar physical or chemical hydrogeological characteristics. Van Tonder and Hodgson (1986) also used cluster analysis alongside discriminant, principal component and factor analysis to interpret hydrogeochemical facies.

Two sets of Cluster Analysis (Set A and Set B), in the present study, were performed using IBM® SPSS® Statistics 21 (IBM). The first set (Set A) used the same seven variables ( $\text{Ca}^{2+}$ ,  $\text{Mg}^{2+}$ ,  $\text{Na}^+\text{+K}^+$ ,  $\text{Cl}^-$ ,  $\text{SO}_4^{2-}$  and  $\text{HCO}_3^-$ ) that were used in the Piper (1994) graphical representation method (section 3 of this chapter). In the analysis of Set A variables, the same percentage meq concentrations of the variables were used to highlight the advantage of cluster analysis in grouping the groundwater samples in to specific hydrochemical facies. The results of this analysis were denoted with CA1, CA2... etc. for distinguishing them in the discussions chapter. The resulting groups from this analysis were compared with the hydrochemical facies interpreted from the classical hydrogeochemical interpretation using the trilinear diagram (Piper, 1944).

The second set of cluster analysis (Set B) used fourteen variables (EC, SAR, TDS, TH, TA, pH,  $\text{Ca}^{2+}$ ,  $\text{Mg}^{2+}$ ,  $\text{Na}^+$ ,  $\text{K}^+$ ,  $\text{Cl}^-$ ,  $\text{SO}_4^{2-}$ ,  $\text{HCO}_3^-$  and  $\text{NO}_3^-$ ). This set was analysed using the raw values and units of the variables and was performed in two steps. The first step classified the groundwater samples in to three groups and the results were denoted as CB1I, CB2I.....etc. Based on the results of the trilinear diagram (Piper, 1944) and major ion chemistry the first cluster containing about 73.5% of the groundwater samples (CB1I) was further classified. The results of the second analysis were then denoted as CB1II, CB2II.....etc.

The groundwater types created through Cluster Analysis were then verified and characterized using discriminant analysis. It should be noted that groundwater samples are grouped according to their similarities and their underlying hydrogeochemical structures. The combination of cluster and discriminant analyses depends upon grouping samples of the groundwater data through cluster analysis and later characterizing them using discriminant analyses (Siad, 1994).

### **4.3. Discriminant analysis**

Discriminant Analysis (DA) employs a set of methods to differentiate among groups in data and to assign new observations into the existing groups. It identifies the most significant parameters responsible for differentiating naturally occurring groups or clusters (minimum two) from a large dataset, and thus, brings about significant dimensionality or data reduction.

The groups (or clusters) provided from cluster analysis were incorporated as dependent variables with their respective hydrogeochemical data as independent variables into Discriminant Analysis (linear and stepwise). The main goal was to characterize these clusters by identifying the variables that discriminate between them and develop functions to compute new variables as a measure of the difference between them (Soldić-Aleksić, 2001). This technique used the Wilk's Lambda method of classification.

### 4.3.1. Linear discriminant analysis

Most hydrogeochemical variables are measured on a continuous ratio scale. However, their ultimate function for the investigator is as an aid to converting them to categorical variables, which may have as few as two values that can give meaning to the entire data set.

These problems can be dealt with by using Discriminant Analysis. This method is applied to situations where there are previously defined "training sets" representing classes, which differ, in some important, observable and important characteristic. From the multivariate observations that make up these training sets, a series of *discriminant functions* are derived, one per defined class. Solution of the functions for the data on a single sample yields a series of indices known as *discriminant scores*. The class whose discriminant score is highest is the one to which that sample would be assigned. The discriminant functions are defined as follows:

$$D_j = a_{j1}X_1 + a_{j2}X_2 \dots \dots \dots - t - a_{jp}X_p \quad \text{eq. 2.7}$$

Where  $X_1, X_2, \dots, X_p$  are the discriminant variables,  $a_{j1}, a_{j2} \dots a_{jp}$  are the discriminant function coefficients,  $D_j$ =the discriminant score of the projection through the data along which the populations show the greatest separation.

The method is useful in two-group situations where suitable training sets are available and it is necessary to discriminate and classify "potable" and "not potable" or "contaminated" and "uncontaminated" or "highly mineralised" and "less mineralised" samples as demonstrated by Clausen and Harpoth (1983), Siad (1994) and Siad et al. (1994), where these characteristics are not directly observable in routine samples. The method is also applicable where more than two groups are identified (for example, when multiple hydrochemical variables are present within dissolved constituents of the groundwater, which is the reality of groundwater chemistry).

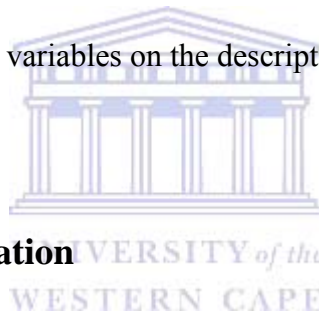
The use of discriminant analysis in the thesis is aimed at understanding the groundwater quality from boreholes located in different lithology and determines the effect of mineralisation and anthropogenic activities on selected boreholes from the study area.

### 4.3.2. Stepwise discriminant analysis

The quantitative and qualitative effect of the variables on the correct classification percentage of the total population and the individual groups was investigated in a stepwise discriminant analysis. When using the method, variables are selected through a statistical test to determine the order in which they are included (entered/removed) in the analysis. At each step, the element that yielded the best classification was entered. In this way, it was possible to test:

1. How many hydrochemical variables are necessary to describe the individual groups in the study area with a specific hydrochemical facies, and separate it from the others?
2. Which variables have the greatest and the smallest importance in the classification?
3. The effect of individual variables on the description of the individual groups.

## 5. Spatial analysis



### 5.1. Spatial data preparation

Data preparation was done using the ArcCatalog, ArcMap and the Spatial Analyst extension of ArcGIS 10.0 from ESRI<sup>®</sup>. Borehole point data was imported into ArcMap using the latitude and longitude coordinates captured using hand held GPS instrument in the field and projected using the WGS\_1984\_UTM\_Zone\_34S projected coordinate system. For the purpose of interpretation of borehole data and statistical analyses results of the variables, different maps were created using different sources and all of them were projected using the above-mentioned projected coordinate system with the WGS\_1984 datum.

The Water Management Areas (based on drainage region boundaries), Catchments-SA (Quaternary catchment boundaries for South Africa) and other vector data were acquired from the Water Resources of South Africa, 2005 study (WR2005) (Middleton & Bailey, 2008). The water management areas and quaternary catchments of the study

area were then extracted from these vector data. The Beaufort West 3222 raster map (GISCOE, 2005) and SRTM3 elevation data of the study area were used to create orthorectified geological map. The raster map of the study area was extracted using the boundaries of the Quaternary catchments that encompass the borehole locations.

Shuttle Radar Topography Mission (SRTM3) digital elevation model (DEM) for the study area was acquired from the U.S. Geological Survey's EROS Data Centre (USGS, 2013(b)). These SRTM3 data are distributed with data sampled at three arc-second intervals in latitude and longitude. The three arc-second data are generated by three by three averaging of the one arc-second samples. Data are divided into one by one degree latitude and longitude tiles in "geographic" projection that make a raster presentation with equal intervals of latitude and longitude in no projection at all but easy to manipulate and mosaic. The SRTM3 data have an extent of about 90 meters (USGS, 2013(a)).

The S33E022 and S33E023 height files with an extension \*.HGT from the SRTM3 were used for the study area. These files are signed two-byte integers and are in Motorola "big-endian" order. The heights are in meters referenced to the WGS84/EGM96 geoid and data voids are assigned the value -32768. The SRTM3 files contain 1201 lines and 1201 samples (USGS, 2013(a)).

The height files were then imported to Integrated Land and Water Information System software (ILWIS) to generate a raster map using the DEM Visualization tool. The results of this visualization (closhadow raster maps) were used in ArcMap 10 to create orthorectified geological raster image of the study area.

The resulting raster maps of the height files created in ILWIS were then converted into a mosaic raster in order to obtain a single DEM raster map of the study area.

The South African National Land Cover 2000 (nlc2000\_vs1.3) (Agricultural Research Council of South Africa) vector data was used for displaying local land cover and land use information of the study area. These vector files were analysed in ArcMap 10.0 and the area of interest was extracted using the boundaries of the quaternary catchments that encompass the groundwater sampling points. Some of the land cover attributes of these vector files were edited to simplify the display of legends created for land use maps.

## 5.2. Spatial data presentation

Data presentation was done using the Spatial Analyst Module of ArcGIS 10.0 from ESRI®.

Based on spatial distribution of the boreholes, univariate, bivariate and multivariate statistical analyses, different maps displaying cation and anion variables, factor score and other multivariate statistical analyses results against geology, quaternary catchments and land use were created for interpretation purposes.

The spatial distribution of the variables such as  $\text{Ca}^{2+}$ ,  $\text{Mg}^{2+}$ ,  $\text{Na}^+$ ,  $\text{K}^+$ ,  $\text{Cl}^-$ ,  $\text{SO}_4^{2-}$ ,  $\text{HCO}_3^-$ ,  $\text{NO}_3^-$  and TDS were displayed using Inverse Distance Weighted (IDW) interpolation method in ArcMap 10.0 to show the distribution of these variables and predict the values surrounding these measured variables. The factor scores and other multivariate statistical analyses results were also displayed using the same methodology based on the display objectives. The WHO (1993) recommended levels of the variables  $\text{Ca}^{2+}$ ,  $\text{Mg}^{2+}$ ,  $\text{Na}^+$ ,  $\text{K}^+$ ,  $\text{Cl}^-$ ,  $\text{SO}_4^{2-}$ ,  $\text{HCO}_3^-$ ,  $\text{NO}_3^-$  and TDS were displayed using reclassification method of the interpolated distributions of these variables.

IDW interpolation explicitly implements the assumption that things that are close to one another are more alike than those that are farther apart. This assumption is based on Tobler's First Law of Geography that states, "Everything is related to everything else, but near things are more related than distant things." This method was used to predict values for unmeasured locations in the study area by using the measured values closest to these locations.

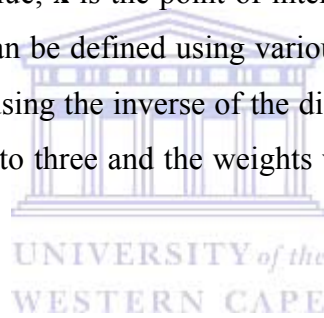
In Inverse Distance Weighted interpolation weights are computed by taking the inverse of distance from an observation's location to the location of the point being estimated. In this interpolation, the optimal power (p) was raised to three in order to model a cubed geometry that gives better interpolation compared to lower powers. This power controls the significance of surrounding points on the interpolated value where a higher power results in less influence from distant points and it is determined by minimizing the root mean square prediction error (RMSPE) through a statistical method known as cross-validation. The computed weights are proportional to the inverse distance ( $\lambda_i$ ) raised to

the power value  $p$ . A variable search radius with twelve nearest sample points and the default value of the map's diagonal extent length (in map units) was used to perform the interpolation. A polyline feature derived from the topography feature of the study area was used as a barrier to break or limit the search for input sample points beyond 900 m elevation excluding areas like the Nuweveld Mountains and above 900 m altitudes of some of the dolerite outcrops.

The interpolation uses equation 2.8 in measuring the unknown values from the known measurements.

$$z(x) = \sum_i w_i z_i + \sum_i w_i \quad \text{eq. 2.8}$$

Where  $z(x)$  is the unknown or unmeasured value;  $z_i$  is the known measurements;  $w_i$  is the weight of the measured value;  $x$  is the point of interest;  $i$  runs from 1 to  $n$  (number of data points). The weights can be defined using various methods and the option most employed is computing them using the inverse of the distance raised to a power. In this method, the power was raised to three and the weights were computed in ArcGIS as in equation 2.9.



$$w_i = 1 + d^3_i \quad \text{eq. 2.9}$$

Where  $d$  is the distance from  $x_i$  to  $x$ .

The southern part of the study area has large gaps in data since most of these properties were strictly prohibited from being accessed. For interpolation purposes, this situation is not ideal as it influences the accuracy of the interpolation in the southern areas. However, the areas in the south were included since they include extensive agricultural activities as well as uranium mining and exploration.

## Chapter III

### Results and Discussion

This section will discuss the results and discussion part based on the groundwater chemistry results, their hydrogeochemical and multivariate statistical analyses and will be describing the dominant hydrogeochemical processes in the fractured rock aquifer and their potential contribution to the overall groundwater quality of the study area.

A variety of chemical reactions between groundwater and the host rock take place during the water's movement along flow paths from the point of recharge to discharge areas. These reactions result in different concentrations of the groundwater constituents, which can be used to identify the intensity of the interaction and chemical reactions. Therefore, the conceptual approach the thesis follows, in discussing the results is, the investigation of the quantity and types of ions detected in the groundwater samples and infer their most likely sources.

#### 1. Univariate and bivariate statistics

Table 3.1 shows the minimum, maximum, mean and standard deviation values generated from the analysis of the 49 borehole samples. The range, mean and standard deviation values reveal considerable variations in the groundwater samples with respect to their chemical composition. The hydrochemical variables were analysed for the purpose of comparisons with different standards. Some of the standards used for the classification and comparison of the groundwater in the study area include:

- SAWQG (DWAf, 1996) Domestic water use
- WHO (1993) Guidelines for drinking water quality
- Davis and DeWiest (1996) Water classification based on TDS
- Freeze and Cherry (1979) Water classification based on TDS
- Sawyer and McCarty (1967) Water classification based on TH and
- US Salinity Laboratory Staff (1954) Salinity hazard classification based on EC

The pH of the groundwater samples is alkaline, ranges between 6.60 and 8.3 and meets the WHO (1993) and SAWQG (DWAF, 1996) drinking water criteria. According to SAWQG (DWAF, 1996) the mean pH of 7.51 is in the range of the Target Water Quality (6.0 to 9.0) and has no significant effects on health due to toxicity of dissolved metal ions and protonated species, or on taste is expected.  $\text{Ca}^{2+}$  and  $\text{Na}^+$  dominate the observed cation concentration with mean values of 139.86 mg/L and 159.69 mg/L, respectively and are noticeably higher than the SAWQG (DWAF, 1996) Target Water Quality concentrations. These ions represent 41.7% and 39.4% of the total major cations, respectively while  $\text{Mg}^{2+}$  represents 18% and  $\text{K}^+$  represents only 0.96% of the total cations (Table 3.2).  $\text{Cl}^-$  and  $\text{HCO}_3^-$  dominate the anion concentration with mean values of 224.88 mg/L and 393.59 mg/L respectively (Table 3.1). These ions represent 31.5% and 43.4% of the total major anions, respectively while  $\text{SO}_4^{2-}$  represents 22.2% and  $\text{NO}_3^-$  is only 3% of the total anions (Table 3.3). The  $\text{Cl}^-$  concentration is noticeably higher than the SAWQG (DWAF, 1996) target quality and renders the water in the study area to have a distinctly salty taste. As expected, the TDS values for 93.878% of the groundwater samples is above the SAWQG (DWAF, 1996) target water quality (Table 3.1). This dominance of some of the major ions is also reflected in the water type classification discussed in section 2 of this chapter. The standard deviations of the hydrochemical variables in general and  $\text{Cl}^-$  in particular indicates that the water in the study area is heterogeneous and reveals the influence of complex contamination sources and geochemical processes. This variation could be attributed to differences in salinity and ionic composition.

The groundwater samples were compared to the WHO (1993) drinking water guidelines as shown in Table 3.4. About 29% of the groundwater samples fall above the minimum WHO (1993)  $\text{Cl}^-$  limit of 250 mg/L. The high concentration will naturally affect the taste and palatability of the water and could cause corrosion.

**Table 3.1 Groundwater physical and chemical quality descriptive statistics\* with SAWQG (DWAf, 1996) Limits**

Variables	Minimum	Maximum	Mean	Std. Deviation	SAWQG (DWAf, 1996) (mg/L) Target Water Quality	Effect beyond target limit including mean values
pH	6.0	8.30	7.51	0.409	6.0 to 9.0	
EC	56.00	477.00	170.34	92.763	≤70	Consumption of water does not appear to produce adverse health in the short term.
TDS	424.00	3000.00	1202.34	614.299	≤450	Water has marked salty taste & would probably not be used on aesthetic grounds if alternative supplies were available.
TA	102.992	785.63	319.27	119.519	-	
TH	157.80	1733.843	514.49	304.343	-	
SAR	0.832	6.792	2.856	1.411	-	
Ca <sup>2+</sup>	45.90	392.50	139.86	73.557	≤32	No health effects, severe scaling problems & lathering of soap severely impaired.
Mg <sup>2+</sup>	2.60	205.48	40.20	32.846	≤30	No bitter taste, slight scaling problems may occur & no health effects.
Na <sup>+</sup>	47.41	390.80	159.69	90.949	≤100	Faintly salty taste, threshold for taste & no health effects.
K <sup>+</sup>	0.01	30.57	5.39	5.116	≤50	No aesthetic (bitter taste) or health effects.
HCO <sub>3</sub> <sup>-</sup>	125.60	950.81	393.59	149.039	-	
Cl <sup>-</sup>	35.20	1088.68	224.88	205.767	≤100	Water has a distinctly salty taste, but no health effects. Likelihood of noticeable increase in corrosion rates in domestic appliances.
SO <sub>4</sub> <sup>2-</sup>	14.89	954.48	211.31	184.538	≤200	Tendency to develop diarrhoea in sensitive and non-adapted individuals. Slight taste noticeable
NO <sub>3</sub> <sup>-</sup>	0.10	69.60	7.08	12.284	≤6	Rare instances of methaemoglobinaemia in infants; no effects in adults. Concentrations in this range are generally well tolerated.

\*N=49. All values are in mg/L except EC, in mS/m and pH (no units); - no standard available

**Table 3.2 Major cation mean concentrations percentages (meq/L)**

Cations	Na <sup>+</sup>	K <sup>+</sup>	Ca <sup>2+</sup>	Mg <sup>2+</sup>
% Mean	39.442	0.956	41.743	17.860

**Table 3.3 Major anions mean concentrations percentages (meq/L)**

Anions	NO <sub>3</sub> <sup>-</sup>	SO <sub>4</sub> <sup>2-</sup>	Cl <sup>-</sup>	HCO <sub>3</sub> <sup>-</sup>
% Mean	2.954	22.147	31.470	43.430

Most of the groundwater samples that showed high Cl<sup>-</sup> concentrations are situated on the calcrete deposits, near hard pans, dry watercourses and irrigation farms. Some of them are in close proximity with the wastewater treatment plant (Figure 3.2a). SO<sub>4</sub><sup>2-</sup> concentrations were also found to be higher than WHO (1993) levels for about 29% of the samples (Figure 3.2b).

**Table 3.4 Comparison of the groundwater samples from Beaufort West area with WHO (1993) drinking water standards**

Substance characteristic Essential characteristics	WHO (1993) recommended limit (mg/L)	Undesirable effect outside the desirable limit	No. of samples exceeding recommended value	% samples exceeding recommended value
TDS	1000	Beyond this palatability decreases and may cause gastro intestinal irritation	30	61.22
Ca <sup>2+</sup>	250	Encrustation in water supply structure and adverse effects on domestic use	3	6.12
Mg <sup>2+</sup>	100	Encrustation in water supply structure and adverse effects on domestic use	2	4.08
Na <sup>+</sup>	200		13	26.53
K <sup>+</sup>	12		3	6.12
Cl <sup>-</sup>	250	Beyond this limit, taste, corrosion and palatability are effected	14	28.57
SO <sub>4</sub> <sup>2-</sup>	250	Cause gastro intestinal irritation when Mg <sup>2+</sup> or Na <sup>+</sup> are present	14	28.57
NO <sub>3</sub> <sup>-</sup>	50		2	4.08

These groundwater samples are more or less the same samples as those that displayed high  $\text{Cl}^-$  concentrations except for the sample collected from the Tweeling borehole. High  $\text{SO}_4^{2-}$  concentrations in groundwater can cause gastro intestinal irritation when  $\text{Mg}^{2+}$  or  $\text{Na}^+$  is present.  $\text{Na}^+$  was the third ion that showed typically high concentrations compared to the WHO (1993) for about 27% of the groundwater samples. These samples coincide with the samples that showed high  $\text{Cl}^-$  concentrations except for one sample (Steenboki A), which is situated on the Teekloof formation (Figure 3.1c). Only 4.08% of the groundwater samples showed  $\text{NO}_3^-$  values above the WHO (1993) limit and these samples are located near irrigation farms (Figure 3.2c).

TDS values indicated that 61.22% of the groundwater samples (30 boreholes) are above the WHO (1993) desirable limit of 1000 mg/L (Table 3.4) and ranged between 424 and 3000 mg/L with mean and standard deviation of 1202.34 mg/L and 614.299 mg/L (Table 3.1), respectively. The spatial distribution of the cations, anions and TDS based on WHO (1993) limits are shown in Figures 3.1, 3.2 and 3.3 respectively using an Inverse Distance Weighted interpolation method.

According to Davis and Dewiest (1966) groundwater classification based on TDS (Table 3.5), only 8.2% of the groundwater in the study area is desirable for drinking while 30.6% of the groundwater samples indicate permissible TDS values. Furthermore, 61.2% of the groundwater in the study area is useful for irrigation purposes.

Freeze and Cherry (1979) classification based on TDS values (Table 3.6) shows that 38.8% of the groundwater is considered as fresh while 61.2% of the water is classified as brackish. This is consistent with Davis and DeWiest (1966) classification of the water that is useful for irrigation and WHO (1993) recommended limit (Figure 3.3). These high TDS concentrations are due to the presence of high  $\text{HCO}_3^-$ ,  $\text{SO}_4^{2-}$ ,  $\text{Cl}^-$ ,  $\text{Ca}^{2+}$  and  $\text{Na}^+$  as evidenced in Tables 3.1 to 3.4 as well as Figures 3.1 and 3.2. Jaine et al. (2003) indicated that groundwater containing such high concentration of TDS could cause gastrointestinal irritation. High values of TDS also influence the taste, hardness, and corrosive property of the water (Haran, 2002; Joseph & Jaiprakash, 2000; WHO, 1993).

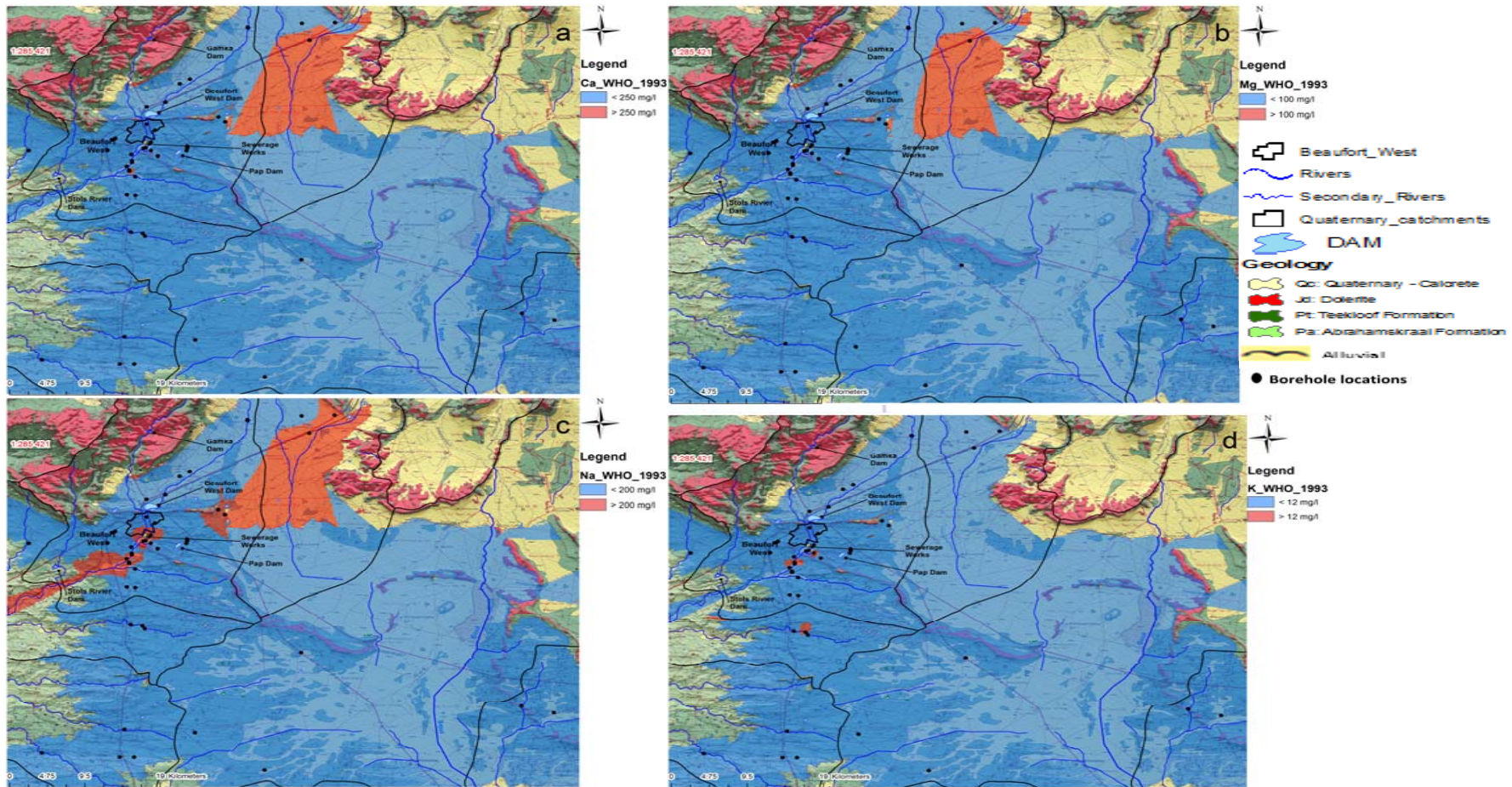


Figure 3.1 Cation (a) Ca<sup>2+</sup>, (b) Mg<sup>2+</sup>, (c) Na<sup>+</sup> and (d) K<sup>+</sup> concentration classification of the groundwater samples based on WHO (1993) drinking water guidelines: Inverse Distance Weighted Interpolation representation.

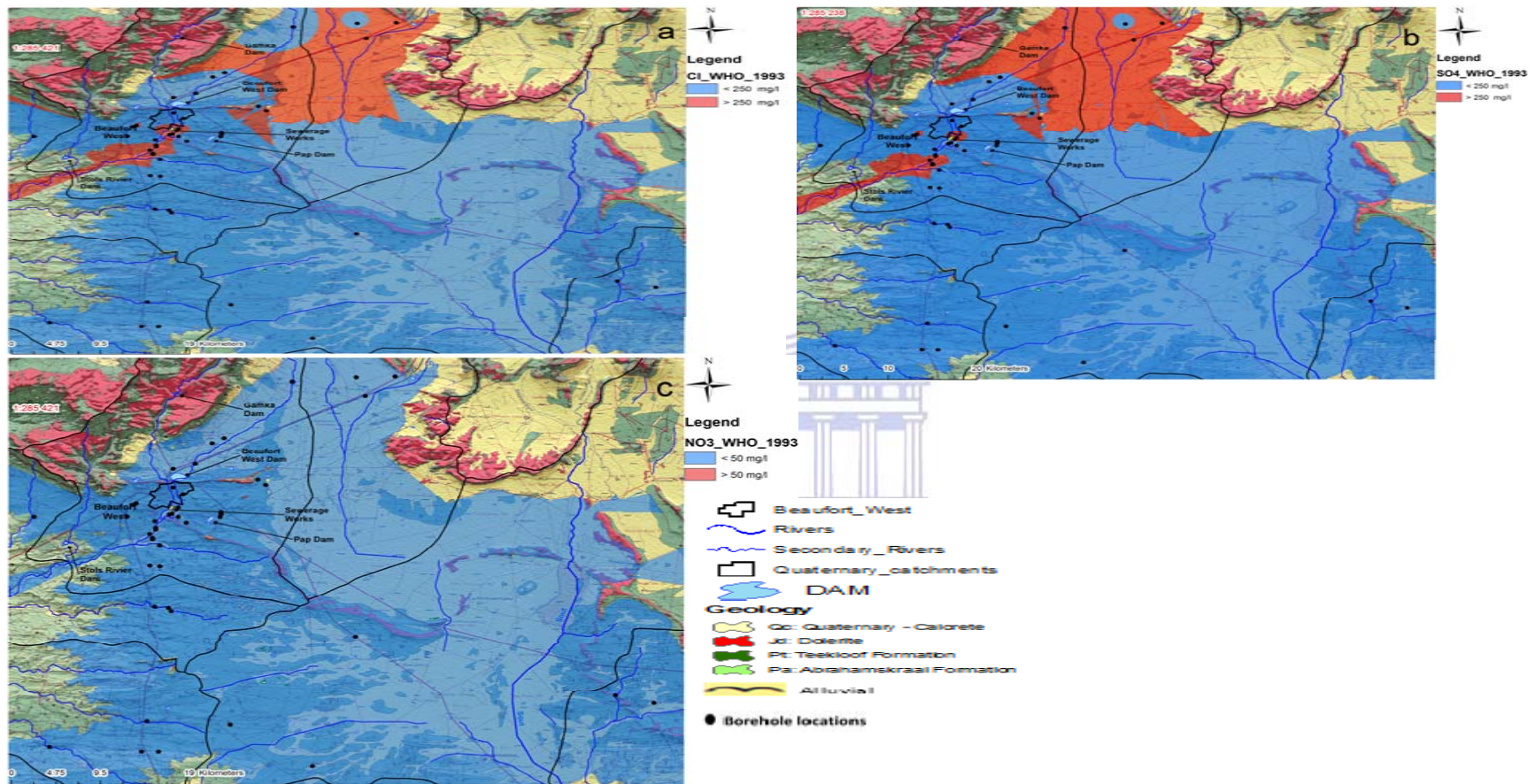


Figure 3.2 Anion (a) Cl<sup>-</sup>, (b) SO<sub>4</sub><sup>2-</sup> and (c) NO<sub>3</sub><sup>-</sup> concentration classification of the groundwater samples based on WHO (1993) drinking water guidelines: Inverse Distance Weighted Interpolation representation.

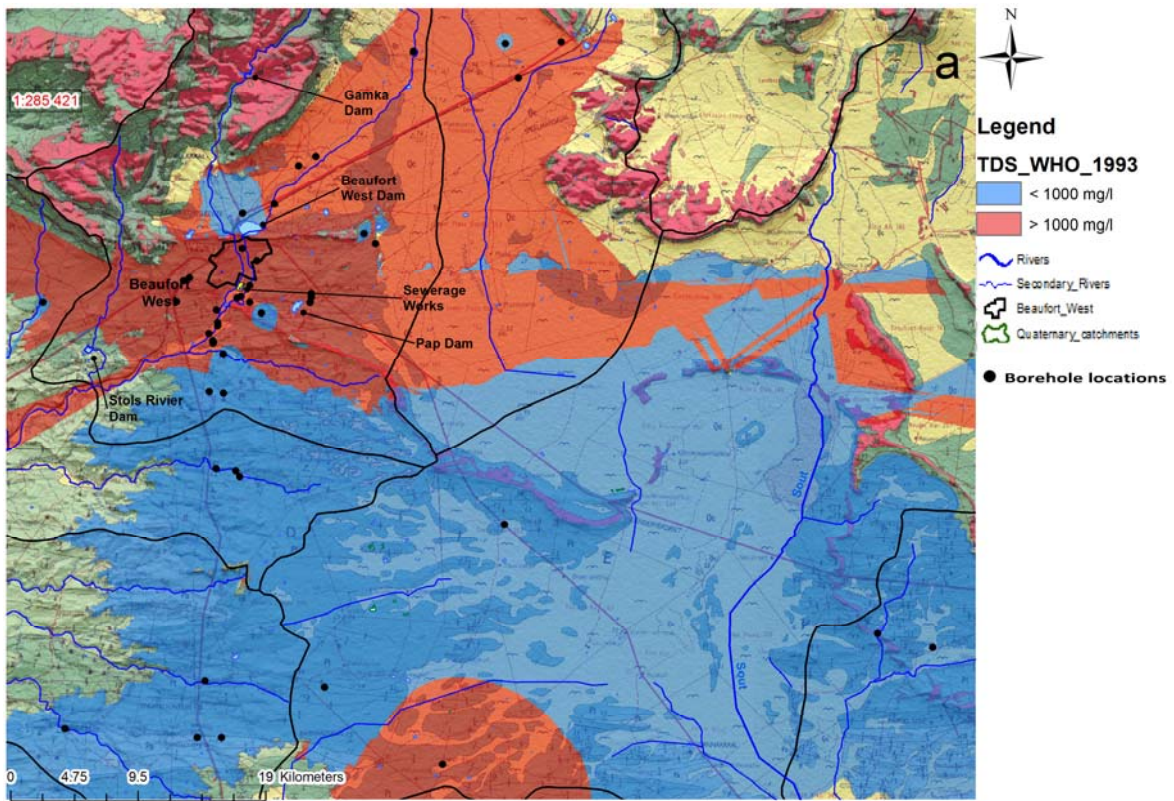


Figure 3.3 TDS level classification of the groundwater samples based on WHO (1993) drinking water guidelines.

Table 3.5 Classification of water based on TDS (Davis & DeWiest, 1966)

TDS (mg/L)	Class	No. of samples	% of samples
<500	Desirable water	4	8.2
500 - 1000	Permissible water	15	30.6
1000 - 3000	Useful for irrigation	30	61.2
>3000	Unfit for drinking and irrigation	0	0
Total		49	100

Table 3.6 Classification of water based on TDS (Freeze & Cherry, 1979)

TDS (mg/L)	Class	No. of samples	% of samples
<1000	Fresh water	19	38.8
1000 – 10,000	Brackish water	30	61.2
10,000 – 100,000	Saline water type	0	0
>100,000	Brine water	0	0
Total		49	100

Groundwater classification based on hardness value (Sawyer & McCarty, 1967) is given in Table 3.7. The hardness (TH) values ranged from 157.8 to 1733.843 mg/L with mean

and standard deviation of 514.49 mg/L and 304.343 mg/L (Table 3.1), respectively. Groundwater exceeding the limit of 300 mg/L is considered very hard (Sawyer and McCarty 1967) and accordingly all the groundwater samples are classified as hard to very hard type of water (Table 3.7), and will definitely require softening prior to domestic use although they are good for irrigation purposes (Table 3.9). The hardness is mostly due to the high TDS compared to  $\text{Ca}^{2+}$  and  $\text{Mg}^{2+}$  concentrations.

**Table 3.7 Classification of water based on hardness (Sawyer & McCarty, 1967)**

TH (mg/L)	Class	No. of samples	% of samples
0 – 75	Soft	0	0
75 – 150	Moderately hard	0	0
150 – 300	Hard	9	18.4
>300	Very hard	40	81.6
Total		49	100

The term salinity refers to the presence of the major dissolved inorganic solutes (essentially  $\text{Na}^+$ ,  $\text{Mg}^{2+}$ ,  $\text{Ca}^{2+}$ ,  $\text{K}^+$ ,  $\text{Cl}^-$ ,  $\text{SO}_4^{2-}$ ,  $\text{HCO}_3^-$ ,  $\text{NO}_3^-$  and  $\text{CO}_3^{2-}$ ) in aqueous samples. As applied to soils, it refers to the soluble and readily dissolvable salts in the soil or, operationally, in an aqueous extract of a soil sample. Salinity is quantified in terms of the total concentration of such soluble salts, or more practically, in terms of the EC of the solution, because the two are closely related (US Salinity Laboratory, 1954). The EC values of the groundwater samples varied between 56 and 477 mS/m, with a mean and standard deviation of 170.34 mS/m and 92.763 mS/m (Table 3.1), respectively. According to the US Salinity Laboratory (1954) standard, 81.6% of the groundwater samples have low while 18.4% have medium salinity hazard as shown in Table 3.8.

**Table 3.8 Classification of water based on EC (US salinity Laboratory, 1954)**

Salinity hazard	EC (mS/m) at 25°C	No. of samples	% of samples
Low	<250	40	81.6
Medium	250 - 750	9	18.4
High	750 - 2250	0	0
Very high	>2250	0	0
Total		49	100

Sodium concentration is one of the important parameters in the classification of groundwater for irrigation purpose. Soils containing a large proportion of  $\text{Na}^+$  with  $\text{HCO}_3^-$  as predominant anion are characterized alkali soils while soils with  $\text{Cl}^-$  or  $\text{SO}_4^{2-}$  as predominant anion are designated as saline soils, which affect plant growth (Todd & Mays, 2007). Sodium content in groundwater used for irrigation purpose is usually expressed in terms of  $\text{Na}^+$  percentage defined by equation 3.1.

$$\% \text{Na}^+ = \frac{(\text{Na}^+ + \text{K}^+)}{(\text{Ca}^{2+} + \text{Mg}^{2+} + \text{Na}^+ + \text{K}^+)} \quad \text{eq. 3.1}$$

Where all ionic concentrations are expressed in meq/L. Percentage sodium classification is presented in Table 3.9, which indicates that 97.96% of the groundwater samples are suitable for irrigation purposes.

**Table 3.9 Classification of water based on percentage  $\text{Na}^+$  (US salinity Laboratory, 1954)**

$\text{Na}^+$ (%)	Class	No. of samples	% of samples
<20	Excellent	0	0
20-40	Good	28	57.14
40-60	Permissible	20	40.82
60-80	Doubtful	1	2.04
>80	Unsuitable		
Total		49	100

The US Salinity Laboratory (1954) recommends Sodium Adsorption Ratio (SAR), which indicates the effect of relative cation concentration on sodium accumulation in the soil, as a more reliable method for determining this effect than sodium percentage. The Sodium Adsorption Ratio (SAR) is defined by equation 3.2.

$$\text{SAR} = \frac{\text{Na}^+}{\sqrt{(\text{Ca}^{2+} + \text{Mg}^{2+})}} + 2 \quad \text{eq. 3.2}$$

Where all ionic concentrations are expressed in meq/L. The US Salinity laboratory (1954) states that, low- $\text{Na}^+$  water (based on SAR value less than 10) can be used for irrigation on almost all soils with little danger of the development of harmful levels of exchangeable sodium. However,  $\text{Na}^+$  crops, such as stone-fruit trees and avocados, may

accumulate injurious concentrations of  $\text{Na}^+$ . The groundwater samples' SAR shows 2.856 and 1.411 mean and standard deviation values respectively (Table 3.1). The mean SAR is low and classification of the analysed groundwater for irrigation, based on SAR and EC (Table 3.8) indicated a low sodium alkali hazard and low to medium salinity hazard.

### 1.1. Correlation analysis

The degree of linear association between any two-groundwater quality parameters is measured by the correlation coefficient ( $r$ ) value. The Correlation matrix for the different groundwater quality parameters along with the significance level (2 tailed) is shown in Table 3.10. The significant correlation between EC and the other hydro-geochemical parameters is highly positive with the exception of  $\text{K}^+$ ,  $\text{HCO}_3^-$  and  $\text{NO}_3^-$ .

The  $r$  value between EC and TDS is 0.980, which means TDS is highly positively correlated with EC and can be predicted from EC with 96%. Additionally, the EC value of the groundwater samples has high positive correlation with  $\text{Cl}^-$ , TH,  $\text{SO}_4^{2-}$ ,  $\text{Mg}^{2+}$ ,  $\text{Ca}^{2+}$  and  $\text{Na}^+$  with relative positive coefficient  $r$  values of 0.952, 0.928, 0.924, 0.902, 0.875, and 0.858 respectively. Groundwater Samples that are strongly correlated (0.01 level of significance) are shown in bold (Table 3.10). These positive correlations between EC and some of the major ions indicate that an increase in these ions' concentrations would increase the EC value of the groundwater. The strong correlation of the major elements  $\text{Ca}^{2+}$ ,  $\text{Mg}^{2+}$ ,  $\text{Na}^+$ ,  $\text{Cl}^-$  and  $\text{SO}_4^{2-}$  with EC is an indication of the contribution of these elements to the salinity/hardness of the groundwater due to concentration of ions from evaporation of recharge water and groundwater interaction with the geological formations.  $\text{K}^+$  was found to be positively correlated (0.05 level) to pH and this could be attributed to the anthropogenic influence on the groundwater of the study area.

Table 3.10 also shows a strong positive correlation between TH and the cations  $\text{Ca}^{2+}$  and  $\text{Mg}^{2+}$ . This relationship is in line with fact that TH is determined based on these two cations. Naturally, the TDS values of the groundwater samples also show strong positive correlation with the major ions that constitute it in the groundwater solution.

Ca<sup>2+</sup> shows highly positive correlation with Mg<sup>2+</sup> compared to Na<sup>+</sup> and strong correlation with Cl<sup>-</sup> and SO<sub>4</sub><sup>2-</sup> compared to HCO<sub>3</sub><sup>-</sup>. This could be an indication of the source of Ca<sup>2+</sup> in the groundwater (e.g. calcite, dolomite, gypsum and silicates) due to its strong association with Mg<sup>2+</sup> and suggest the type of groundwater found in the study area (Ca-Mg-Cl-SO<sub>4</sub>) type of water.

**Table 3.10 Correlation matrix (Pearson) of the groundwater sample parameters (N= 49). All values are in mg/L unless indicated otherwise**

	pH <sup>b</sup>	EC <sup>a</sup>	SAR <sup>b</sup>	Ca <sup>2+</sup>	Mg <sup>2+</sup>	Na <sup>+</sup>	K <sup>+</sup>	HCO <sub>3</sub> <sup>-</sup>	Cl <sup>-</sup>	SO <sub>4</sub> <sup>2-</sup>	TDS	TA	TH	NO <sub>3</sub> <sup>-</sup>
pH <sup>b</sup>	1													
EC <sup>a</sup>	0.203	1												
SAR <sup>b</sup>	0.323*	<b>0.504</b>	1											
Ca <sup>2+</sup>	0.009	<b>0.875</b>	0.228	1										
Mg <sup>2+</sup>	0.121	<b>0.902</b>	0.274	<b>0.821</b>	1									
Na <sup>+</sup>	0.228	<b>0.858</b>	<b>0.706</b>	<b>0.657</b>	<b>0.631</b>	1								
K <sup>+</sup>	0.348*	0.064	0.063	-0.025	0.040	0.071	1							
HCO <sub>3</sub> <sup>-</sup>	0.035	0.251	0.218	0.051	0.085	<b>0.458</b>	0.013	1						
Cl <sup>-</sup>	0.149	<b>0.952</b>	<b>0.375</b>	<b>0.863</b>	<b>0.960</b>	<b>0.729</b>	0.071	0.076	1					
SO <sub>4</sub> <sup>2-</sup>	0.205	<b>0.924</b>	<b>0.494</b>	<b>0.842</b>	<b>0.857</b>	<b>0.766</b>	-0.010	0.036	<b>0.890</b>	1				
TDS	0.136	<b>0.980</b>	<b>0.532</b>	<b>0.838</b>	<b>0.864</b>	<b>0.891</b>	0.011	0.308*	<b>0.913</b>	<b>0.907</b>	1			
TA	0.011	0.235	0.168	0.060	0.078	<b>0.437</b>	0.014	<b>0.991</b>	0.066	0.012	0.288*	1		
TH	0.059	<b>0.928</b>	0.259	<b>0.968</b>	<b>0.939</b>	<b>0.676</b>	0.002	0.068	<b>0.946</b>	<b>0.888</b>	<b>0.889</b>	0.071	1	
NO <sub>3</sub> <sup>-</sup>	0.054	0.273	0.208	0.307*	0.240	0.241	-0.031	0.040	0.270	0.145	0.241	0.054	0.292*	1
<b>Bold.</b> Correlation is significant at the 0.01 level (2-tailed).														
* Correlation is significant at the 0.05 level (2-tailed).														
<sup>a</sup> mS/m														
<sup>b</sup> No units														

Na<sup>+</sup> showed strong positive correlation with Cl<sup>-</sup> and SO<sub>4</sub><sup>2-</sup> besides TDS compared to HCO<sub>3</sub><sup>-</sup>, which is an indication of the salinity found in some of the groundwater samples as discussed in the preceding section. The strong positive correlation between SO<sub>4</sub><sup>2-</sup> and Cl<sup>-</sup> could be an indication of surface contamination due to agricultural activities in the study area. The linear relationship between all the hydrochemical variables considered in this section is further discussed in the proceeding section.

## 1.2. Regression analysis

To clarify the linear relationships observed in the correlation analysis further, stepwise multiple linear regressions were performed using IBM<sup>®</sup> SPSS<sup>®</sup> Statistics 21 (IBM)

software. Most of the multiple linear regression model used in predicting EC, TDS, TH,  $\text{Ca}^{2+}$ ,  $\text{Mg}^{2+}$ ,  $\text{Na}^+$ ,  $\text{K}^+$ ,  $\text{HCO}_3^-$ ,  $\text{Cl}^-$  and  $\text{SO}_4^{2-}$  are presented in Tables 3.11 and 3.12. All the independent variables were noticed to have a significant effect ('t' test for the partial regression coefficients at 5% level of probability) on the corresponding dependent variables.  $\text{Ca}^{2+}$  followed by  $\text{Mg}^{2+}$  dominates the prediction of TH from the cations describing 100% of the observed TH in the groundwater samples of the study area (Table 3.11).  $\text{Ca}^{2+}$  alone predicts 93.6% of the TH. This trend is also observed with the anions where  $\text{Cl}^-$  alone predicts 89.5% of the TH while  $\text{SO}_4^{2-}$  predicts a mere 1% of the TH. It is also observed that the rest of the ions do not predict TH. This is an indication that the TH could be attributed to carbonate and silicate weathering and halite dissolutions in the groundwater resulting in a Ca-Mg-Cl type of water.

$\text{Mg}^{2+}$  followed by  $\text{Na}^+$  dominates the prediction of EC by the cations.  $\text{Mg}^{2+}$  alone gives 81.4% of the variability of EC (Table 3.11).  $\text{Na}^+$  explains 13.8% of the total 96.8% prediction of EC by the cations.  $\text{Cl}^-$  is the major predictor of EC from the anions considered. It predicts 90.6% of EC while  $\text{SO}_4^{2-}$  and  $\text{HCO}_3^-$  predict only 3.2% and 3.3% of EC respectively. These dominant predictions of EC by  $\text{Mg}^{2+}$ ,  $\text{Na}^+$  and  $\text{Cl}^-$  agree with classification of the groundwater of the study area as having low to medium salinity hazard (Table 3.8) and suitability of the water for irrigation (Table 3.9).

The multiple  $R^2$  value (0.941) indicates that 94.1% of the variability in TDS is ascribed to the combined effect of  $\text{Cl}^-$ ,  $\text{HCO}_3^-$  and  $\text{SO}_4^{2-}$  of which 83.4% was due to  $\text{Cl}^-$  alone (Table 3.11). On the other hand, 95.3% of the variability of TDS can be predicted with the combination  $\text{Na}^+$ ,  $\text{Mg}^{2+}$  and  $\text{Ca}^{2+}$  of which  $\text{Na}^+$  alone describes 79.4%.

The two dominant anions,  $\text{HCO}_3^-$  and  $\text{Cl}^-$ , in the groundwater samples are distinctly predicted by the cations  $\text{Na}^+$ ,  $\text{Mg}^{2+}$  and  $\text{Ca}^{2+}$ . The 32% of variability of  $\text{HCO}_3^-$  is attributed to the combined effect of  $\text{Na}^+$  and  $\text{Ca}^{2+}$  as shown in Table 3.12 while 95.4% of the variability of the observed  $\text{Cl}^-$  is ascribed to the combined effect of  $\text{Mg}^{2+}$ ,  $\text{Na}^+$  and  $\text{Ca}^{2+}$  whereby 92.1% was due to  $\text{Mg}^{2+}$  alone.

**Table 3.11 Multiple linear regression analysis result of TH, EC and TDS\***

	TH	%Total TH	EC	%Total EC	TDS	%Total TDS
Ca <sup>2+</sup>	93.6%	100%	1.6%	96.8%	0.8%	95.3%
Mg <sup>2+</sup>	6.4%		81.4%		15.1%	
Na <sup>+</sup>	-		13.8%		79.4%	
K <sup>+</sup>	-		-		-	
Cl <sup>-</sup>	89.5%	90.5%	90.6%	97.4%	83.4%	94.1%
SO <sub>4</sub> <sup>2-</sup>	1%		3.2%		5.0%	
HCO <sub>3</sub> <sup>-</sup>	-		3.3%		5.7%	
NO <sub>3</sub> <sup>-</sup>	-		0.3%		-	

\* All values are in mg/L except EC, in mS/m; - no prediction

**Table 3.12 Multiple linear regression analysis result of the ions\***

	Ca <sup>2+</sup>	Mg <sup>2+</sup>	Na <sup>+</sup>	K <sup>+</sup>	Total
Cl <sup>-</sup>	0.8%	92.1%	2.5%	-	95.4%
SO <sub>4</sub> <sup>2-</sup>	2.5%	73.5%	8.4%	-	84.4%
HCO <sub>3</sub> <sup>-</sup>	11%	-	21.0%	-	32.0%
NO <sub>3</sub> <sup>-</sup>	9.4%	-	-	-	9.4%

\* All values are in mg/L; - no prediction

In predicting SO<sub>4</sub><sup>2-</sup>, 84.4% of the variability could be ascribed to the combined effect of Mg<sup>2+</sup>, Na<sup>+</sup>, and Ca<sup>2+</sup> with Mg<sup>2+</sup> alone contributing 73.5% of the variability. It is also observed that Ca<sup>2+</sup> alone could predict 9.4% of NO<sub>3</sub><sup>-</sup>.

## 2. Hydrogeochemistry

Based on the percentage of the chemical constituents present, groundwater is classified into different types. These classifications of groundwater generally reflect the sources of the chemical constituents, i.e. rock water interaction and/or anthropogenic influence. Generally, Ca-HCO<sub>3</sub>, Ca-Mg-HCO<sub>3</sub>, Ca-Cl, Na-HCO<sub>3</sub>, Na-Cl, Ca-SO<sub>4</sub> and Na-SO<sub>4</sub> are the important groundwater types found throughout the world. The Piper (1994) diagram graphical presentation shows the concentrations of individual samples plotted as percentages of the total cation and/or anion concentrations, such that the samples with very different total ionic concentrations can occupy the same position in the diagrams. Such presentation formats represent the relative abundance of the ions. A piper trilinear diagram (Piper, 1944) used in the thesis generally classifies the groundwater samples as

in Figure 3.4. When the major source of the chemical constituents in groundwater is rock water interaction, the dissolution of calcite, dolomite, gypsum and halite will give rise to a Ca-HCO<sub>3</sub>, Ca-Mg-HCO<sub>3</sub>, Ca-SO<sub>4</sub>, and Na-Cl type of groundwater, respectively. In addition to dissolution of the above minerals, cation exchange processes can also result in Na-HCO<sub>3</sub>, Ca-Cl and Na-SO<sub>4</sub> groundwater types as shown in Figure 3.4.

As it is evident in Figure 3.4, most of the groundwater samples of the study area could not be clearly classified into one of the four-groundwater types. Most of the groundwater samples showed mixed type of groundwater ranging from Na-HCO<sub>3</sub> to Ca-Cl.

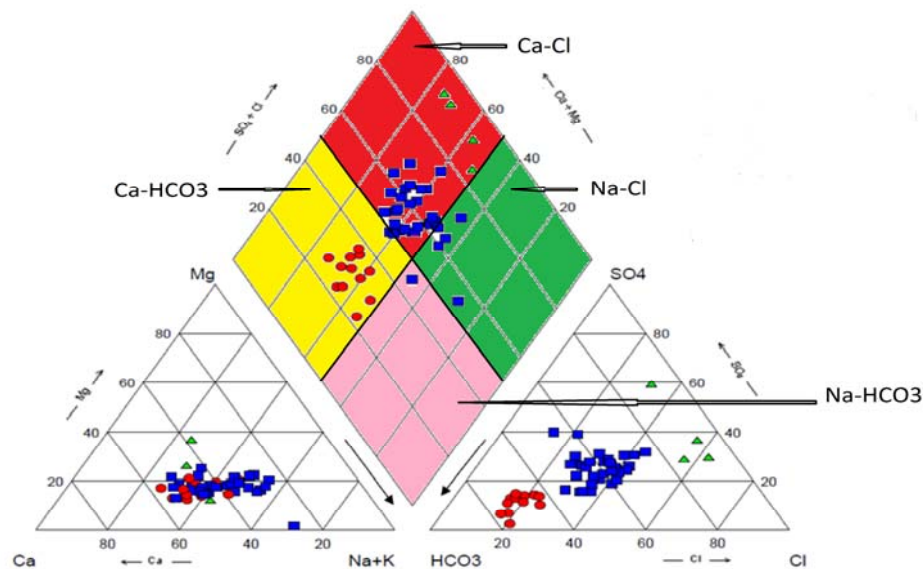


**Figure 3.4 General trilinear diagrammatic classifications of hydrochemical facies.**

Further classification based on the percentage meq/L concentrations of the ions considered resulted in three groundwater types based on the dominant cations and anions and are displayed in Figure 3.5. This classification produced three hydrochemical facies that are listed below:

1. Ca-HCO<sub>3</sub>
2. Ca-Na-Cl-HCO<sub>3</sub> (Mixed water)
3. Ca-Cl

The groundwater evolves from Ca-HCO<sub>3</sub> recharge water type to Ca-Cl through carbonate dissolution and ion exchange processes. The majority of the groundwater remains as mixed water between the two ends (Figure 3.5).

Most of the Ca-HCO<sub>3</sub> type water is situated near recharge areas such as the Nuweveld Mountains in the north, river downstream in the south and dolerite outcrops as can be seen in Figure 3.6. The boreholes in the north are mostly located near or on the calcrete deposits while the boreholes in the south of the study area are mainly on the lithofeldspathic sandstones of the Teekloof formation. The chemical composition of this water type is attributed to carbonate dissolution and reverse cation exchange process. The boreholes in the north of the study area mostly located in the Droerivier, Tweeling and Brandwag compartments. According to Rose (2008), the regional groundwater flow in the study area is from north to south (Figure 1.4) and this could explain the recharge composition of these boreholes.

The Ca-Na-Cl-HCO<sub>3</sub> (Mixed water) water type comprises most of the borehole samples in the study area (Figure 3.5 and Figure 3.6).

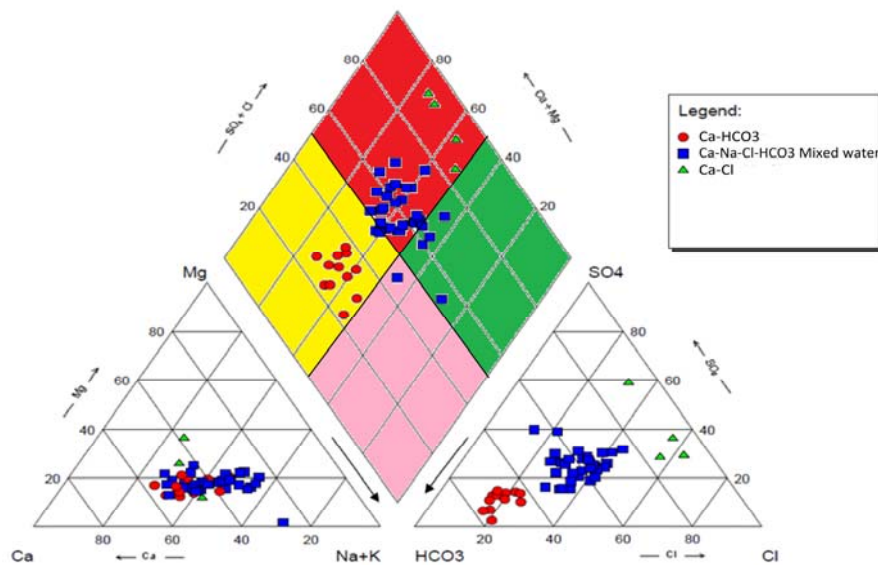


**Figure 3.5 Trilinear diagrammatic classifications of study area hydrochemical facies.**

High Ca<sup>2+</sup>, Na<sup>+</sup>, Cl<sup>-</sup> and HCO<sub>3</sub><sup>-</sup> and mixing of different waters along the groundwater flow path, characterizes this water type. The boreholes in this group are located in the

Droerivier, Hansrivier and Town compartments (Figure 1.4) in the north while the rest of them are in the southern part of the study area. This water type is distributed along calcrete deposits, dolerite intrusions and the lithofeldspathic sandstones of the Teekloof formation (Figure 3.6). The chemical composition of this water type is attributed to a combination of carbonate dissolution, silicate weathering, ion exchange and halite dissolution.

The Ca-Cl water type comprises only four boreholes (Figure 3.5). Most of them are situated in the Brandwag compartment, which is characterized by calcrete deposits (Figure 3.6) except for one borehole that is located in the Droerivier compartment (Figure 1.4) to the east of the Town dyke. The composition of this water type is attributed to carbonate and halite dissolution followed by ion exchange processes.

The descriptive statistics of the three water types determined using the trilinear diagrammatic representation (Piper, 1944) is shown in Table 3.13. The mixed Groundwater type, Ca-Na-Cl-HCO<sub>3</sub> is the dominant water type in the study area representing about 67.4% of the total sample, while groundwater type Ca-Cl is the least dominant representing only 8.2% of the total water type. The Ca-HCO<sub>3</sub> recharge water represents 24.5% of the groundwater in the study area. The Ca-Na-Cl-HCO<sub>3</sub> and Ca-Cl water types have mean TDS values above 1000 mg/L, indicating mineralised water-types in comparison to the less mineralised Ca-HCO<sub>3</sub> water-type. The high TDS attributes to abundance of carbonate/dolomitic, calcrete sediments and dolerite intrusions in the study area. The mean NO<sub>3</sub><sup>-</sup> concentrations of the Ca- Na-Cl- HCO<sub>3</sub> mixed water and Ca-Cl water-types are 7.386 and 13.06 mg/L respectively and are above the SAWQG (DWA, 1996) target water quality level of 6 mg/L (Table 3.13). These high levels can be associated with the agricultural activities in the study area. Elevated nitrate concentration can be also associated with recharge from precipitation and irrigation-carrying nitrogen compounds from soil into the aquifer.

Non-agricultural sources of nitrate in the study area would include municipal and industrial discharges containing nitrogen bearing effluent and atmospheric deposition.

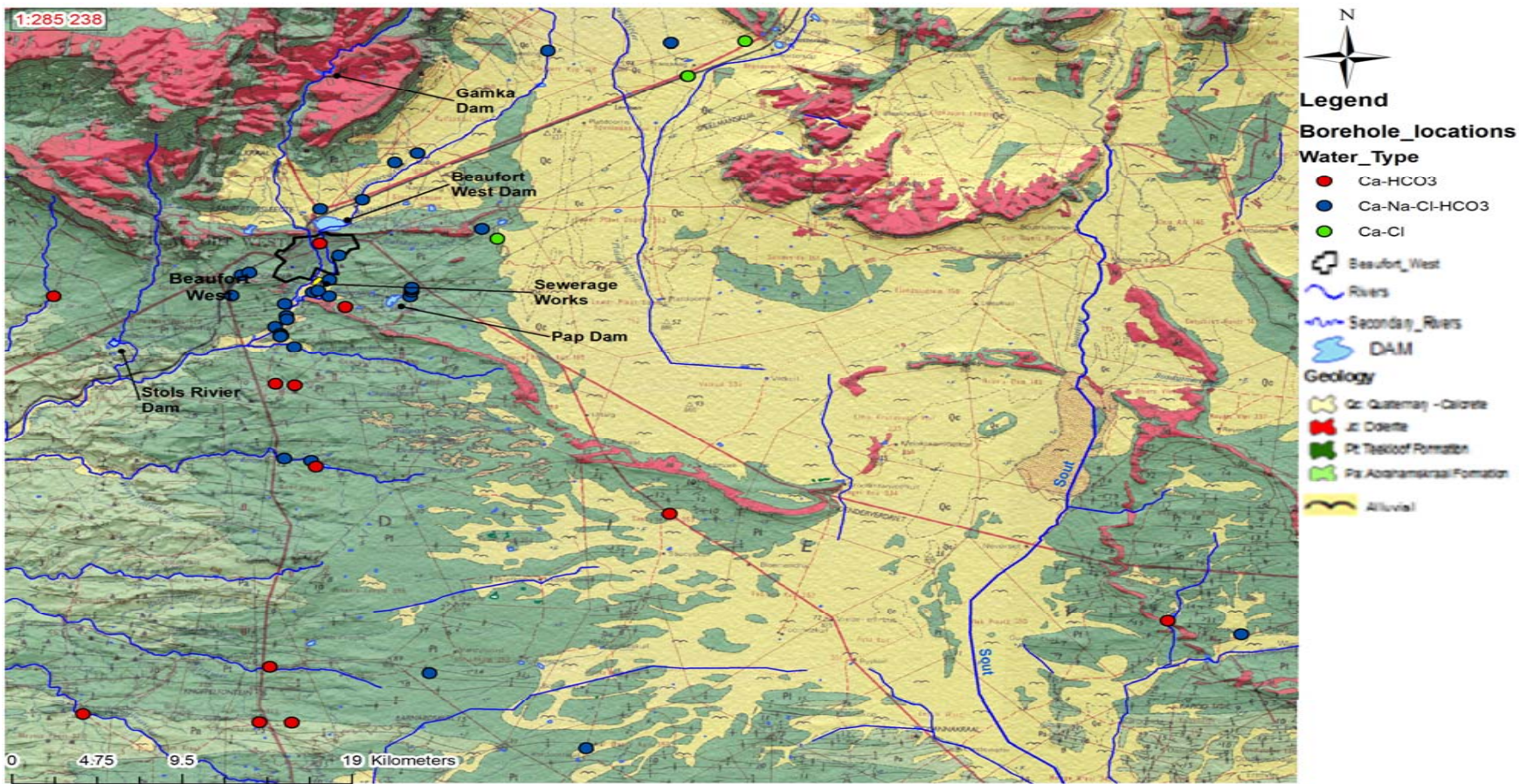


Figure 3.6 Spatial distribution of the different hydrochemical facies in the study area.

**Table 3.13 Descriptive statistics of the hydrochemical facies**

Parameters*	Ca-HCO <sub>3</sub> Recharge water N=12			Ca-Na-Cl-HCO <sub>3</sub> N=33			Ca-Cl Hard/Saline water N=4		
	Range	Mean	SD	Range	Mean	SD	Range	Mean	SD
pH	7.0-8.2	7.542	0.3397	6.6-8.3	7.485	0.448	7.3-7.9	7.675	0.263
EC	56-124	83.867	19.852	83.1-405	179.885	67.764	241-477	351	113.243
SAR	1.231-3.165	1.882	0.514	1.624-6.792	3.426	1.364	2.792-5.025	3.771	0.987
Ca <sup>2+</sup>	45.9-115.79	83.626	17.041	71.27-392.5	142.412	55.861	172.31-388.6	287.54	102.080
Mg <sup>2+</sup>	9.81-32.70	18.511	7.579	2.6-78.3	39.36	15.987	37-205.48	112.238	74.27
Na <sup>+</sup>	47.41-135.20	72.465	24.954	63.14-390.8	177.174	85.088	249.8-307.91	277.17	25.304
K <sup>+</sup>	0.01-9.72	4.499	2.746	0.5-30.57	5.852	5.965	2-6.67	4.265	2.107
HCO <sub>3</sub> <sup>-</sup>	246.5-627.80	368.94	116.105	251.1-950.81	425.436	150.313	125.6-260.29	204.808	62.187
Cl <sup>-</sup>	35.2-91.64	58.982	18.540	57.39-621.2	227.904	114.230	263.5-1088.68	697.568	359.018
SO <sub>4</sub> <sup>2-</sup>	14.89-65.00	42.896	14.342	84.55-607.0	220.98	111.107	390.82-954.48	636.825	237.773
NO <sub>3</sub> <sup>-</sup>	0.370-10.950	4.248	3.087	0.1-69.6	7.386	12.521	0.1-50.6	13.06	25.029
TDS	424-1011.9	636.625	149.4	449-2689	1273.182	494.828	1682.8-3000	2315.05	581.574
TA	202.13-514.796	302.531	92.206	205.902-785.63	343.703	120.352	102.992-213.438	167.942	50.994
TH	157.8-414.607	284.959	66.796	188.835-1302.28	517.406	190.727	723.392-1733.843	1179.024	527.239

\*All parameters are expressed in mg/L except pH, EC (mS/m) and SAR



Elango and Kannan (2007) described the chemical composition of groundwater as the imprints of the rock-water interaction and chemical processes. Thus, these imprints can be used to identify the rock-water interaction and other chemical processes. Because the study area experiences dry and semi-arid climatic conditions evaporation could also play important role in the groundwater chemistry. Gibbs (1970) reported that the presence of rock-water interaction in groundwater could be identified using TDS vs.  $\text{Na}^+ / (\text{Na}^+ + \text{Ca}^{2+})$  and TDS vs.  $\text{Cl}^- / (\text{Cl}^- + \text{HCO}_3^-)$  scatter diagrams. The Gibbs plot (1970) displays distribution of the samples and divides the curve into three sections where the centre of the curve indicates rock-water interaction while the top and bottom parts indicated evaporation precipitation processes respectively. Such diagrams provide comprehensive indication about the intensity of rock-water interaction.

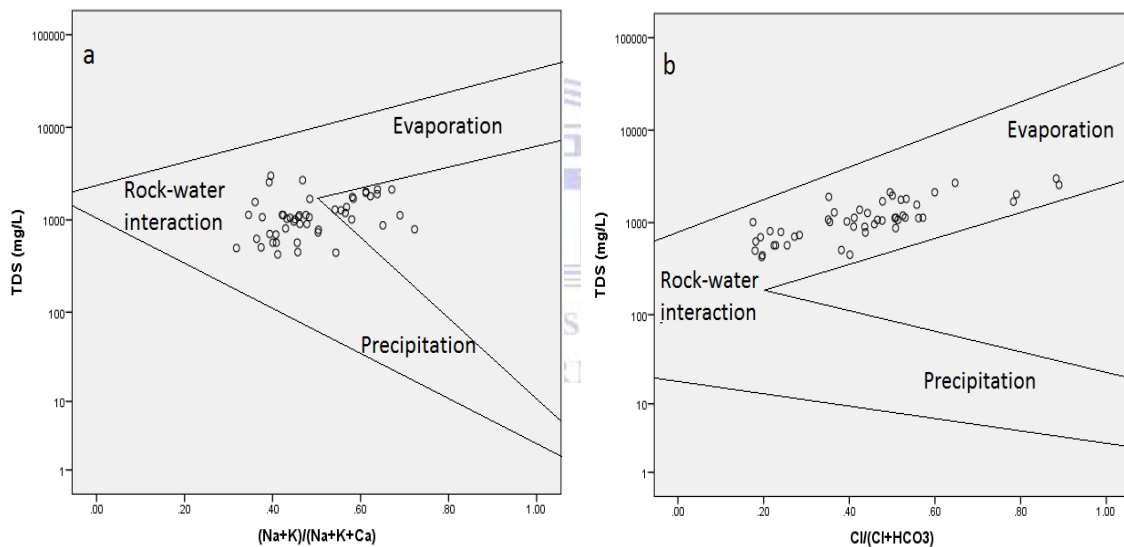


**Figure 3.8 Rock-water interaction diagrams (Gibbs, 1970).**

The Gibbs plot in Figures 3.8a and 3.8b clearly shows that rock-water interaction is the dominant source of the chemical constituents of the sampled groundwater with few samples plotting on the evaporation zone. This is an indication that the weathering of the host rocks is the primary factor that controls the hydrochemistry of the groundwater in the study area. Based on the general perspective gained from the Gibbs (1970) plot in Figures 3.8a and 3.8b, this section attempts to determine the source of the major ions using their concentrations and the mineralogy of the different rocks in the study area.

The groundwater samples have high  $\text{Ca}^{2+}$  and  $\text{HCO}_3^-$  concentrations (Tables 3.2 and 3.3) and a scatter plot of these ions in conjunction with their associated ions ( $\text{Mg}^{2+}$  and  $\text{SO}_4^{2-}$ ) is shown in Figures 3.9a, 3.9b and 3.9c.

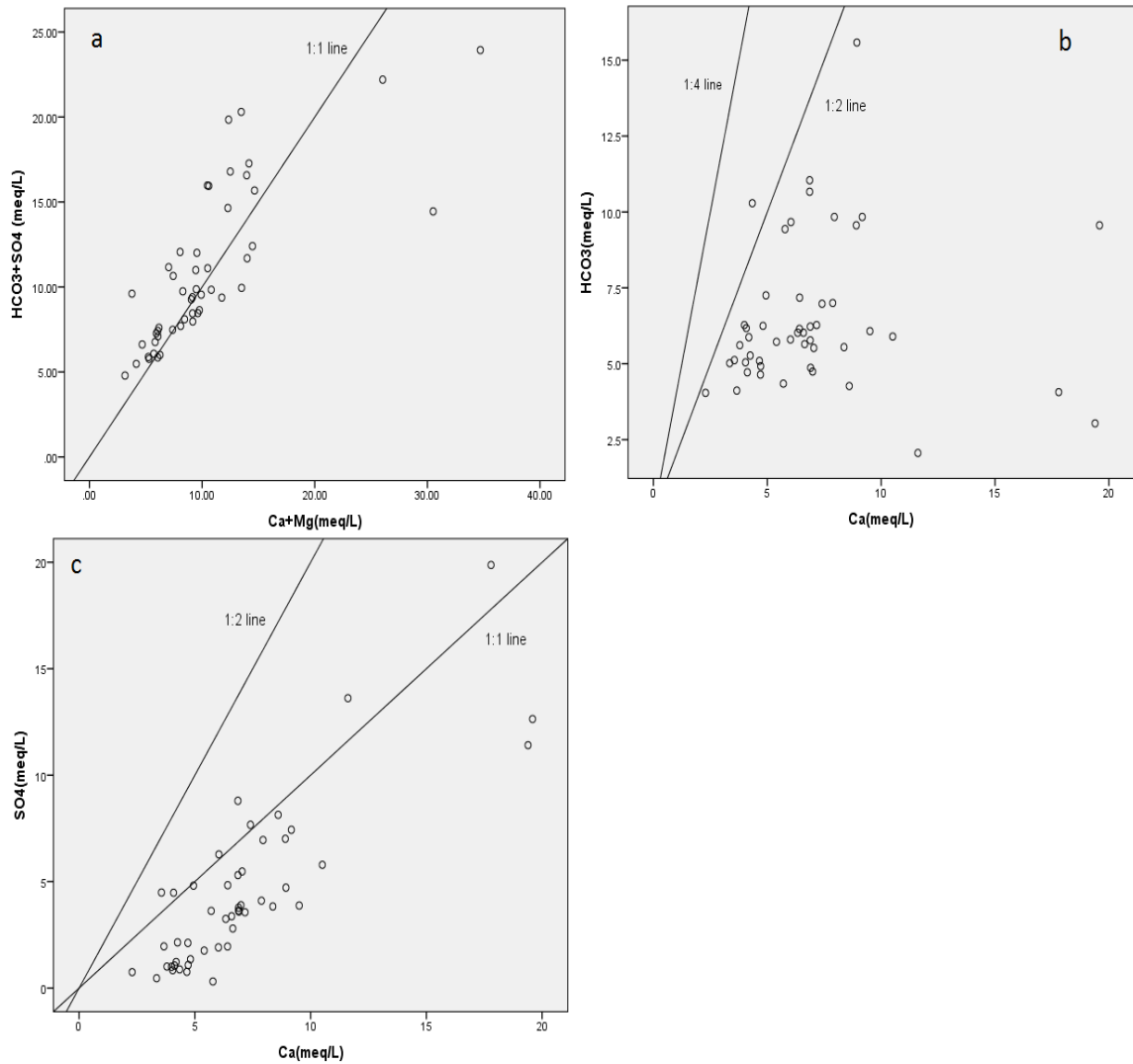


**Figure 3.9 Relationships between  $\text{Ca}^{2+}$ ,  $\text{Mg}^{2+}$ ,  $\text{SO}_4^{2-}$  and  $\text{HCO}_3^-$ .**

Datta and Tyagi (1996) explained that groundwater samples that fall above the equiline of the  $\text{Ca}^{2+} + \text{Mg}^{2+}$  vs.  $\text{HCO}_3^- + \text{SO}_4^{2-}$  scatter plot indicate dominant carbonate weathering while those that fall on the equiline of the indicate weathering of carbonates, sulphate minerals (gypsum or anhydrite) and silicates (Figure 3.9a). Furthermore, the authors indicate that groundwater samples that fall below the equiline showing excess  $\text{Ca}^{2+}$  and  $\text{Mg}^{2+}$  would normally be balanced by  $\text{HCO}_3^-$  alone if carbonate and silicate weathering

are the only source of these cations. Most of the groundwater samples plot on or very close to the equiline, suggesting that carbonate, sulphate minerals and silicates are the main source of these ions. The few samples (e.g. Nigrini Farm 2, RK1 and Steenrotsfontein 2) that plot below the equiline have high  $\text{Ca}^{2+} + \text{Mg}^{2+}$  concentrations that are not balanced by  $\text{HCO}_3^-$  which suggest that other processes such as ion exchange (reverse) could be the source of these cations.

In lithofeldspathic and carbonate, sandstones such as those of the study area calcite and/or dolomite and silicates would be the major source of dissolved  $\text{Ca}^{2+}$  and  $\text{HCO}_3^-$ . In the case of carbonate dissolution, when the equivalent  $\text{Ca}^{2+}$  to  $\text{HCO}_3^-$  ratio is 1:2 calcite is considered to be the sole source of these ions whereas dolomite would be their source when they have a 1:4 ratio as shown in Figure 3.9b (Garrels & Mackenzie, 1971; Holland, 1978). Some of the groundwater samples follow the 1:2 line and none of the samples follow the 1:4 line (Figure 3.9b). This indicates that calcite is the sole source of the carbonate weathering that contributes to these ions for those samples that follow the 1:2 line. The same three-groundwater samples, with very high  $\text{Ca}^{2+}$  concentrations that could not be balanced by  $\text{HCO}_3^-$  in Figure 3.9a, plot in the far right end of  $\text{Ca}^{2+}$ . This indicates that the  $\text{Ca}^{2+}$  in these samples comes from other geochemical processes such as plagioclase weathering besides calcite weathering.

Das and Kaur (2001) indicated that the dissolution of gypsum or anhydrite could be the source of dissolved  $\text{Ca}^{2+}$  and  $\text{SO}_4^{2-}$  in groundwater if their equivalent ratio is 1:1. Few of the groundwater samples in Figure 3.9c fall on the 1:1 line suggesting gypsum or anhydrite dissolution as the source of these ions. The rest of the groundwater samples show excess  $\text{Ca}^{2+}$  compared to  $\text{SO}_4^{2-}$  which indicate additional geochemical process contribute to the excess  $\text{Ca}^{2+}$  in solution. The few groundwater samples that show excess  $\text{SO}_4^{2-}$  over  $\text{Ca}^{2+}$  express the removal of the cation from solution through processes such as precipitation.

The distinction between the contribution of calcite and dolomite to  $\text{Ca}^{2+}$  and  $\text{Mg}^{2+}$  ions in solution can be identified by calculating the molar ratios of these cations. Mayo and Loucks (1995) explained that dissolution of dolomite occurs when the  $\text{Ca}^{2+}/\text{Mg}^{2+}$  molar ratio is 1:1 and a higher ratio would indicate that calcite dissolution has greater

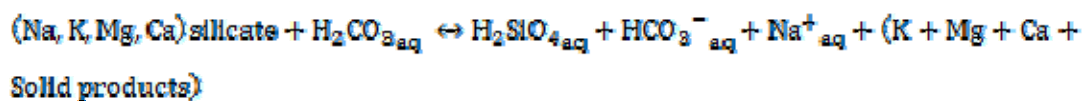
contribution. Katz et al. (1997) further illustrated that higher ratios (greater than 2) indicate silicate-weathering sources. About 65% of the groundwater samples clearly show a  $\text{Ca}^{2+}/\text{Mg}^{2+}$  ratio greater than 2 and the samples, in general, have a mean ratio of 2.7342 (Table 3.14). This designates the dissolution of calcite and silicate minerals as dominant geochemical processes.

**Table 3.14 Descriptive Statistics of  $\text{Ca}^{2+}/\text{Mg}^{2+}$  ratio**

Minimum	Maximum	Mean	Std. deviation	% of samples >2 ratio
1.05	16.62	2.7342	2.17890	65.31

Based on the results shown in Figures 3.9a 3.9b and 3.9c, it can be concluded that the dissolution calcite and silicate minerals followed by ion exchange are the dominant geochemical processes that determine the sources of these ions. To further clarify the influence of silicate weathering on the groundwater chemistry of the study area the relationships between  $\text{Na}^+ + \text{K}^+$ ,  $\text{Ca}^{2+} + \text{Mg}^{2+}$  and Total Cations ( $\text{TZ}^+$ ) is discussed below.

Das and Kaur (2001) explained that the solution products of silicate weathering are difficult to quantify because of the degradation of silicates is incongruent, generating a variety of solid phases (mostly clays) along with dissolved species. The authors depicted general silicate weathering of rocks with carbonic acid (due to the  $\text{HCO}_3^-$  dominance over  $\text{SO}_4^{2-}$  in the study area) as in equation 3.3 and stated that it can be understood by estimating the ratio between these cations and their total.



eq. 3.3

The relationship between  $\text{Na}^+ + \text{K}^+$  and  $\text{TZ}^+$  of the groundwater samples from the study area (Figure 3.10a) show that most of the samples plot along the  $\text{Na}^+ + \text{K}^+ = 0.5 * \text{TZ}^+$  line except for few samples. This relationship indicates the importance of silicate weathering (plagioclase and K-feldspars) in contributing towards the  $\text{Na}^+ + \text{K}^+$  and  $\text{Ca}^{2+}$  concentrations in the groundwater (Stallard & Edmond, 1983). The groundwater

samples that deviate from the  $\text{Na}^+ + \text{K}^+ = 0.5 \cdot \text{TZ}^+$  line have either high  $\text{Na}^+ + \text{K}^+$  (below the line, e.g. SR9 and Steenboki A) or low  $\text{Na}^+ + \text{K}^+$  (above the line, e.g. Nigrini Farm 2, RK1 and Steenrotsfontein 2) due to a possible  $\text{Ca}^{2+} / \text{Na}^+$  ion exchange process.

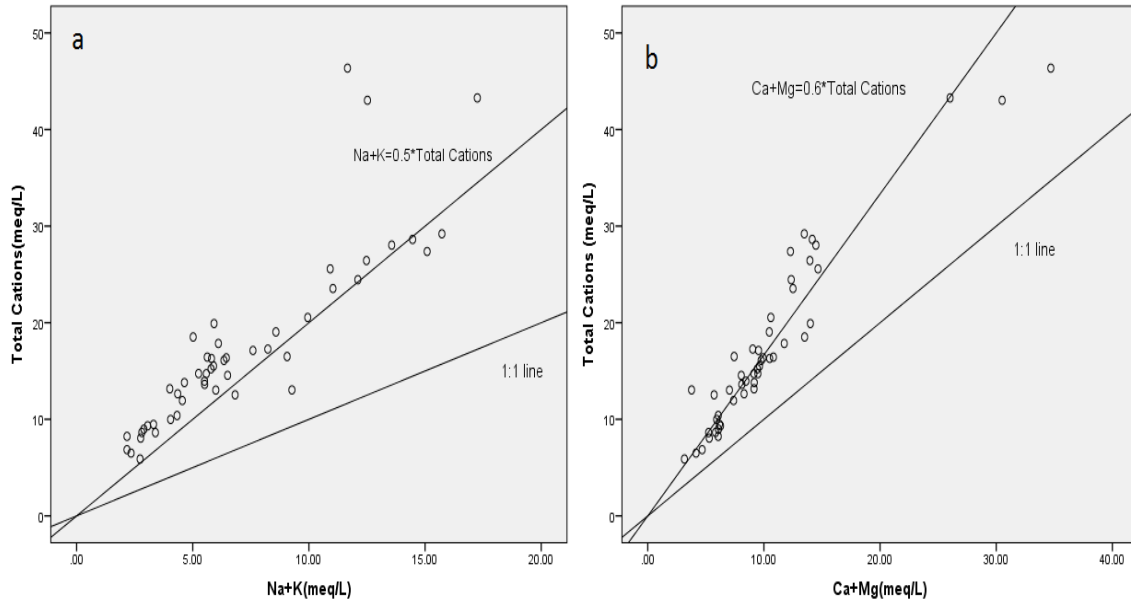


**Figure 3.10 Relationship between total cations,  $\text{Na}^+ + \text{K}^+$  and  $\text{Ca}^{2+} + \text{Mg}^{2+}$ .**

The average equivalent  $\text{Ca}^{2+} + \text{Mg}^{2+}$  to  $\text{HCO}_3^-$  (Table 3.15) and  $\text{Ca}^{2+} + \text{Mg}^{2+}$  to  $\text{TZ}^+$  ratio indicate that silicate weathering plays an important role besides carbonate dissolution.

**Table 3.15 Descriptive Statistics of equivalent  $\text{Ca}^{2+} + \text{Mg}^{2+}$  to  $\text{HCO}_3^-$  ratio**

Minimum	Maximum	Mean	Std. deviation
0.68	10.05	1.8636	1.834

The linear spread along the 0.6:1 line in Figure 3.10b indicates that the cations  $\text{Ca}^{2+}$  and  $\text{Mg}^{2+}$  in the groundwater could have resulted from silicate weathering. These results are in line with the presence of plagioclase and orthoclase in the immature sedimentary rocks of the study area.

**Table 3.16 Descriptive Statistics of equivalent  $\text{Ca}^{2+} + \text{Mg}^{2+}$  to  $\text{TZ}^+$  ratio**

Minimum	Maximum	Mean	Std. deviation
0.29	0.75	0.5961	0.08969

According to Fisher and Mullican (1997), a scatter diagram representing the relationship between  $\text{Na}^+ - \text{Cl}^-$  and  $\text{Ca}^{2+} + \text{Mg}^{2+} - \text{HCO}_3^- - \text{SO}_4^{2-}$  (Figure 3.11) shows a linear relationship with a negative slope when reverse ion exchange processes control the groundwater chemistry. Most of the groundwater samples in Figure 3.11 follow this line with a slope of  $-0.78$  ( $R^2=0.64$ ) indicating  $\text{Ca}^{2+}$  fixation and release of  $\text{Na}^+$  into solution resulting in a  $\text{Na-HCO}_3$  type of water (bottom right). Most of the groundwater samples that plot to the left of the  $\text{Na}^+ + \text{K}^+ - \text{Cl}^- = 0$  represent ion exchange process of  $\text{Na}^+$  fixation resulting in a  $\text{Ca-Cl}$  type of water.

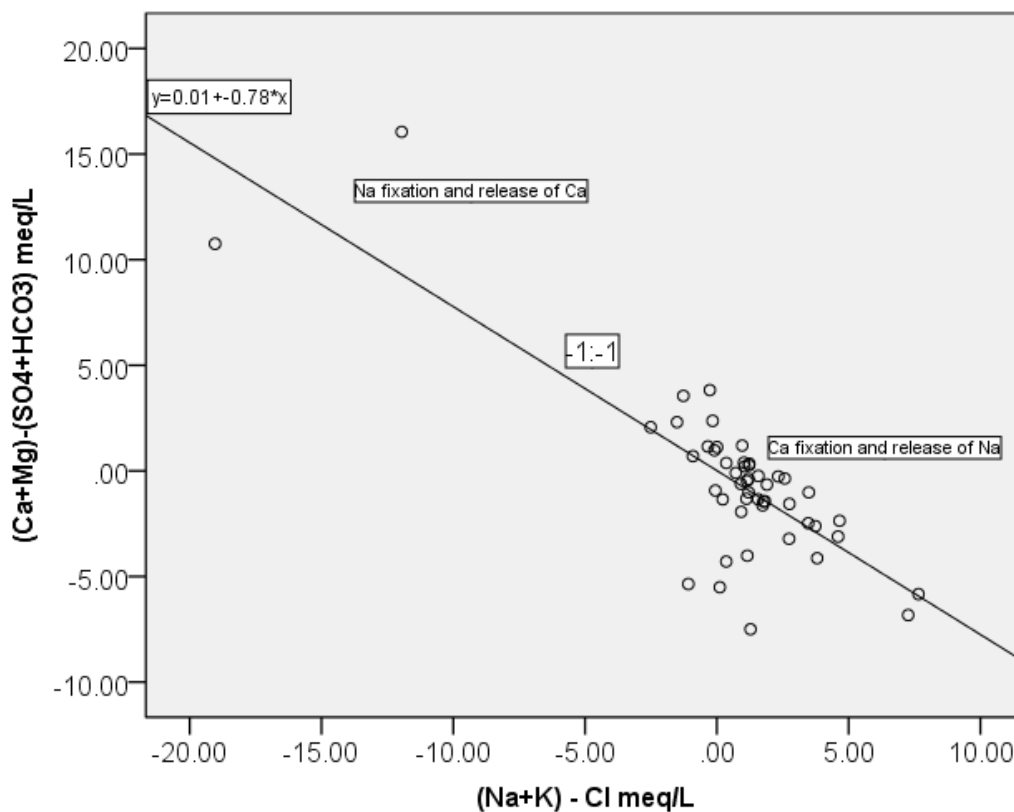


**Figure 3.11 Ion exchange scatter diagram.**

The dissolution of halite ( $\text{NaCl}$ ) is seen as a source of both sodium and chloride in ground water. A plot of  $\text{Na}^+$  vs.  $\text{Cl}^-$  is used to determine the influence of halite dissolution. Because sodium and chloride ions enter solution in equal quantity during the dissolution of halite, an approximately linear relationship may be observed between these ions (Hem, 1985).

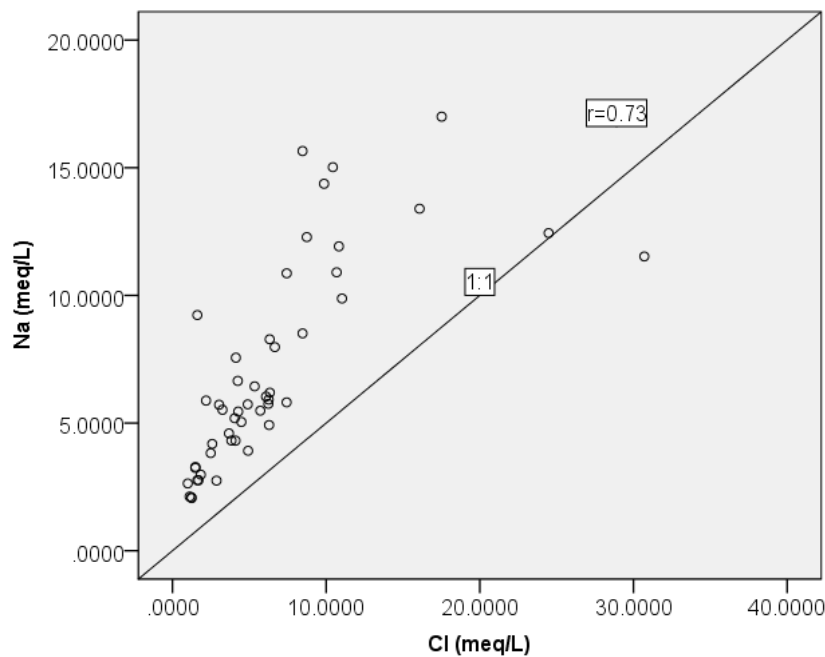


**Figure 3.12 Relationships between Na<sup>+</sup> and Cl<sup>-</sup>.**

A Na<sup>+</sup> vs. Cl<sup>-</sup> scatter plot with a slope equal to one should describe this linear relationship. However, the groundwater samples from the study area do not show this linear relationship (Figure 3.12). This indicates that the Na<sup>+</sup> and Cl<sup>-</sup> concentrations of the ground water of the study area are heavily influenced by factors other than the dissolution of halite. Most of the groundwater samples from the study area plot above the 1:1 line, thus indicating the source of Na<sup>+</sup> could be mainly silicate weathering and not halite dissolution. There is no parallel enrichment of the ions, suggesting that the source of both the ions is not due to dissolution of chloride salts.

The Gibbs plot (Figures 3.8a and b) shows that there is some influence of evaporation on the groundwater chemistry besides the dominant rock-water interaction processes discussed previously. Evaporation is a common process in surface and ground waters of semi-arid areas. Although evaporation process in groundwater increases TDS concentration, Na<sup>+</sup>/Cl<sup>-</sup> ratio in solution remains the same and this ratio could be used to indicate this process. Jankowski and Acworth (1997) explained that a scatter plot that shows constant Na<sup>+</sup>/Cl<sup>-</sup> ratio as the EC of the groundwater increases determines the dominance of evaporation processes. The trend line in Figure 3.13 shows a decrease in Na<sup>+</sup>/Cl<sup>-</sup> with an increase in EC for almost all the groundwater samples except for few.

This trend suggests that evaporation is not a dominant process compared to the above discussed rock-water interaction process.

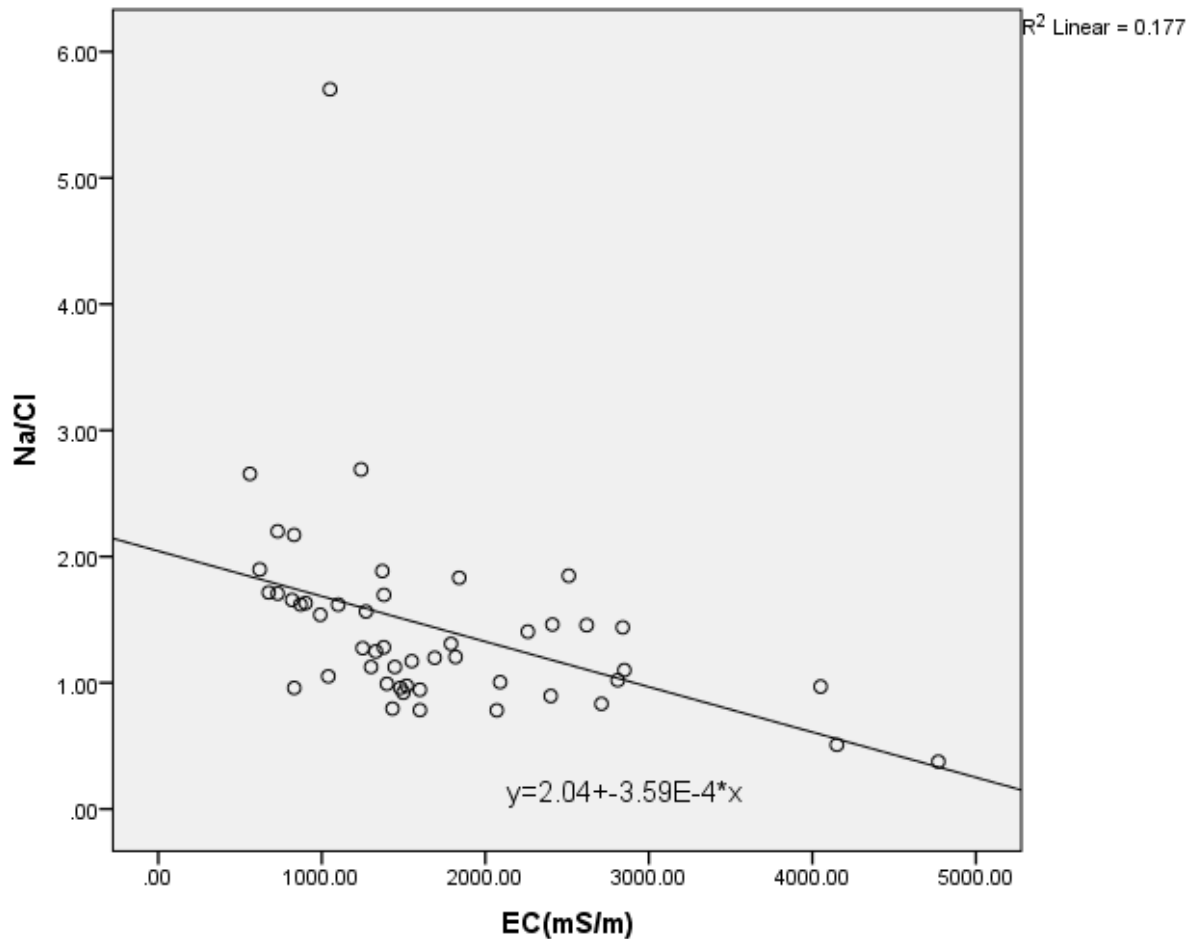


**Figure 3.13 Relationships between EC and Na<sup>+</sup>/Cl<sup>-</sup>.**

Finally, the effect of land use on groundwater chemistry can be explained by Cl<sup>-</sup> vs. SO<sub>4</sub><sup>2+</sup> scatter diagram. The groundwater in the study area is extensively used for stock watering and irrigation besides domestic and municipal uses and contamination from these anthropogenic activities is expected to influence the groundwater chemistry. Figure 3.14 shows a strong correlation between Cl<sup>-</sup> and SO<sub>4</sub><sup>2-</sup> of the groundwater samples with R<sup>2</sup>=0.792. This strong correlation suggests the effect of surface contamination besides rock-water interaction due to anthropogenic activities.

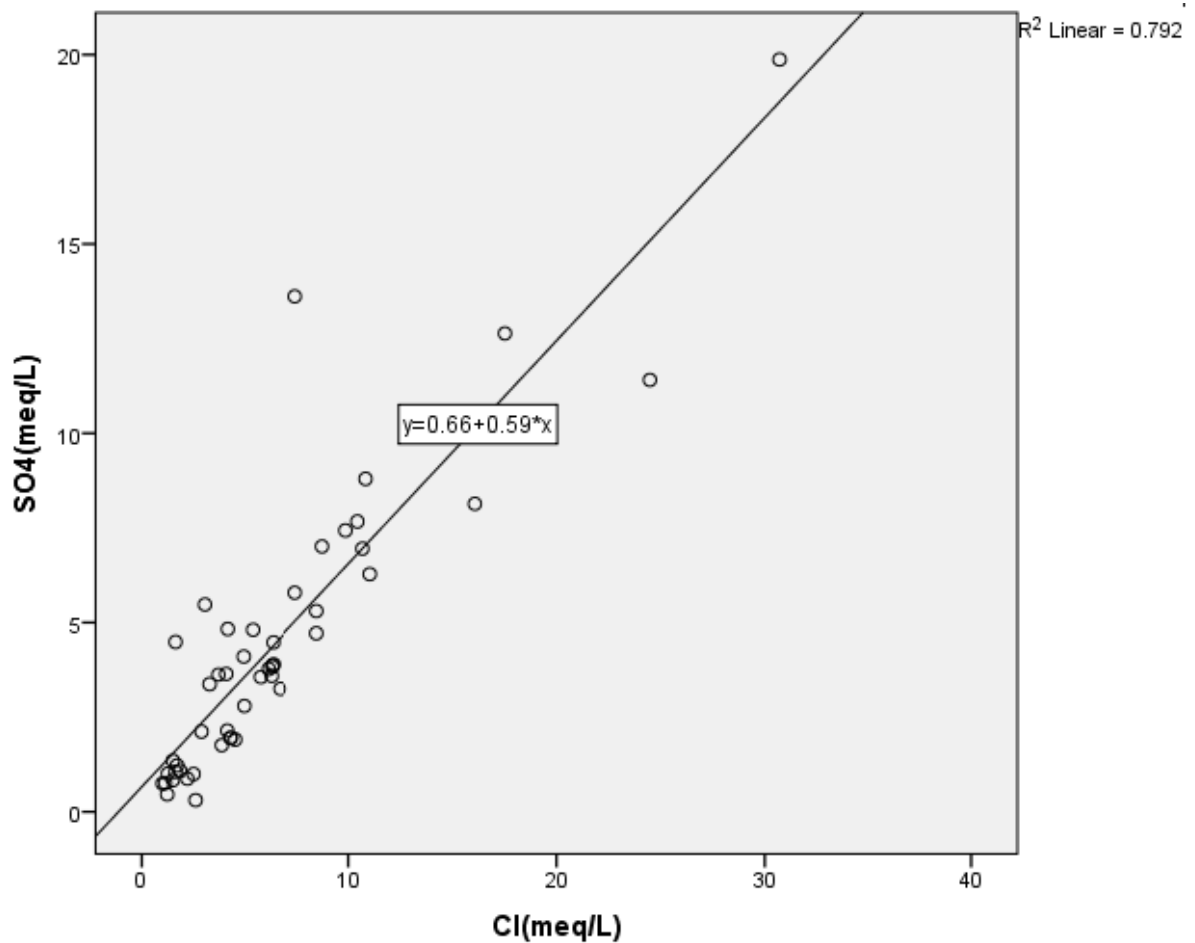


Figure 3.14 Effect of land use on groundwater chemistry.

## 2.2. Spatial distribution of ions

The spatial distribution of the major ions  $\text{Ca}^{2+}$ ,  $\text{Mg}^{2+}$ ,  $\text{Na}^+$ ,  $\text{Cl}^-$  and  $\text{SO}_4^{2-}$  in the study area (Figures 3.15 and 3.16) show higher concentrations on the alluvial sedimentary (calcrete) deposit compared to the lithofeldspathic sandstone of the Teekloof formation (northern part of the study area). This trend is also observed on the southern part of the study area where the calcareous deposition is thinner and combined with Teekloof formation. These higher concentrations are attributed to calcite dissolution, silicate weathering, ion exchange, evaporation processes and surface contamination (the northern part of the study area) as discussed in section 2.1 of this chapter.

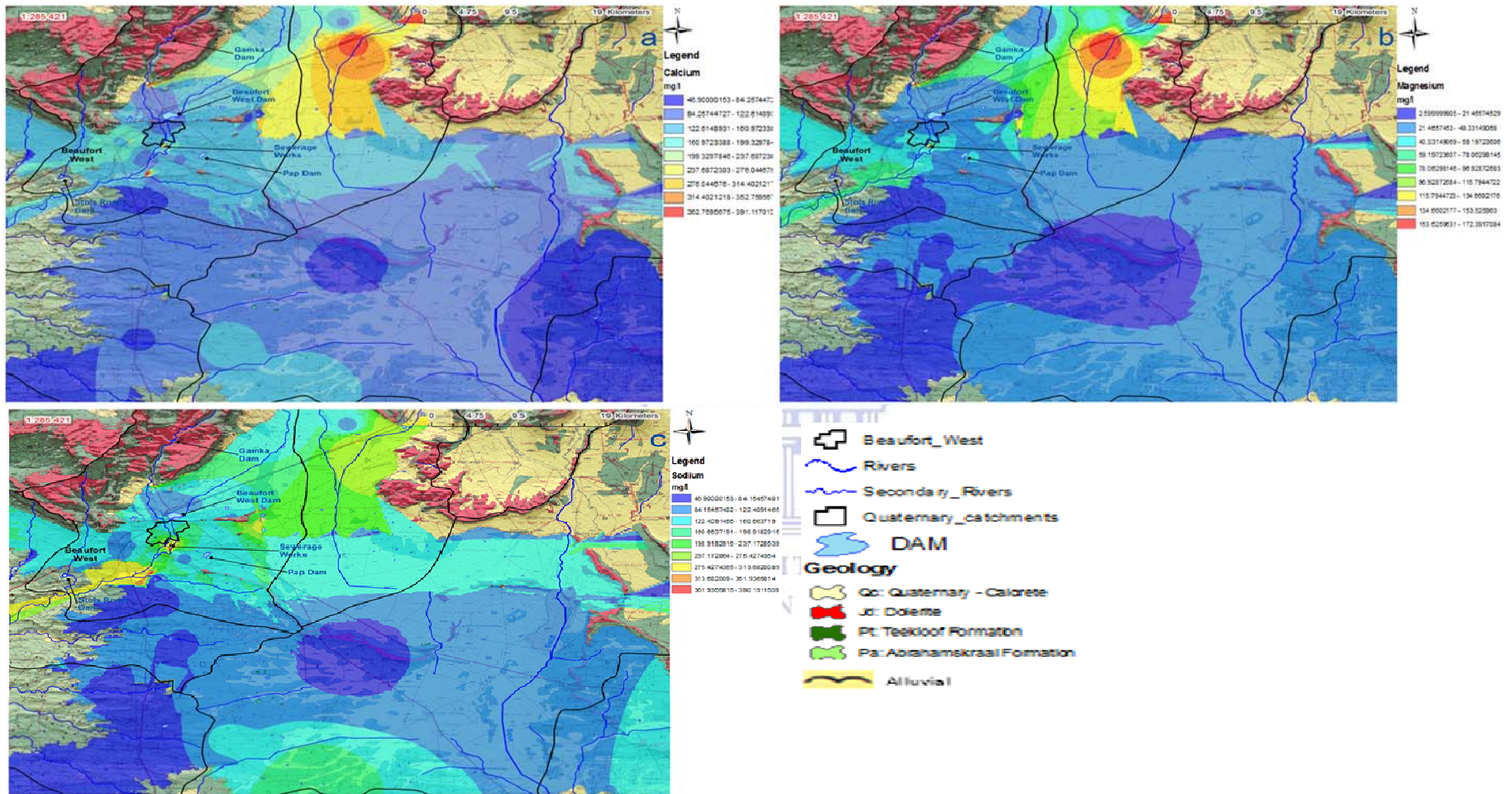


Figure 3.15 Spatial distribution of major ions (a)  $\text{Ca}^{2+}$ , (b)  $\text{Mg}^{2+}$  and (c)  $\text{Na}^+$  against catchment and lithological background: Inverse Distance Weighted Interpolation representation.

The concentration of these major ions is also higher on the Teekloof formation where there is a contact with dolerite intrusions around the town of Beaufort West. The dolerite intrusions increase the major ion ( $\text{Ca}^{2+}$ ,  $\text{Mg}^{2+}$  and  $\text{Na}^+$ ) concentrations in the groundwater through their contribution to silicate weathering. Lower concentration of the above mentioned cations and anions are mainly observed in areas where the mudstone arenite of the Abrahamskraal formation dominates without dolerite intrusions.

In relation to the quaternary catchments, higher concentration of these major ions (Figures 3.15 and 3.16) is mainly observed in the J21A, L11F and northern part of L11G. These catchments have higher Cumulative Mean Annual Precipitation (CMAP) and more weathering of high lying areas as a result compared to catchments J21B, J21C and L12B.

The interaction with the lithology like the carbonates, lithofeldspathic sandstones and dolerites could result in higher concentrations of  $\text{Ca}^{2+}$ ,  $\text{Mg}^{2+}$ ,  $\text{Cl}^-$  and  $\text{SO}_4^{2-}$  due to dissolution and precipitation of evaporites and calcrete (Figures 3.15a and 3.15b; Figures 3.16a and 3.16b). The high  $\text{Ca}^{2+}$  and  $\text{Mg}^{2+}$  concentrations in Figures 3.14a and 3.14b are mostly distributed on the calcareous deposits on the northern part of the study area and south west of the town. These high concentrations are attributed to the weathering and dissolution of calcite and dolomite in the calcrete although  $\text{Ca}^{2+}$  is often the dominant ion in the calcite mineral (Parsons & Abrahams, 1994). Based on the results from section 2.1 (of this chapter) these high concentrations are also due to silicate weathering and reverse ion exchange processes. The groundwater in these areas is characterized as hard.

The  $\text{Na}^+$  is distributed in a similar manner as that of  $\text{Ca}^{2+}$  and  $\text{Mg}^{2+}$  with higher concentrations displayed on the calcrete deposits northeast, east and south east of the town (Figure 3.15c). These high concentrations are mainly attributed to silicate weathering of the lithofeldspathic sandstones and ion exchange processes with some evaporation and halite dissolution.

The  $\text{Cl}^-$  distribution (Figure 3.16a) is similarly high like that of  $\text{Mg}^{2+}$  and  $\text{Na}^+$  (Figures 3.15b and 3.15c) and is attributed to evaporation, surface contamination as well as halite dissolution.

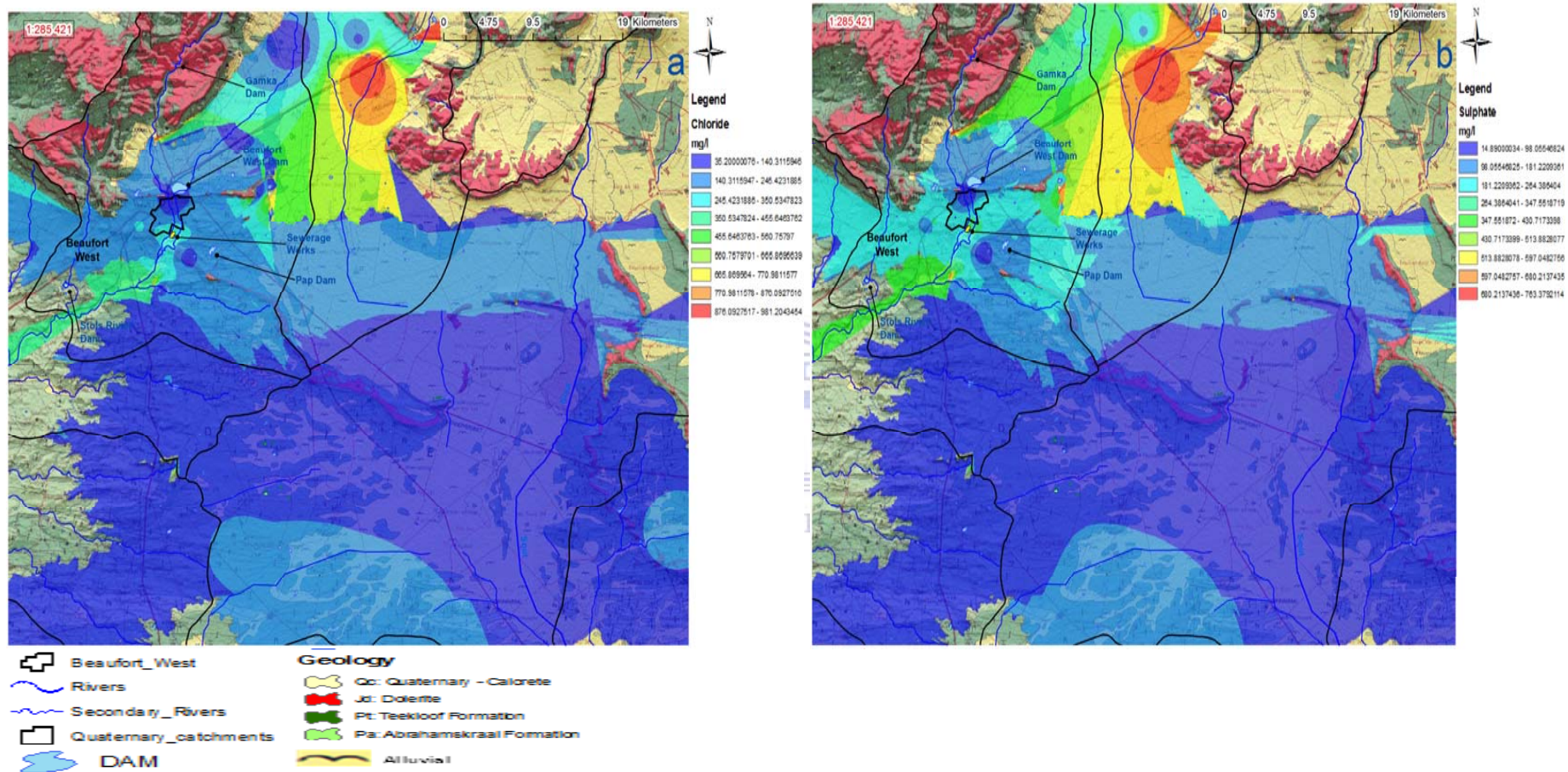
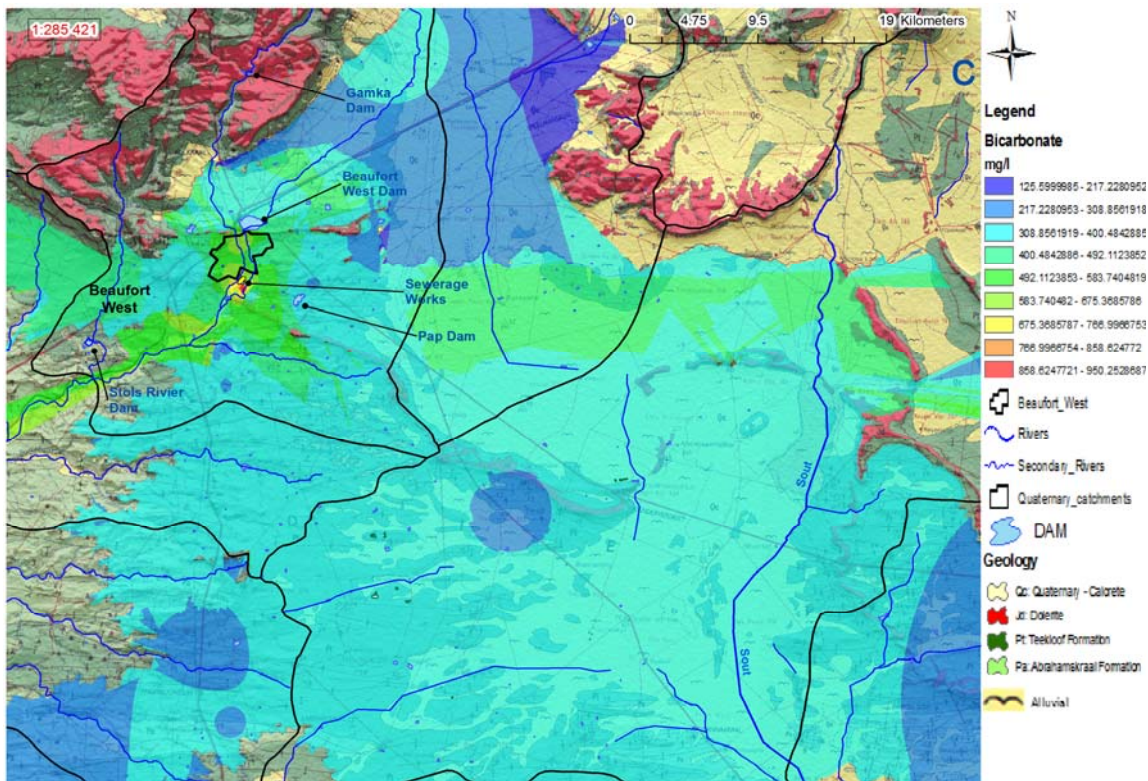


Figure 3.16 Spatial distribution of major ions (a)  $\text{Cl}^-$  and (b)  $\text{SO}_4^{2-}$  against catchment and lithological background: Inverse Distance Weighted Interpolation representation.

On the other hand, the  $\text{SO}_4^{2-}$  distribution (Figure 3.16b) is similar to that of  $\text{Ca}^{2+}$  and  $\text{Mg}^{2+}$  in the northern part of the study area suggesting gypsum and/or anhydrite dissolution. To the south west of the town the  $\text{SO}_4^{2-}$  distribution is also high and is ascribed to surface contamination besides sulphate dissolution.

It is also observed that the  $\text{Cl}^-$  and  $\text{SO}_4^{2-}$  concentrations in the J21A catchment's downstream (especially to the south of the town) are higher (Figures 3.16a and 3.16b). These high concentrations are attributed to possible contamination from domestic wastages and effluents from the sewerage works located in the area.



**Fig 3.17 Spatial distribution of  $\text{HCO}_3^-$  against catchment and lithological background: Inverse Distance Weighted Interpolation representation.**

The  $\text{HCO}_3^-$  spatial distribution (Figure 3.17) shows higher concentrations mainly in the sandstones (basal arenaceous Poortjie Member) and mudstones areas of the sedimentary rocks compared to the calcrete deposits. This could be attributed to the dissolution of soil limestone (which is predominantly calcite) in sediments during recharge. Similar higher concentrations are also observed in areas where there is a sedimentary rock

contact with dolerite intrusion. This observed high concentration in the dolerite contact zones could be the result of chemical weathering (carbonate dissolution and silicate weathering). A relatively lower concentration is observed in the low-lying areas covered by the calcrete formation. The J21A quaternary catchment shows the highest  $\text{HCO}_3^-$  concentration compared to the other catchments.

The spatial distribution of  $\text{K}^+$  and  $\text{NO}_3^-$  was analysed against catchment and land cover/use information of the study area. Catchment J21A is densely populated with the town of Beaufort West being at the centre. This catchment has three major dams, recreational centres (e.g. swimming pools, golf estates etc.), a wastewater treatment plant and commercially cultivated lands. The rest of the catchments are sparsely populated with most of them having non-perennial water bodies and commercially cultivated lands and game farms. Figure 3.18 and 3.19 show the distribution of  $\text{K}^+$  and  $\text{NO}_3^-$  across the six catchments. In catchments J21A and J21B,  $\text{K}^+$  (Figure 3.18) and  $\text{NO}_3^-$  (Figure 3.19) concentrations were observed to be higher in areas with urbanization, commercial farms, game farms and sewerage works compared to the other catchments of the study area. The high  $\text{K}^+$  and  $\text{NO}_3^-$  concentrations observed in Figures 3.18 and 3.19 is attributed to domestic effluent and agricultural contaminants while chemical weathering and cation exchange processes in the lithofeldspathic sandstones of the Teekloof formation could also contribute to the observed high  $\text{K}^+$  concentrations. Catchments J21C, L11F, L11G and L12B show lower concentrations of  $\text{K}^+$  (Figure 3.18) while the  $\text{NO}_3^-$  (Figure 3.19) concentrations are higher in comparison which could be attributed due to commercial irrigation and game farming.

About 35% of the groundwater samples show elevated levels of  $\text{NO}_3^-$  which is well above the SAWQG (DWAF, 1996) target water quality of 6 mg/L and three of these samples have concentrations higher than the maximum tolerable amount rendering the water unfit for human consumption.

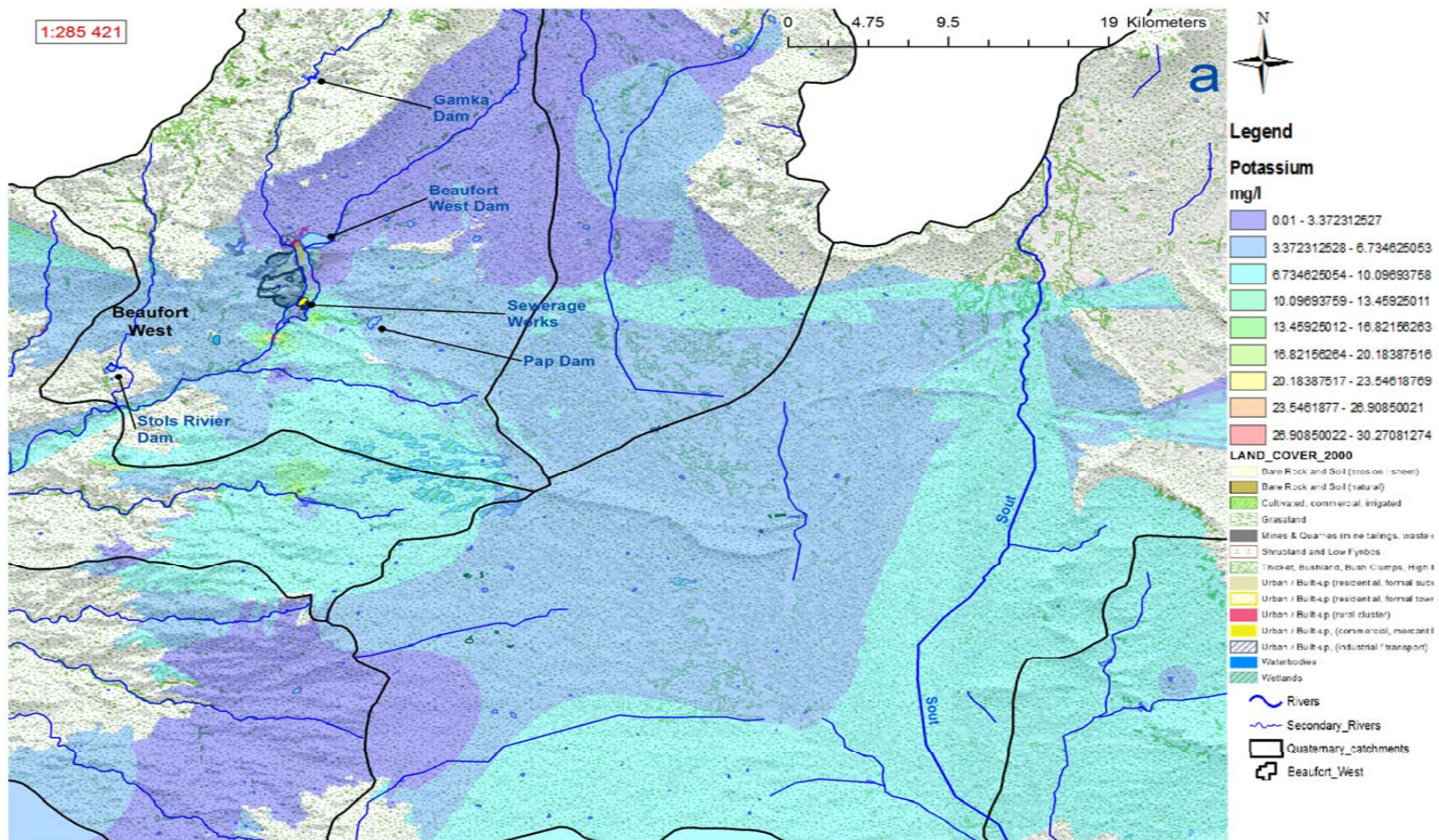


Fig 3.18 Spatial distribution of  $K^+$  against catchment and land cover background: Inverse Distance Weighted Interpolation representation.

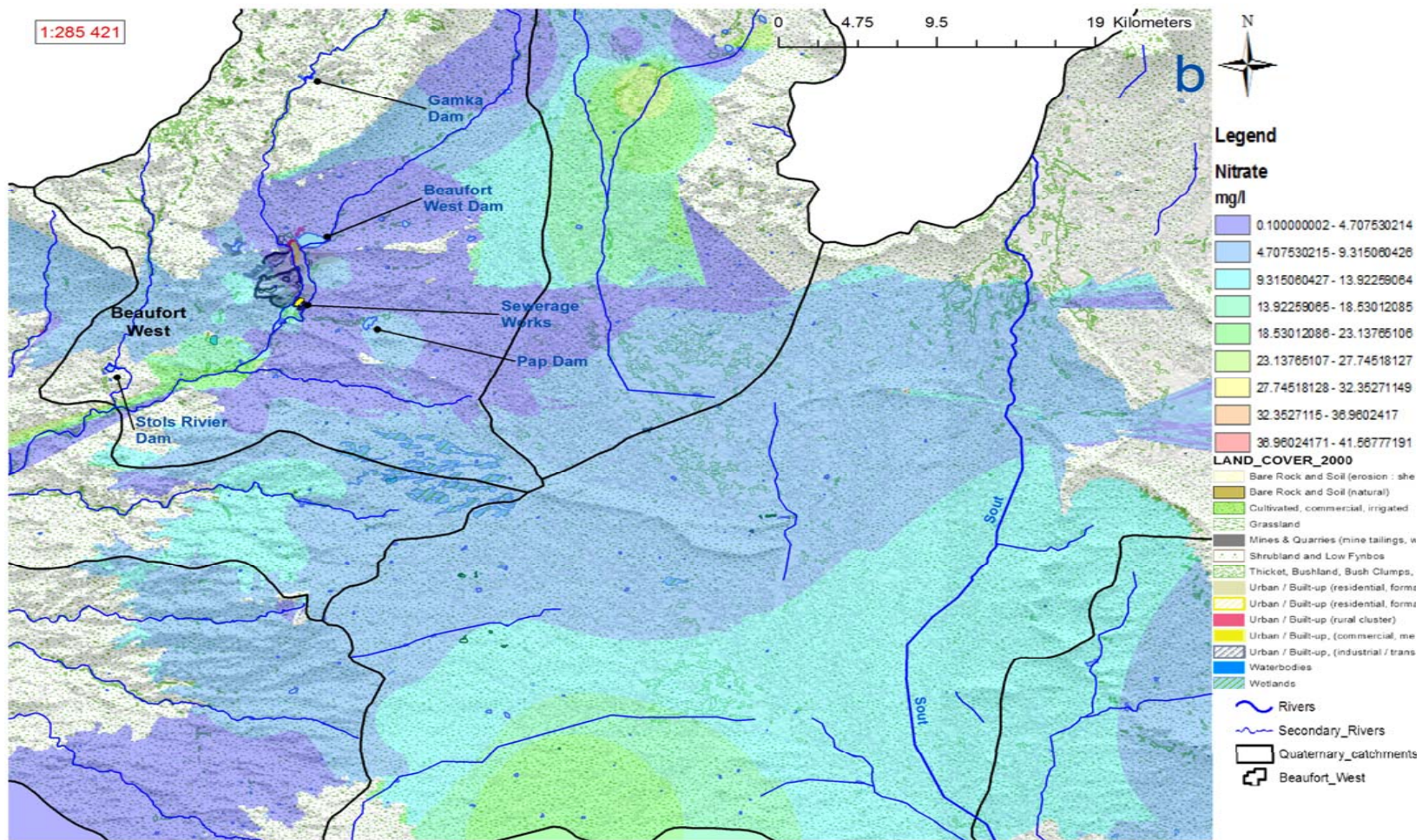


Fig 3.19 Spatial distribution of  $\text{NO}_3^-$  against catchment and lithological background: Inverse Distance Weighted Interpolation representation.

These groundwater samples (Katddornkuil, Nigrini Farm 2 and Steenrotsfontein 1) are all on or near farms and have  $\text{NO}_3^-$  concentrations of 21.58 mg/L, 50.6 mg/L and 69.6 mg/L respectively. The major anthropogenic sources for the high  $\text{NO}_3^-$  concentrations are likely to be due to the stock farming and irrigation occurring on these farms.

### 3. Multivariate statistics

Multivariate statistics was typically used to get a deeper insight in to the complex groundwater data analysed using classic hydrochemical (trilinear), major ion chemistry and spatial analyses. Although trilinear diagrams such as Piper are widely used to analyse, classify and identify mixing of waters they fail in certain situations due to the fact that

- Ion concentrations or variable values are renormalized and
- Some ions or variables that could have significant concentrations or values cannot be easily accommodated in such diagrams or analyses.

#### 3.1. Factor analysis

Factor analysis was performed on 12 variables (EC, TDS, TH, TA,  $\text{Ca}^{2+}$ ,  $\text{Mg}^{2+}$ ,  $\text{Na}^+$ ,  $\text{K}^+$ ,  $\text{Cl}^-$ ,  $\text{SO}_4^{2-}$ ,  $\text{HCO}_3^-$  and  $\text{NO}_3^-$ ) of the groundwater samples. Table 3.17 shows the initial determined factors, their Eigenvalues and the percent of variance contributed in each factor using Varimax rotation method with Kaiser Normalization and unrotated factor solution. Only factors with Eigenvalues  $\geq 1$  were taken into consideration and this resulted in three factors that were sufficient in explaining 85.086% of the variance. The total variance explained by these three factors; factor one, factor two and factor three are 59.124%, 16.564% and 9.397% respectively.

The three factors shown in Table 3.18 are dominated by certain variables based on the prevailing hydrogeochemical processes and land use practices.

**Table 3.17 Factor analysis results: Total variance**

Total Variance Explained									
Component	Initial Eigenvalues			Extraction Sums of Squared Loadings			Rotation Sums of Squared Loadings		
	Total	% of Variance	Cumulative %	Total	% of Variance	Cumulative %	Total	% of Variance	Cumulative %
1	7.095	59.124	59.124	7.095	59.124	59.124	6.946	57.879	57.879
2	1.988	16.564	75.688	1.988	16.564	75.688	2.119	17.662	75.542
3	1.128	9.397	85.086	1.128	9.397	85.086	1.145	9.544	85.086
4	0.964	8.031	93.117						
5	0.412	3.430	96.547						
6	0.187	1.555	98.102						
7	0.107	0.892	98.994						
8	0.059	0.494	99.488						
9	0.039	0.324	99.812						
10	0.017	0.142	99.954						
11	0.004	0.037	99.991						
12	0.001	0.009	100.000						

Extraction Method: Principal Component Analysis.

These three factors were named as “Hardness Factor” for factor 1, “Alkalinity Factor” for factor 2 and “Anthropogenic Factor” for factor 3, based on the major contributing variables of the factor loadings, geochemical processes and anthropogenic activities influencing the groundwater chemistry (Table 3.18).

The main major ion contributors of the Hardness Factor are  $\text{Ca}^{2+}$ ,  $\text{Mg}^{2+}$ ,  $\text{Na}^+$ ,  $\text{Cl}^-$  and  $\text{SO}_4^{2-}$  (Table 3.18). This Factor describes 59.124% of the total variance (Table 3.17), and is ascribed to hardness and salinity of the groundwater due to carbonate, silicate, gypsum and halite dissolution as well as infiltration of concentrated saline surface water resulting from evaporation. Figure 3.20 shows that the Hardness factor score is higher in the low-lying areas covered by calcrete deposits and the lithofeldspathic sandstones of the Teekloof formations near the dolerite intrusions to the south of the town.

The southern part of the study area also shows high Hardness factor score distribution that could be attributed to surface contamination in addition to the rock-water interaction processes. The effect of fluctuating groundwater level coupled with interaction with these geological formations results in the leaching of  $\text{Ca}^{2+}$  and  $\text{Mg}^{2+}$  from rock formations through the processes of carbonate and silicate weathering.

**Table 3.18 Factor analysis result: Rotated Component Matrix**

	Components		
	Hardness	Alkalinity	Anthropogenic
EC	0.975		
Cl <sup>-</sup>	0.965		
TH	0.958		
TDS	0.956		
SO <sub>4</sub> <sup>2-</sup>	0.916		
Ca <sup>2+</sup>	0.912		
Mg <sup>2+</sup>	0.879		
Na <sup>+</sup>	0.874		
HCO <sub>3</sub> <sup>-</sup>		0.987	
TA		0.984	
NO <sub>3</sub> <sup>-</sup>			0.820
K <sup>+</sup>			0.561

Extraction Method: Principal Component Analysis.  
Rotation Method: Varimax with Kaiser Normalization.

The dissolution of these cations with Cl<sup>-</sup> and SO<sub>4</sub><sup>2-</sup> gives rise to the hardness of the groundwater explained by the high TDS contribution to this factor. Na<sup>+</sup> contributes the least to this factor compared to the other cations and has lower correlation with Cl<sup>-</sup> and SO<sub>4</sub><sup>2-</sup> as compared to Ca<sup>2+</sup> and Mg<sup>2+</sup> (Table 3.10). This is an indication that this factor is of low salinity and high hardness due to Ca-Mg-Cl-SO<sub>4</sub> type of groundwater chemistry. The low Na<sup>+</sup> loading on the Hardness factor is also an indication of the influence of reverse ion exchange processes in conjunction with carbonate and silicate weathering in the groundwater samples characterized by this factor.

The Hardness factor has high distribution in the J21A, L11F and southern parts of the L11G quaternary catchments (Figure 3.20).

The Alkalinity Factor accounts for 16.564% (Table 3.17) and indicates the effect of alkalinity with HCO<sub>3</sub><sup>-</sup> and TA being the main contributors (Table 3.18).

This factor is related to carbonate and silicate weathering processes and the observed high TA loading is attributed to alkali carbonates and bicarbonates.

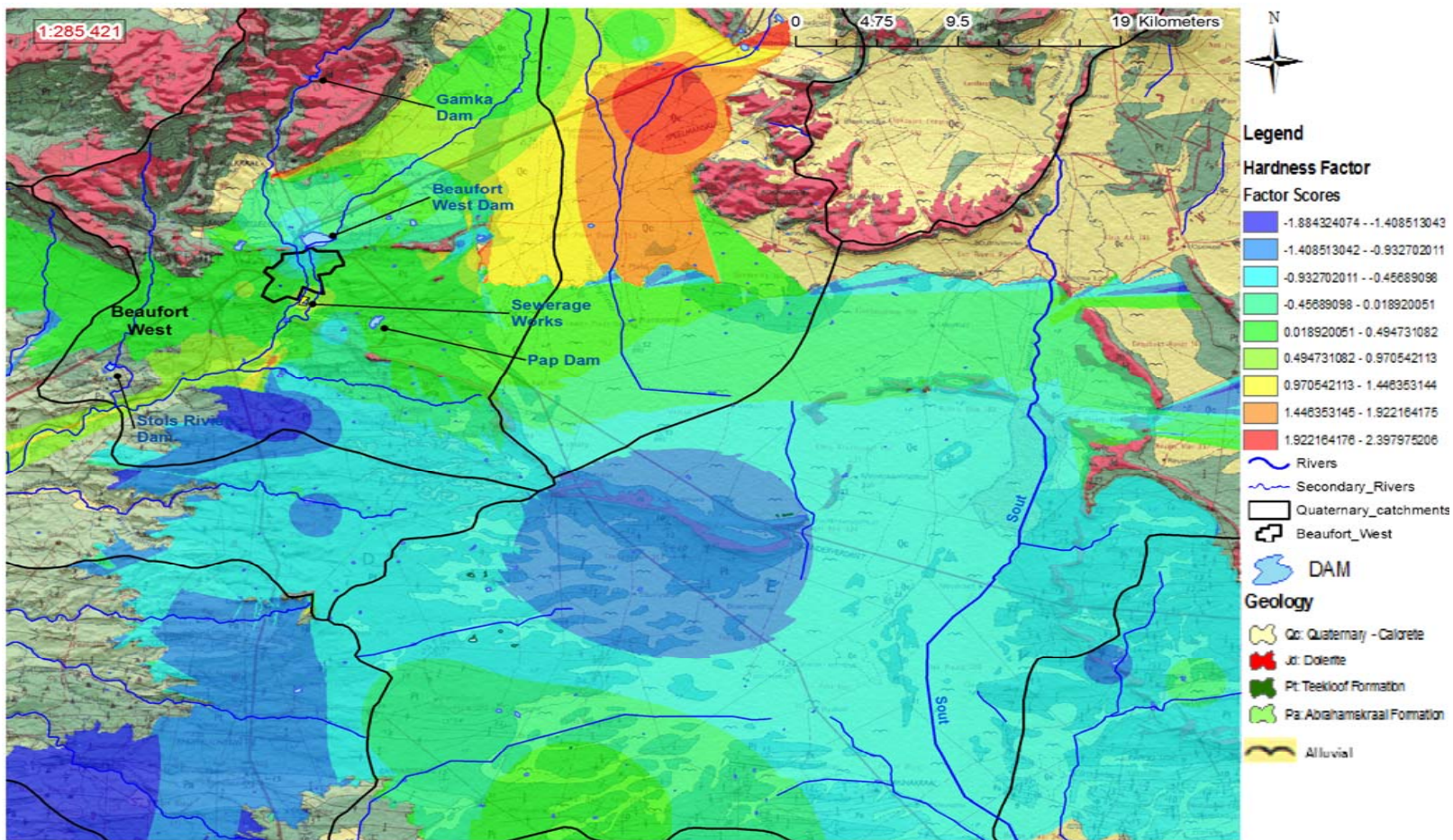
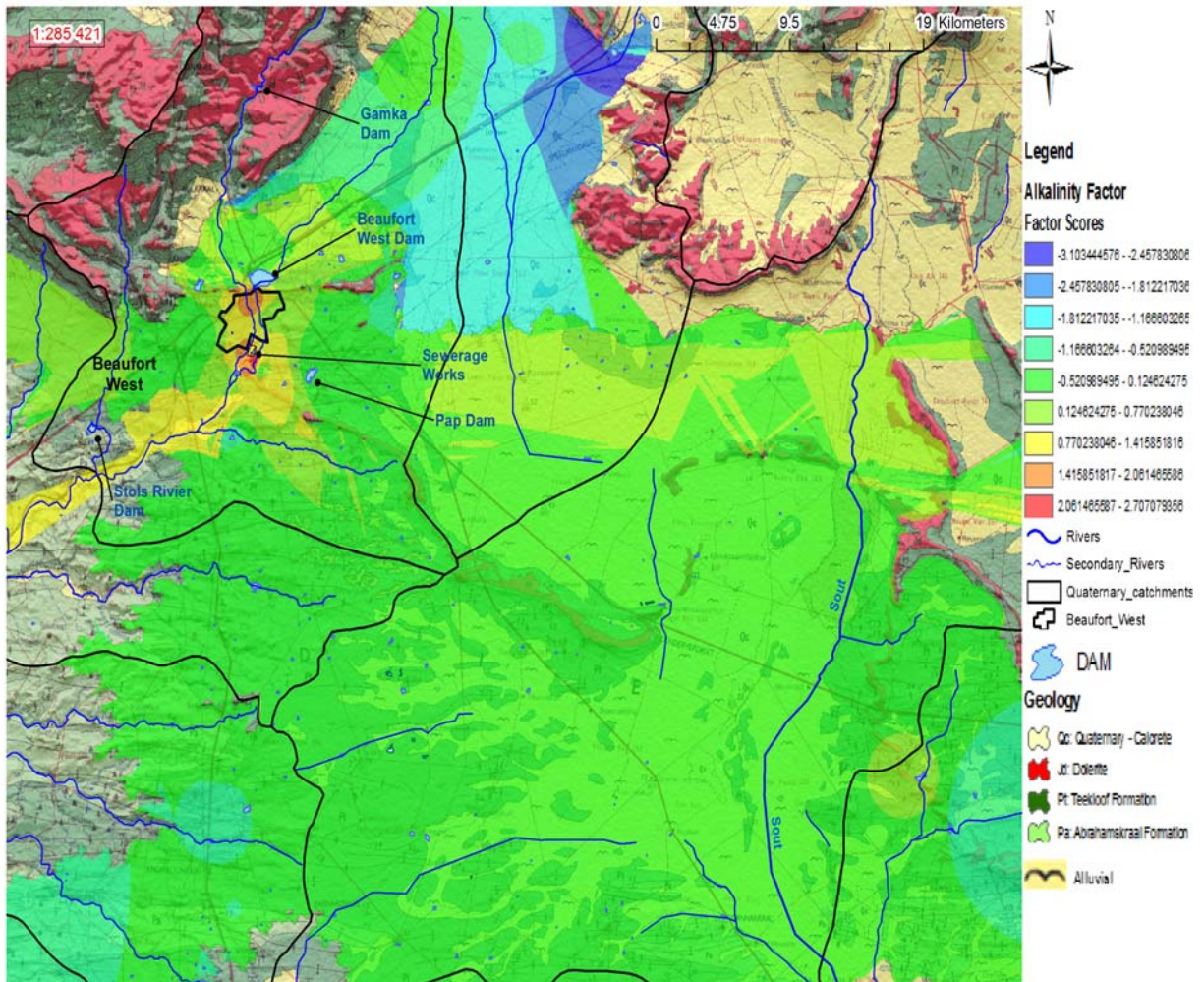


Fig 3.20 Spatial distribution of the Hardness Factor scores against catchment and lithological background: Inverse Distance Weighted Interpolation representation.

The spatial distribution of the Alkalinity factor presents high values in areas covered by the lithofeldspathic sandstones of the Teekloof formation especially in and around Beaufort west town, where there is a contact with dolerite intrusion (Figure 3.21). Lower scores are observed in the low-lying calcrete deposit areas and the southern part of the study area. The J21A quaternary catchment shows highest alkalinity factor scores compared to the other catchments.



**Fig 3.21 Spatial distribution of the Alkalinity Factor scores against catchment and lithological background: Inverse Distance Weighted Interpolation representation.**

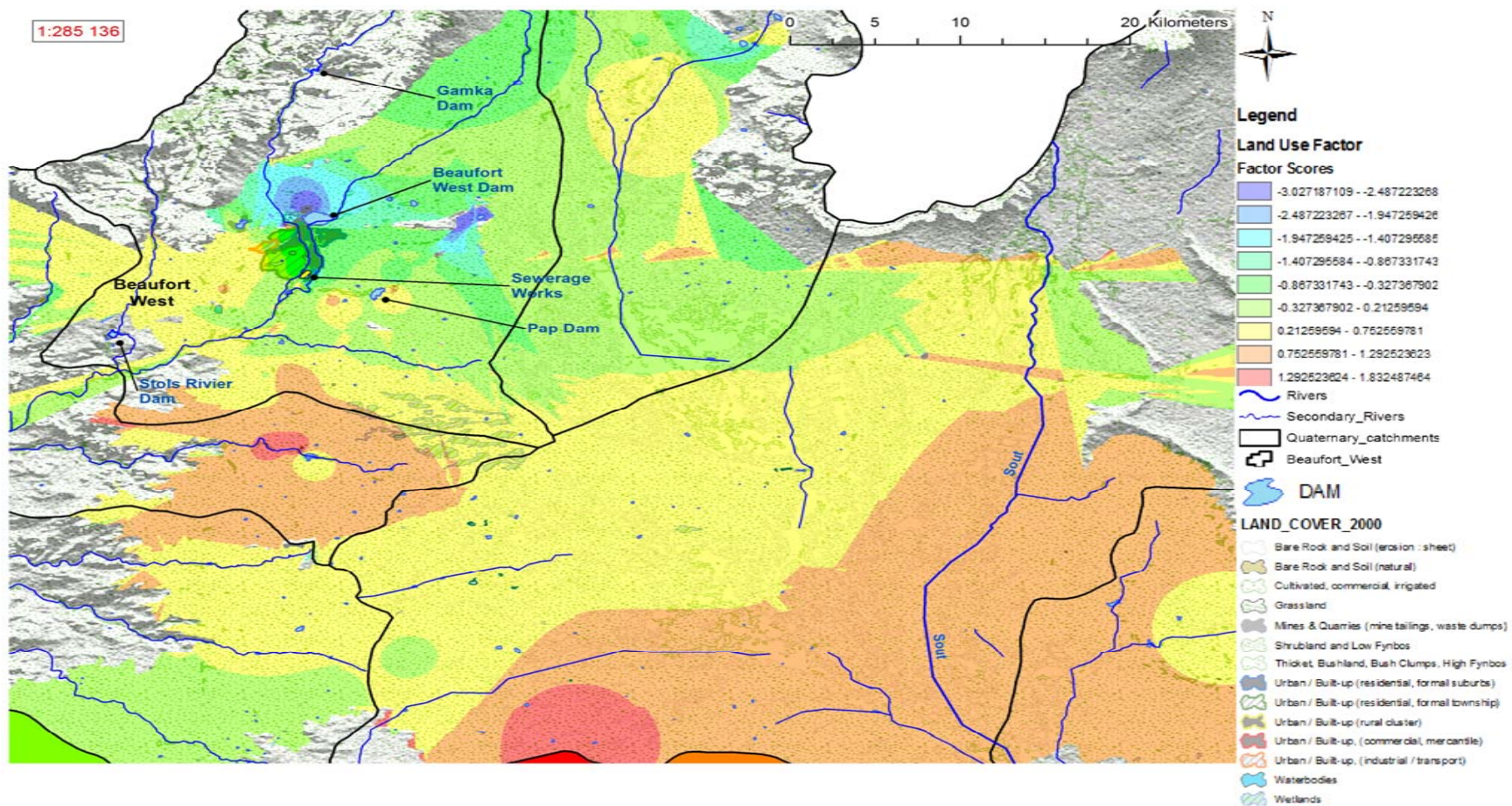


Figure 3.22 Spatial distribution of Anthropogenic Factor scores against catchment and land cover background: Inverse Distance Weighted Interpolation representation.

The anthropogenic Factor accounts 9.397% (Table 3.17) and indicates the effect of human activities on groundwater quality and is dominated by  $K^+$  and  $NO_3^-$ . The J21A, J21B and J21C quaternary catchments, especially areas around wastewater treatment and informal settlement show highest anthropogenic factor score (Figure 3.22). Additionally, L11F and L11G quaternary catchments where both animal and olive farming are practiced show also high anthropogenic factor scores. Elevated nitrate concentration can be also associated with recharge from precipitation and irrigation-carrying nitrogen compounds from soil into the aquifer. Non-agricultural sources of nitrate in the study area would include municipal and industrial discharges containing nitrogen bearing effluent and atmospheric deposition.

### 3.2. Cluster and discriminant analysis

The multivariate statistical techniques such as hierarchical cluster analysis (HCA) and discriminant analysis (DA) have been widely used as unbiased methods in analysing groundwater quality data to draw meaningful information. The HCA and DA techniques and the methodology used for their application are described in detail in many studies (Chen et al., 2007; Davis, 1986; Lambrakis et al., 2004).

The groundwater samples of the study area were analysed using a combination of HCA and DA for two reasons:

- In order to compare with the conventional techniques for water quality studies like, Piper (1994) diagram. In this case, similar variables as in the trilinear diagram were used.
- Since groundwater parameters are multivariate, a combination CA and DA were used to test the hypothesis that these multivariate statistical techniques can provide more information than trilinear diagrams on groundwater quality by using all the available variables.

The analysis was done in two sets. The first set (Set A) comprised the same seven variables used in the trilinear diagram (Piper, 1944) analysis of the groundwater samples in percentage meq/L. It is important to note that this set of data was not standardized as all the variables were measured in the same unit, i.e. percentage meq/L.

The second set (Set B) comprised all the raw values of the available fourteen variables that were used in the correlation analysis (section 1.1 of this chapter). The analysis results and figures of the Set A variables are denoted with the suffix I while the results of Set B and the consequent analysis results and figures are denoted with suffixes II and III.

### 3.2.1. Analysis 1: Set A

The cluster analysis of Set A ( $\text{Ca}^{2+}$ ,  $\text{Mg}^{2+}$ ,  $\text{Na}^+\text{+K}^+$ ,  $\text{Cl}^-$ ,  $\text{HCO}_3^-$  and  $\text{SO}_4^{2-}$  in % meq/L) resulted in a dendrogram showing three distinct groups or hydrochemical facies, namely Ca-Mg-(Na+K)- $\text{HCO}_3^-$  as CA1, Ca-Mg-(Na+K)-Cl- $\text{SO}_4$ - $\text{HCO}_3^-$  as CA2 and Ca-Mg-Cl- $\text{SO}_4$  as CA3 (Figure 3.23). These three groundwater types are hydrochemically different and through linear discriminant analysis were verified to be 100% different from each other using all the available six variables as shown in Table 3.21.

These groups are similar to the water types obtained using the trilinear diagram (Piper, 1944) in section 2 of this chapter. The discriminant analysis of the groups derived from Set A produced two discriminant functions that are correlated to the variables used in this set (Table 3.19) and the group centroid of these functions are shown in Table 3.20.

Function 1 is highly positively correlated to  $\text{HCO}_3^-$  and highly negatively correlated to  $\text{Cl}^-$  and  $\text{SO}_4^{2-}$ . This function clearly separates the  $\text{HCO}_3^-$  water type from the  $\text{Cl}^-$  and  $\text{SO}_4^{2-}$  dominated water type. The second function shows high positive correlation with  $\text{Ca}^{2+}$  and  $\text{Mg}^{2+}$  while it is significantly negatively correlated to  $\text{Na}^+$ . This function separates the groundwater samples as alkali water type and  $\text{Ca}^{2+}$  and  $\text{Mg}^{2+}$  (alkali earth) dominated water type.

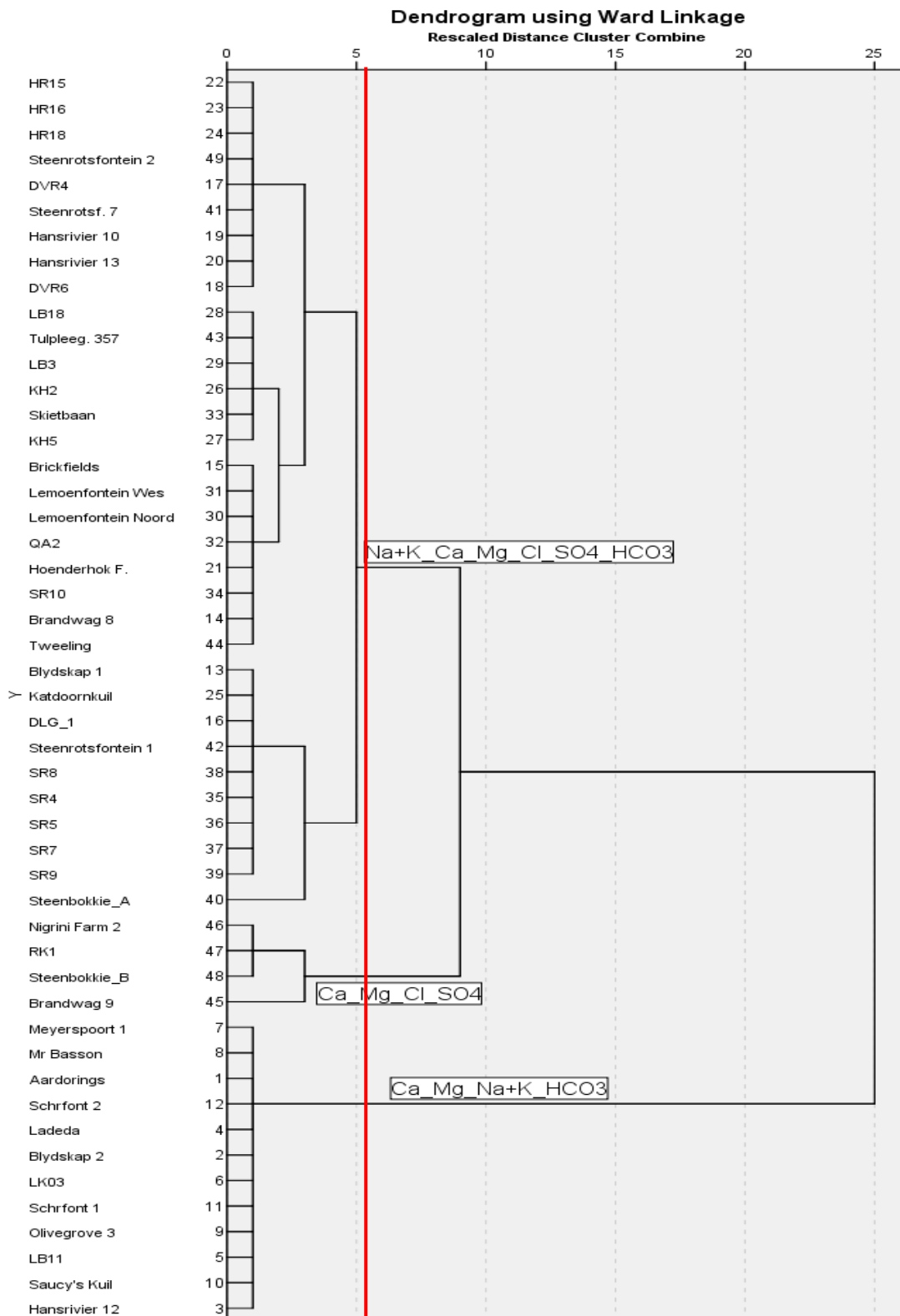


**Figure 3.23** Water type groups cluster of the groundwater samples using Set A variables (red line indicates level of similarity or distance between groups).

**Table 3.19 Structure matrix of Set A variables and their functions**

	Function	
	1	2
HCO <sub>3</sub> <sup>-</sup>	0.964*	-0.162
Cl <sup>-</sup>	-0.473*	0.221
SO <sub>4</sub> <sup>2-</sup>	-0.423*	-0.075
Na <sup>+</sup> +K <sup>+</sup>	-0.052	-0.985*
Ca <sup>2+</sup>	0.115	0.776*
Mg <sup>2+</sup>	-0.102	0.523*
Pooled within-groups correlations between discriminating variables and standardized canonical discriminant functions		
Variables ordered by absolute size of correlation within function		
*. Largest absolute correlation between each variable and any discriminant function		

**Table 3.20 Functions at Group Centroids (Set A variables)**

Predicted Group Analysis 1	Function	
	1	2
CA1	4.341	0.257
CA2	-0.780	-0.202
CA3	-5.424	0.679
Unstandardized canonical discriminant functions evaluated at group means		

**Table 3.21 Classification Results (Set A variables)<sup>a</sup>**

		Predicted Group for Analysis 1	Predicted Group Membership			Total
			CA1	CA2	CA3	
Original	Count	CA1) Ca-Mg-(Na+K)-HCO <sub>3</sub>	12	0	0	12
		CA 2) Ca-Mg-(Na+K)-Cl-SO <sub>4</sub> -HCO <sub>3</sub>	0	32	0	32
		CA 3) Ca-Mg-Cl-SO <sub>4</sub>	0	0	5	5
	%	CA 1) Ca-Mg-(Na+K)-HCO <sub>3</sub>	100	0.0	0.0	100
		CA 2) Ca-Mg-(Na+K)-Cl-SO <sub>4</sub> -HCO <sub>3</sub>	0.0	100	0.0	100
		CA 3) Ca-Mg-Cl-SO <sub>4</sub>	0.0	0.0	100	100
<sup>a</sup> . 100% of original grouped cases correctly classified						

The three-groundwater types that resulted from CA and DA and the number of samples predicted in each group are 100% different as shown in Table 3.21. These groups, based on the discriminant functions and their correlated variables, are classified as

- a) CA1: Recharge water dominated by Ca<sup>2+</sup>, Mg<sup>2+</sup> and HCO<sub>3</sub><sup>-</sup>, which could be attributing to carbonate dissolution and silicate weathering.
- b) CA2: Mixed water that indicates the contribution of carbonate and silicate weathering as well as ion exchange and evaporation processes.

c) CA3: Hard water dominated by  $\text{Ca}^{2+}$ ,  $\text{Mg}^{2+}$ ,  $\text{Cl}^-$  and  $\text{SO}_4^{2-}$  which could be attributing to carbonate and silicate weathering as well as dissolution of gypsum and halite followed by reverse ion exchange.

The three groups that resulted from this analysis are displayed in Figure 3.24, based on the two discriminant functions and their descriptive statistics is given in Table 3.22.

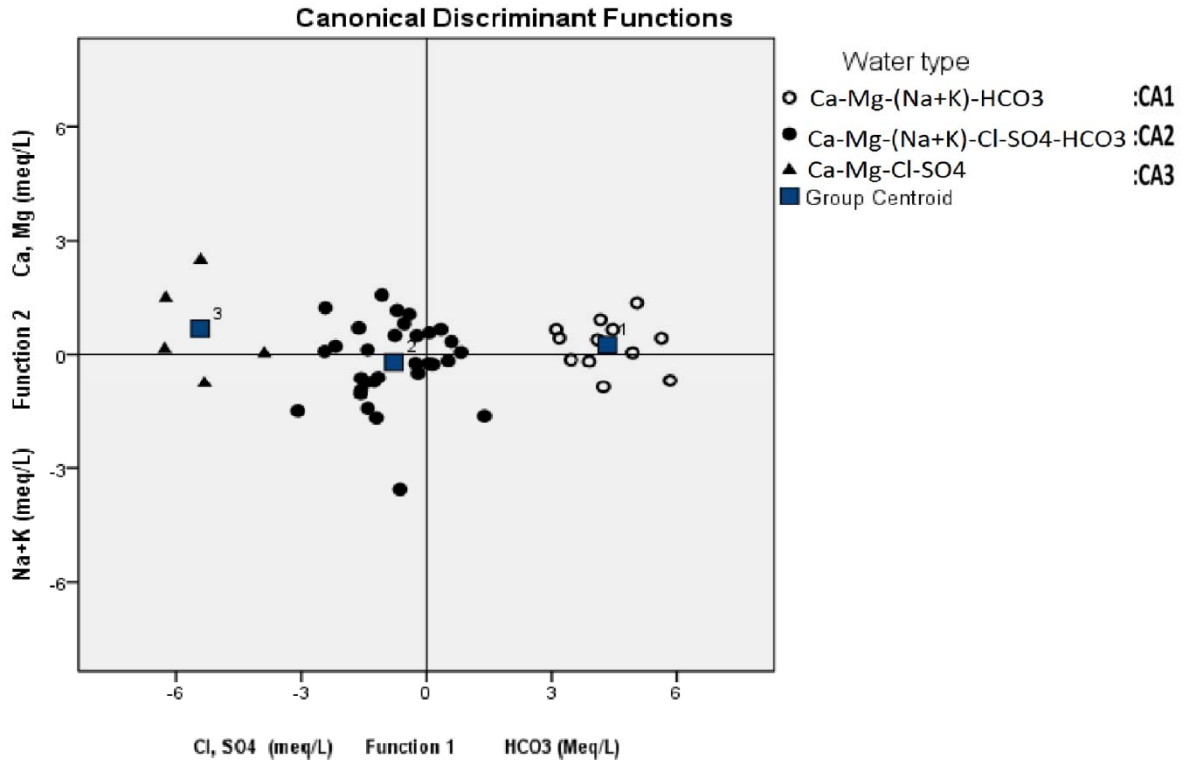


**Figure 3.24 Groundwater sample groups (CA1, CA2 and CA3) vs. discriminant functions (Set A variables).**

The descriptive statistics of the three water types given in Table 3.22 shows that the mean and range of all the hydrochemical variables except  $\text{K}^+$ ,  $\text{HCO}_3^-$  and TA are higher in the hard water type (CA3) in comparison to the mixed (CA2) and recharge water (CA1). This is an indication of the contribution of some of these variables, especially  $\text{Ca}^{2+}$ ,  $\text{Mg}^{2+}$ ,  $\text{Cl}^-$  and  $\text{SO}_4^{2-}$ , towards its characteristic hardness.  $\text{Na}^+$  and  $\text{NO}_3^-$  are also high and contribute to its high TDS. The mixed water type (CA2) has moderate values of the above-discussed variables with the exception of  $\text{K}^+$ ,  $\text{HCO}_3^-$  and TA. These variables have the highest values in this group followed by the recharge water type

while the hard water type has the least. The stepwise discriminant analysis of Set A variables revealed that  $\text{HCO}_3^-$  alone separates the three groups.

**Table 3.22 Descriptive statistics of the three water types (A)\***

	Ca-Mg-(Na+K)- $\text{HCO}_3^-$ (CA1) N=12			Ca-Mg-(Na+K)-Cl- $\text{SO}_4$ - $\text{HCO}_3^-$ (CA2) N=32			Ca-Mg-Cl- $\text{SO}_4$ (CA3) N=5		
	Mean	Min-Max	St.Dev.	Mean	Min-max	St.Dev	Mean	Min-max	St.Dev
PH	7.5	7.0-8.2	0.3	7.5	6.6-8.3	0.5	7.7	7.3-7.9	0.2
EC <sup>a</sup>	83.9	56-124	19.9	172.9	83.1-285	55.3	361.8	241-477.0	101.0
SAR	1.8	0.8-3.2	0.6	3.1	1.0-6.8	1.5	4	2.8-5	1.0
Ca <sup>2+</sup>	83.6	45.9-115.8	17	134.6	71.3-210.5	33.8	308.5	172.3-392.5	100.0
Mg <sup>2+</sup>	18.5	9.8-32.7	7.6	38.1	2.6-66.7	14.6	150.5	37-205.5	66.1
Na <sup>+</sup>	72.5	47.4-135.2	25	170.5	63.1-359.8	77.2	300	249.8-390.8	55.3
K <sup>+</sup>	4.5	0.01-9.7	2.8	5.7	0.5-30.6	6.1	5.4	2-9.8	3.1
$\text{HCO}_3^-$	368.9	246.5-627.8	116.1	420.5	251.1-950.8	150.0	280.5	125.6-583.3	177.6
Cl <sup>-</sup>	59.0	35.2-91.6	18.5	215.6	57.4-391.2	91.2	682.3	263.5-1088.7	312.8
$\text{SO}_4^{2-}$	42.9	14.9-65	14.3	208.9	84.6-422.5	91.2	630.9	390.8-954.5	206.4
$\text{NO}_3^-$	4.3	0.4-11	14.3	7.5	0.1-69.6	12.7	11.2	0.1-50.6	22.1
TDS	636.6	424-1011	166.5	1228.9	449-2130	431.3	2389.9	1682.8-3000	530.7
TA	302.5	202.1 – 514.8	95.2	339.5	205.9 – 785.6	205.9	230	103-478.3	145.7

\*All units in mg/L except SAR an pH; <sup>a</sup>mS/m

### 3.2.2. Analysis 2: Set B

The first attempt on cluster analysis of Set B (EC, TDS, TA, TH, pH, SAR, Ca<sup>2+</sup>, Mg<sup>2+</sup>, Na<sup>+</sup>, K<sup>+</sup>, Cl<sup>-</sup>,  $\text{HCO}_3^-$ ,  $\text{NO}_3^-$  and  $\text{SO}_4^{2-}$ ) resulted in a dendrogram showing three groups or hydrochemical facies (Figure 3.25a). These three groundwater types are hydrochemically different and through linear discriminant analysis were verified to be 100% different from each other using all the available fourteen variables as shown in Table 3.25. Although this analysis classified 100% of the original groundwater samples as shown in Tables 3.25 and Figure 3.26, cluster CB1I (Water TDS<1000mg/L) has large number of samples in contrast to cluster CB3I (Hard water  $\text{NO}_3^-$ >50mg/L) which has only two samples.

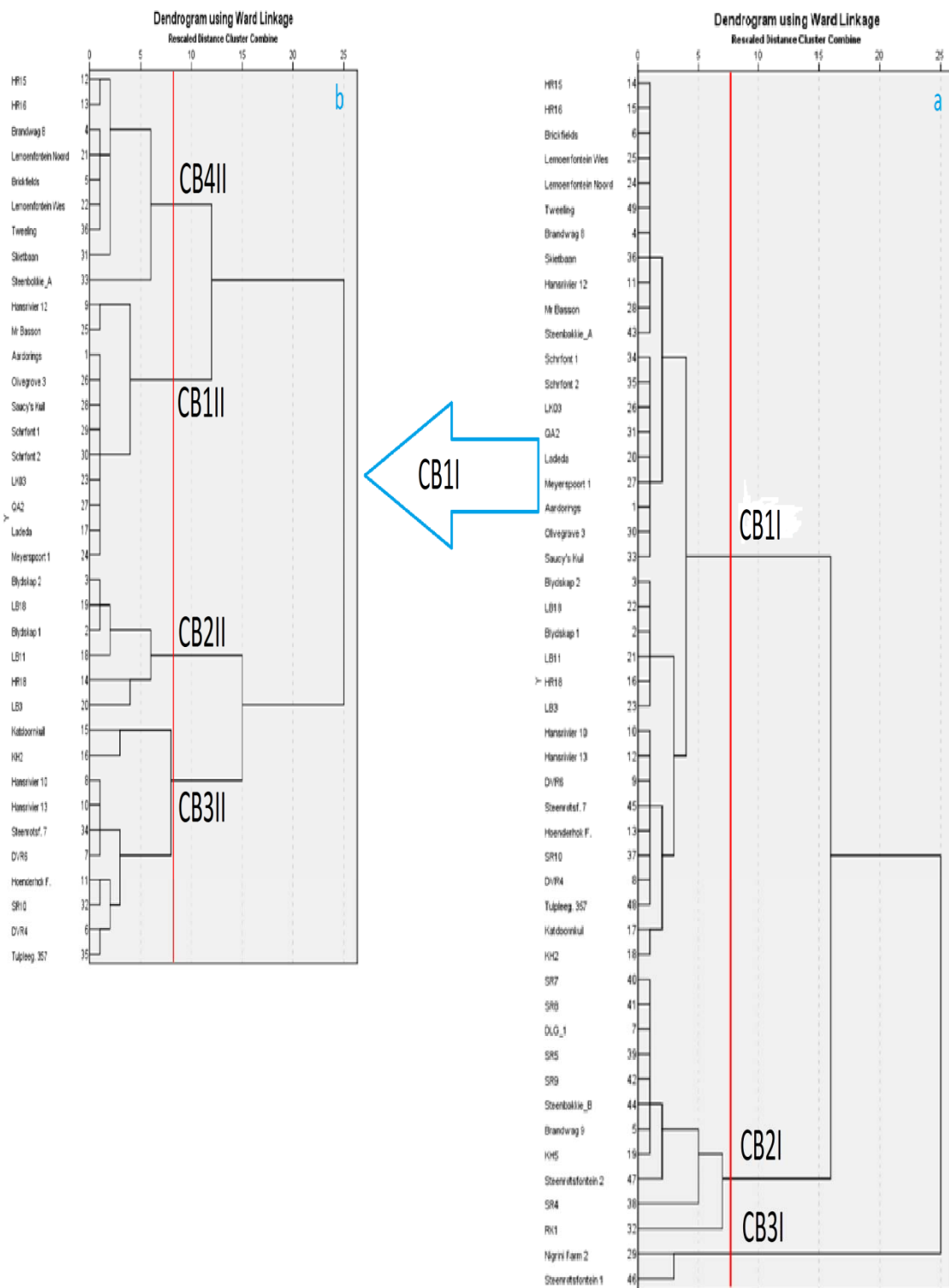


**Figure 3.25** Water type groups cluster of the groundwater samples using Set B variables: a) First attempt (BI) b) Further classification of CB1I in to 4 groups (BII). Red line indicates level of similarity or distance between groups).

The discriminant analysis of the groups derived from Set B produced two discriminant functions correlated to the variables used in this set (Table 3.23) and the group centroids of these functions are shown in Table 3.24. Function 1 is highly positively correlated to  $\text{NO}_3^-$  only. Cluster CB1I and Cluster CB3I are characterized by this function.

Function 2 is highly positively correlated to  $\text{Na}^+$ , TDS, EC,  $\text{SO}_4^{2-}$ ,  $\text{Cl}^-$ ,  $\text{Mg}^{2+}$ ,  $\text{Ca}^{2+}$ , SAR, pH,  $\text{HCO}_3^-$ , TA and  $\text{K}^+$ . Groups CB2I and CB3I are characterized by this function. These two functions classify the groundwater samples as (Table 3.25 and Figure 3.26):

- a) CB1I: Mixed water TDS<1000mg/L,
- b) CB2I: Hard and Alkaline water and
- c) CB3I: Hard water with  $\text{NO}_3^- > 50\text{mg/L}$

The low TDS in CB1I attributes its value to the low values of  $\text{Ca}^{2+}$ ,  $\text{Mg}^{2+}$ ,  $\text{Na}^+$ ,  $\text{K}^+$ ,  $\text{Cl}^-$ ,  $\text{HCO}_3^-$  and  $\text{SO}_4^{2-}$  which are highly positively correlated to function 2 (Table 3.23) and not function 1. Cluster CB1I contains most of the groundwater samples included in the mixed water type (CA2) as well as substantial number of samples from the recharge water type (CA1) classification of Set A. This is a clear indication that CB1I water type has a mixed type of water that could be a result of mixed hydrogeochemical processes and requires detailed statistical analysis. Analysis 2 used larger number of variables in order to classify the water type of the study area better compared to analysis 1. The large size of cluster CB1I and its characterization by  $\text{NO}_3^-$  only suggests the possibility of other hydrogeochemical processes that might be significant under a better classification. Therefore, further classification through cluster analysis of CB1I was performed to get a better grouping that characterizes the groundwater quality of the study area. This problem was also observed in the CA and DA of Set A variables in which the mixed water type group (CA1) had large number of groundwater samples and moderate values of the above-mentioned variables between the two end members of the data set (Table 3.22). Therefore, the groundwater samples in CB1I were classified further and their cluster analysis resulted in four groups (Figure 3.25b).

The Hard and Alkaline water type (CB2I) is attributed to groundwater chemistry

resulting from carbonate and silicate weathering, halite and gypsum dissolution as well as ion exchange processes. The distribution of the groundwater samples in this group correspond to the Hardness factor distribution shown in Figure 3.20. The samples in this group were classified in-group CA2 (mixed water) result of Set A variables along groundwater samples from group CB1I. This new classification of the groundwater samples is attributed due to the inclusion of more variables such as  $\text{NO}_3^-$  that characterize cluster CB3I and separate CB2I from the others. The third cluster (CB3I) is attributed to the same hydrogeochemical processes that control the hydrochemistry of CB2I and anthropogenic influence. The anthropogenic influence is indicated by the higher than WHO (1993)  $\text{NO}_3^-$  content ( $>50\text{mg/L}$ ) in the groundwater samples of these group (Nigrini Farm 2 and Steenrotsfontein 1).

**Table 3.23 Structure matrix of Set B variables and their functions (BI)**

	Function	
	1	2
$\text{NO}_3^-$	0.739*	0.276
$\text{Na}^+$	-0.028	0.758*
TDS	-0.002	0.645*
EC	0.015	0.614*
$\text{SO}_4^{2-}$	-0.032	0.498*
$\text{Cl}^-$	0.039	0.481*
$\text{Mg}^{2+}$	0.039	0.393*
$\text{TH}^b$	0.066	0.389*
$\text{Ca}^{2+}$	0.075	0.337*
SAR	-0.019	0.321*
pH	-0.022	0.190*
$\text{HCO}_3^-$	-0.059	0.153*
TA	-0.052	0.141*
$\text{K}^+$	-0.061	0.073*
Pooled within-groups correlations between discriminating variables and standardized canonical discriminant functions		
Variables ordered by absolute size of correlation within function		
*. Largest absolute correlation between each variable and any discriminant function		
<sup>b</sup> . This variable not used in the analysis		

**Table 3.24 Functions at Group Centroids of Set B variables (BI)**

Predicted Group Analysis 2	Function	
	1	2
CB1I	0.169	-1.321
CB2I	-2.767	3.474
CB3I	12.177	4.672
Unstandardized canonical discriminant functions evaluated at group means		

**Table 3.25 Classification Results of Set B variables (BI)<sup>a</sup>**

		Predicted Group for Analysis 2	Predicted Group Membership			Total
			CB1I	CB2I	CB3I	
Original	Count	CB1I) Mixed water TDS<1000mg/L	36	0	0	36
		CB2I) Hard and Alkaline water	0	11	0	11
		CB3I) Hard water with NO <sub>3</sub> >50mg/L	0	0	2	2
	%	CB1I) Mixed water TDS<1000mg/L	100	0.0	0.0	100
		CB2I) Hard and Alkaline water	0.0	100	0.0	100
		CB3I) Hard water with NO <sub>3</sub> >50mg/L	0.0	0.0	100	100

<sup>a</sup>. 100% of original grouped cases correctly classified

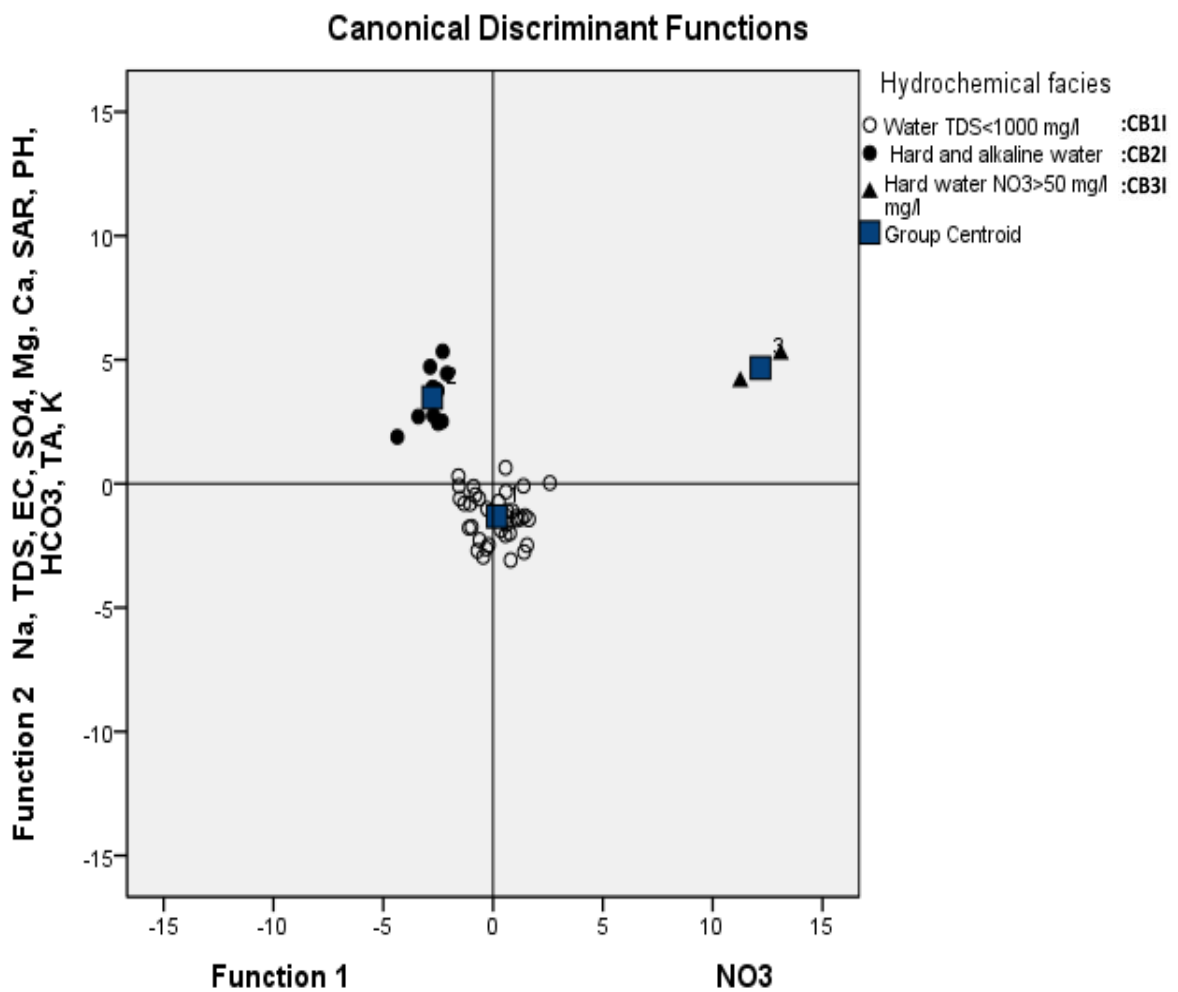


**Figure 3.26 Groundwater sample groups (CB1I, CB2I and CB3I) vs. discriminant functions of Set B variables (BI).**

### 3.2.3. Analysis 3: Set B

The discriminant analysis of the groups derived from cluster CBII of Set B produced three discriminant functions that are correlated to the variables used in this set (Table 3.26) and the group centroid of these functions are shown in Table 3.27. These four groundwater types are hydrochemically different and through linear discriminant analysis were verified to be 100% different from each other using all the available fourteen variables as shown in Table 3.28. Function 1 is highly positively correlated to EC, TDS  $\text{Cl}^-$ ,  $\text{Mg}^{2+}$  and  $\text{Ca}^{2+}$  while function 2 is only positively correlated to  $\text{K}^+$  and  $\text{NO}_3^-$ . Function 3 on the other hand is highly positively correlated to  $\text{SO}_4^{2-}$ ,  $\text{Na}^+$ , pH and SAR and negatively correlated to TA and  $\text{HCO}_3^-$ . Based on these functions the new groups (BII) were classified as shown in Table 3.28 and Figure 3.27. Cluster CBIII (Alkaline water) is characterized as an alkaline water with high TA and  $\text{HCO}_3^-$ . Carbonate and silicate weathering influence the chemistry of the groundwater in this group. This group corresponds to the recharge water type (CA1) in Figure 3.23 (with the exception of two groundwater samples: Blydskap2 and LB11) and the group's distribution corresponds with the Alkalinity factor distribution map in Figure 3.21.

**Table 3.26 Structure matrix of Set B variables and their functions (BII)**

	Function		
	1	2	3
EC	0.540*	0.076	0.411
TDS	0.487*	-0.102	0.287
$\text{Cl}^-$	0.455*	0.120	0.386
$\text{TH}^b$	0.372*	-0.036	0.205
$\text{Mg}^{2+}$	0.362*	0.046	0.155
$\text{Ca}^{2+}$	0.327*	-0.073	0.203
$\text{K}^+$	-0.085	0.663*	0.337
$\text{NO}_3^-$	0.242	0.450*	-0.068
$\text{SO}_4^{2-}$	0.491	-0.218	0.515*
$\text{Na}^+$	0.293	-0.047	0.427*
pH	-0.316	0.189	0.414*
TA	0.094	0.038	-0.188*
$\text{HCO}_3^-$	0.095	0.026	-0.176*
SAR	0.117	-0.047	0.141*
Pooled within-groups correlations between discriminating variables and standardized canonical discriminant functions			
Variables ordered by absolute size of correlation within function			
*. Largest absolute correlation between each variable and any discriminant function			
<sup>b</sup> . This variable not used in the analysis			

**Table 3.27 Functions at Group Centroids of Set B variables (BII)**

Predicted Group Analysis 3	Function		
	1	2	3
CB1II	-2.354	-0.366	-1.464
CB2II	-2.037	2.876	1.278
CB3II	-0.090	-1.875	1.331
CB4II	4.335	0.614	-0.541

Unstandardized canonical discriminant functions evaluated at group means

**Table 3.28 Classification Results of Set B variables (BII) <sup>a</sup>**

		Predicted Group for Analysis 3	Predicted Group Membership				Total
			CB1II	CB2II	CB3II	CB4II	
Original	Count	CB1II) Alkaline water	11	0	0	0	11
		CB2II) Na-SO <sub>4</sub> -K-NO <sub>3</sub> water	0	6	0	0	6
		CB3II) Na-SO <sub>4</sub> -SAR water	0	0	10	0	10
		CB4II)Hard (Ca-Mg-Cl) water	0	0	0	9	9
	%	CB1II) Alkaline water	100	0.0	0.0	0.0	100
		CB2II) Na-SO <sub>4</sub> -K-NO <sub>3</sub> water	0.0	100	0.0	0.0	100
		CB3II) Na-SO <sub>4</sub> -SAR water	0.0	0.0	100	0.0	100
		CB4II)Hard (Ca-Mg-Cl) water	0.0	0.0	0.0	100	100

<sup>a</sup>. 100% of original grouped cases correctly classified

Silicate weathering, possible gypsum dissolution, reverse ion exchange and anthropogenic activities influence cluster CB2II is characterized by high K<sup>+</sup>, NO<sub>3</sub><sup>-</sup>, Na<sup>+</sup> and SO<sub>4</sub><sup>2-</sup> and its groundwater chemistry. The boreholes in this group are all found in and around irrigation farms (Lombard's Kraal, Blydskap and Hansrivier area) and the high NO<sub>3</sub><sup>-</sup> values are attributed to surface contamination through recharge of irrigation water. The distribution of the groundwater sample of this group corresponds to the anthropogenic factor spatial distribution shown in Figure 3.22.

Cluster CB3II illustrates further the importance of NO<sub>3</sub><sup>-</sup> in the separation of these groups. This cluster has also high values of Na<sup>+</sup> and SO<sub>4</sub><sup>2-</sup> like cluster CB2II but low values of K<sup>+</sup> and NO<sub>3</sub><sup>-</sup>. The groundwater chemistry is influenced by possible gypsum dissolution, reverse ion exchange, silicate weathering and evaporation and is similar to that of cluster CB2I with the exception of high Na<sup>+</sup> and SO<sub>4</sub><sup>2-</sup>. The groundwater in this group is generally used for drinking water although it tends to be slightly hard and its distribution corresponds to the Hardness factor distribution map in Figure 3.20.

High EC, TDS, Ca<sup>2+</sup>, Mg<sup>2+</sup> and Cl<sup>-</sup>, moderate K<sup>+</sup> and NO<sub>3</sub><sup>-</sup>, and low alkalinity

characterize cluster CB4II. The groundwater in this group is of the hard water type (Ca-Mg-Cl) and carbonate and silicate weathering, anthropogenic activities as well as evaporation influence its groundwater. The distribution of the groundwater samples in this group also correspond to the Hardness factor distribution map in Figure 3.20 with noticeably high alkali earth and chloride concentrations compared to cluster CB3II.

The four groups that resulted from further classification of cluster CB1I are displayed in Figure 3.27 against the discriminant functions.

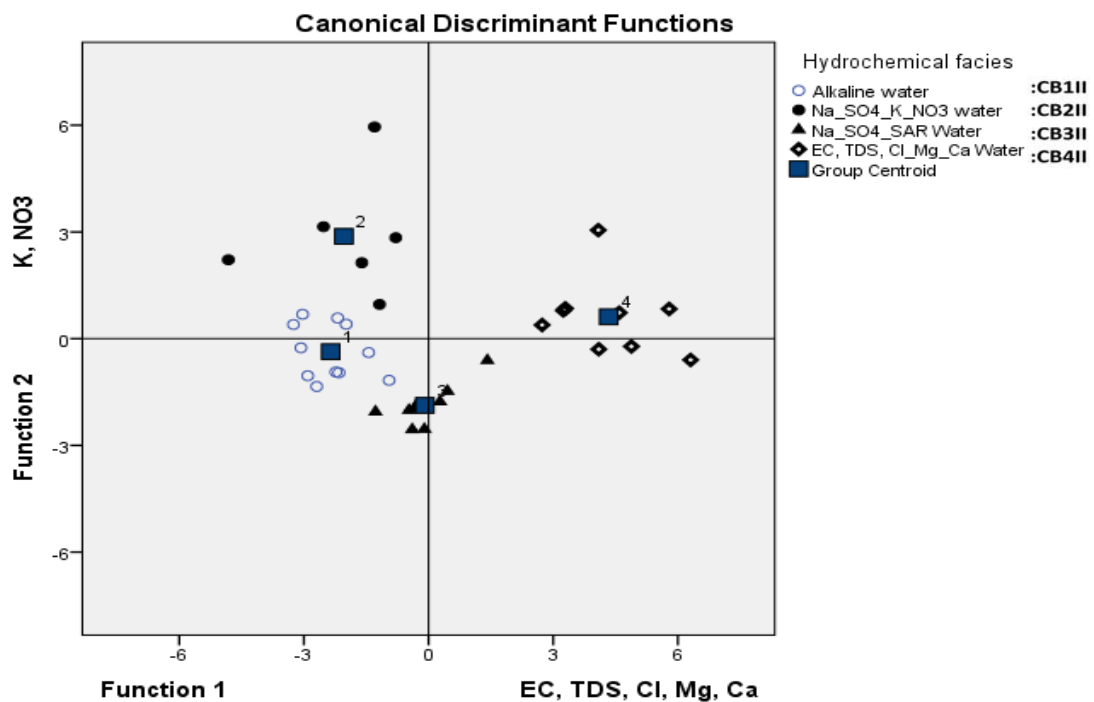


**Figure 3.27** Groundwater sample groups (CB1II, CB2II, CB3II and CB4II) vs. discriminant functions of Set B variables (BII).

Stepwise discriminant analysis of the variables in analysis 3 showed that EC, K<sup>+</sup>, pH, NO<sub>3</sub><sup>-</sup> separate these four hydrochemical facies up to 97.2% where EC alone discriminates the groups up to 61.1%.

### 3.2.4. Analysis 4: Set B

Further discriminant analysis of the fourteen variables used in Set B and the groups derived from them revealed six groups (CB1III, CB2III, CB3III, CB4III, CB5III and

CB6III). These six groundwater types are hydrochemically different and through linear discriminant analysis were verified to be 100% different from each other using all the available fourteen variables as shown in Table 3.31. Their structure matrix, group means of the functions and classification results are given in Tables 3.29, 3.30 and 3.31 respectively. The five functions that resulted from the discriminant analysis and their correlation to the variables are discussed below.

Function 1 is significantly negatively correlated to  $\text{NO}_3^-$  only. Function 2 is highly positively related to  $\text{Na}^+$ , TDS, EC,  $\text{SO}_4^{2-}$ ,  $\text{Cl}^-$ ,  $\text{Mg}^{2+}$ ,  $\text{Ca}^{2+}$  and SAR. Interestingly pH plays an important role and is highly positively correlated to function 3 only. Function 4 is negatively correlated to  $\text{K}^+$  only while function 5 is highly positively correlated to TA and  $\text{HCO}_3^-$ . Based on this structure matrix and the group centroids of each function, the groups are characterized as follows.

**Table 3.29 Structure matrix of Set B variables and their functions (BIII)**

	Function				
	1	2	3	4	5
$\text{NO}_3^-$	-0.667*	0.495	0.144	-0.011	0.129
$\text{Na}^+$	0.106	0.717*	-0.069	0.215	0.014
TDS	0.069	0.648*	-0.220	0.313	0.129
EC	0.043	0.581*	-0.145	0.070	0.205
$\text{SO}_4^{2-}$	0.072	0.433*	-0.122	0.233	0.011
$\text{Cl}^-$	0.013	0.404*	-0.059	0.092	0.364
$\text{TH}^b$	-0.10	0.338*	-0.094	0.208	0.100
$\text{Mg}^{2+}$	0.007	0.326*	-0.063	0.135	0.259
$\text{Ca}^{2+}$	-0.020	0.299*	-0.102	0.230	-0.027
SAR	0.039	0.264*	-0.042	-0.018	-0.112
pH	0.065	0.153	0.629*	-0.395	-0.041
$\text{K}^+$	0.037	0.063	0.110	-0.607*	-0.257
TA	0.038	0.107	-0.105	-0.012	0.320*
$\text{HCO}_3^-$	0.044	0.115	-0.102	-0.005	0.319*
Pooled within-groups correlations between discriminating variables and standardized canonical discriminant functions					
Variables ordered by absolute size of correlation within function					
*. Largest absolute correlation between each variable and any discriminant function					
<sup>b</sup> . This variable not used in the analysis					

Cluster CB1III is characterized by high  $\text{NO}_3^-$ , pH, TA and  $\text{HCO}_3^-$ . This group comprises the same groundwater samples belonging to cluster CB1II, from analysis 3, which was only characterized by TA and  $\text{HCO}_3^-$  in the previous analysis. This characteristic of pH

and  $\text{NO}_3^-$  reveals the influence of agricultural activity on the groundwater quality in addition to the alkalinity effect. This cluster's groundwater chemistry is influenced by carbonate and silicate weathering while the high  $\text{NO}_3^-$  and pH is an indication of the anthropogenic influence. The pH in this group also affects the dissolution and precipitation of carbonates.

**Table 3.30 Functions at Group Centroids of Set B variables (BIII)**

Predicted Group Analysis 4	Function				
	1	2	3	4	5
CB1II→CB1III	-0.920	-3.062	0.481	0.330	0.279
CB2II→CB2III	-1.765	-1.166	2.075	-1.563	-0.110
CB3II→CB3III	1.560	-1.269	0.472	0.594	-0.298
CB4II→CB4III	-2.539	-0.325	-2.750	-0.358	-0.046
CB2I→CB5III	5.114	3.757	0.060	-0.066	0.107
CB3I→CB6III	-15.810	7.535	1.617	0.794	0.003
Unstandardized canonical discriminant functions evaluated at group means					

Cluster CB2III is characterized by high  $\text{NO}_3^-$ ,  $\text{K}^+$  and pH. This cluster comprise the same groundwater samples belonging to cluster CB2II (analysis 3) with the exception of one sample (HR18) being predicted as belonging to cluster CB3III. The influence of  $\text{Na}^+$  and  $\text{SO}_4^{2-}$ , which were high in analysis 3, is not significant and puts anthropogenic influence as a dominant factor that influences the groundwater chemistry in addition to the rock-water interactions described for cluster CB2II. The significance of pH is an indication of its effect in rock water interaction. The distribution of the groundwater sample in this group corresponds to the anthropogenic factor spatial distribution shown in Figure 3.22.

Cluster CB3III is characterized by pH alone. This group comprise the groundwater samples of cluster CB3II (analysis 3) and an addition of sample HR18 from CB2II. This significance of pH indicates its effect on the possible gypsum dissolution, reverse ion exchange, silicate weathering and evaporation processes that showed high  $\text{Na}^+$  and  $\text{SO}_4^{2-}$  in analysis 3. The groundwater of the samples in this group is generally used for drinking water although it tends to be slightly hard and its distribution corresponds to the Hardness factor distribution map in Figure 3.20.

**Table 3.31 Classification Results of Set B variables (BIII) <sup>a</sup>**

		Predicted Group for Analysis 4	Predicted Group Membership					Total	
			CB1III	CB2III	CB3III	CB4III	CB5III		CB6III
Original	Count	CB1III) Alkaline water with high pH & NO <sub>3</sub> <sup>-</sup>	11	0	0	0	0	0	11
		CB2III) Na-SO <sub>4</sub> -K-NO <sub>3</sub> water	0	5	0	0	0	0	5
		CB3III) Na-SO <sub>4</sub> -SAR water	0	0	11	0	0	0	11
		CB4III)Hard (Ca-Mg-Cl) water	0	0	0	9	0	0	9
		CB5III) Hard and Alkaline	0	0	0	0	11	0	11
		CB6III) Hard water with NO <sub>3</sub> <sup>-</sup> > 50 mg/L	0	0	0	0	0	2	2
	%	CB1III) Alkaline water	100	0.0	0.0	0.0	0.0	0.0	100
		CB2III) Na-SO <sub>4</sub> -K-NO <sub>3</sub> water	0.0	100	0.0	0.0	0.0	0.0	100
		CB3III) Na-SO <sub>4</sub> -SAR water	0.0	0.0	100	0.0	0.0	0.0	100
		CB4III)Hard (Ca-Mg-Cl) water	0.0	0.0	0.0	100	0.0	0.0	100
		CB5III) Hard and Alkaline	0.0	0.0	0.0	0.0	100	0.0	100
		CB6III) Hard water with NO <sub>3</sub> <sup>-</sup> > 50 mg/L	0.0	0.0	0.0	0.0	0.0	100	100

<sup>a</sup>. 100% of original grouped cases correctly classified

Cluster CB4III is characterized by K<sup>+</sup> and NO<sub>3</sub><sup>-</sup>. This cluster consists of the same groundwater samples grouped in cluster CB4II that was characterized by high EC, TDS, Ca<sup>2+</sup>, Mg<sup>2+</sup> and Cl<sup>-</sup>, moderate K<sup>+</sup> and NO<sub>3</sub><sup>-</sup>, and low alkalinity. The significance of K<sup>+</sup> and NO<sub>3</sub><sup>-</sup> in this analysis indicates the dominance of silicate weathering and anthropogenic influence in relation to the other rock-water interaction processes while still contributing to the hardness of the water. The distribution of the groundwater samples in this group also correspond to the Hardness factor distribution map in Figure 3.20

Groups CB5III and CB6III are characterized exactly as the groups CB2I and CB3I (analysis 2) respectively. The Hard and Alkaline water type (CB5III) is attributed to groundwater chemistry resulting from carbonate and silicate weathering, halite and gypsum dissolution as well as ion exchange processes. The distribution of the groundwater samples in this group correspond to the Hardness factor distribution shown in Figure 3.20. Cluster CB6III's groundwater chemistry is attributed to the same hydrogeochemical processes that control the hydrochemistry of CB5III with significant anthropogenic influence. The anthropogenic influence is indicated by the higher than

WHO (1993)  $\text{NO}_3^-$  content ( $>50\text{mg/L}$ ) in the groundwater samples of these group (Nigrini Farm 2 and Steenrotsfontein 1).

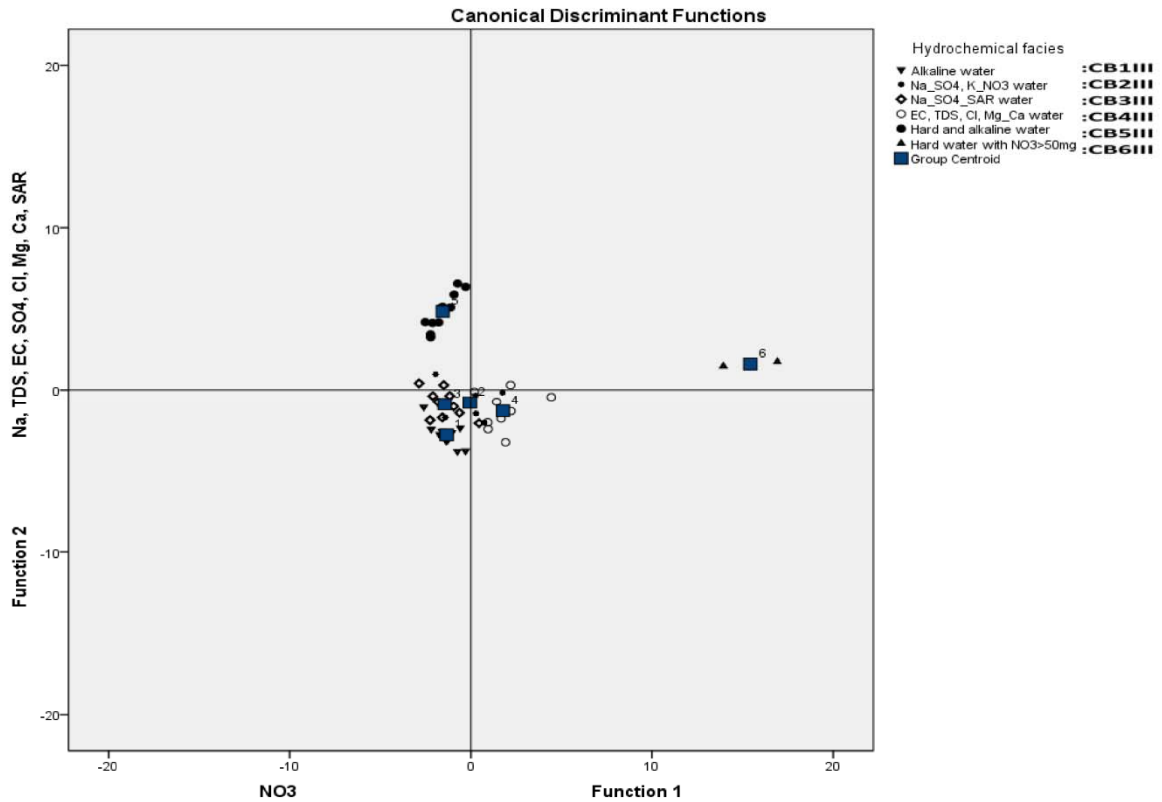


**Figure 3.28** Groundwater sample groups (CB1III, CB2III, CB3III, CB4III, CB5III and CB6III) vs. discriminant functions of Set B variables (BIII).

Since the direct discriminant function method does not show the importance of the individual chemical variables for the description of classified groups, or their importance in the classification itself, a stepwise discriminant method was considered. The result shows that  $\text{NO}_3^-$ ,  $\text{Na}^+$  and pH separate the six groups up to 93.9% with  $\text{NO}_3^-$  alone separating the groups up to 42.9%.

## Chapter IV

### Conclusion and recommendation

#### 1. Summary and conclusion

The aim of thesis was to assess the groundwater quality of the Beaufort West area using multivariate statistical and spatial analyses techniques. To realize this aim, the hydrochemical data was analysed using univariate, bivariate and multivariate statistical techniques in addition to conventional techniques. The analyses results were used to characterize the groundwater quality of the study area. The results of the multivariate statistical analyses were compared to conventional hydrogeochemical classification and interpretation methods and the outcomes were further analysed spatially to map the groundwater quality.

The pH of the groundwater samples was found to be alkaline and meets the WHO and South African drinking water criteria. The observed major ion concentrations is dominated by  $\text{Ca}^{2+}$ ,  $\text{Na}^+$ ,  $\text{Cl}^-$  and  $\text{HCO}_3^-$  and are noticeably higher than the SAWQG Target Water Quality and WHO concentrations except for the latter. About 29% of the groundwater samples have above minimum  $\text{Cl}^-$  and  $\text{SO}_4^{2-}$  WHO limit while about 27% of the groundwater samples have above minimum  $\text{Na}^+$  WHO limit. Most of the groundwater samples that showed high  $\text{Cl}^-$  and  $\text{SO}_4^{2-}$  concentrations are situated on the calcareous alluvial deposits, near hard pans, dry watercourses, irrigation farms and some of them in close proximity to the wastewater treatment plant. Only 4.08% of the groundwater samples showed  $\text{NO}_3^-$  values above the WHO limit and these samples are located near irrigation farms. In accordance to the high concentrations of the major ions, the TDS values for 93.878% and 61.22% of the groundwater samples is above the SAWQG and WHO limits respectively. Different classification methods of the groundwater samples based on TDS showed that only 8.2% of the water is desirable for drinking, 30.6% of the water is permissible while the remaining 61.2% of the water is brackish but useful for irrigation. Further classification of the groundwater based on TH, EC and percentage  $\text{Na}^+$  indicated that the water in the study area is characterized as

hard to very hard with low to medium salinity hazard and about 97% is useful for irrigation.

Significant correlation is noticed among many of the tested hydrochemical variables. The EC of these groundwater samples showed significant positive correlation with some of the hydrogeochemical variables such as  $\text{Cl}^-$ ,  $\text{SO}_4^{2-}$ ,  $\text{Mg}^{2+}$ ,  $\text{Ca}^{2+}$  and  $\text{Na}^+$ . This is an indication of the contribution of these ions to the hardness and salinity of the groundwater due to concentration of these ions from evaporation of recharge water and groundwater interaction with the geological formations. The positive correlation between  $\text{K}^+$  and pH is an indication of the anthropogenic effect on the groundwater of the study area. The influence of calcite, dolomite, halite and gypsum dissolution and silicate weathering as well as surface contamination on the groundwater chemistry is indicated by the significant positive correlations between the major ions  $\text{Ca}^{2+}$ ,  $\text{Mg}^{2+}$ ,  $\text{Cl}^-$ ,  $\text{SO}_4^{2-}$  and  $\text{Na}^+$ .

The linear relationships between the hydrochemical variables highlighted that the cations  $\text{Ca}^{2+}$  and  $\text{Mg}^{2+}$  and the anion  $\text{Cl}^-$  predict 100% and 89.5% of the TH of the groundwater respectively. This is an indication of the influence of carbonate and silicate weathering and halite dissolutions in the groundwater resulting in a Ca-Mg-Cl type of hard water. The cations  $\text{Mg}^{2+}$  and  $\text{Na}^+$  dominate the prediction of EC while  $\text{Na}^+$  is the major predictor of TDS. The anion  $\text{Cl}^-$  is the major predictor of EC and TDS and confirms the low to medium salinity hazard classification of the groundwater of the study area. On the other hand,  $\text{Na}^+$  and  $\text{Ca}^{2+}$  are the major cations that describe  $\text{HCO}_3^-$  variability while  $\text{Mg}^{2+}$  is the major predictor of  $\text{Cl}^-$  and  $\text{SO}_4^{2-}$ . This indicates the evolution of the groundwater from Ca-Na- $\text{HCO}_3$  recharge water to a hard Mg-Cl- $\text{SO}_4$ .

Conventional hydrogeochemical classification and interpretation of the groundwater samples using trilinear diagrams resulted in three hydrochemical facies: Ca- $\text{HCO}_3$ , Ca-Na-Cl- $\text{HCO}_3$  (Mixed water) and Ca-Cl. This illustrates the evolution of the groundwater from Ca- $\text{HCO}_3$  recharge water type to Ca-Cl hard water through carbonate dissolution and ion exchange processes. The majority of the groundwater remains as mixed water between the two ends. Most of the Ca- $\text{HCO}_3$  type water is situated near recharge areas such as the Nuweveld Mountains in the north, river downstream in the south and

dolerite outcrops. The chemical composition of this water type is attributed to carbonate dissolution. High  $\text{Ca}^{2+}$ ,  $\text{Na}^+$ ,  $\text{Cl}^-$  and  $\text{HCO}_3^-$  and mixing of different waters along the groundwater flow path, characterizes the Ca-Na-Cl-HCO<sub>3</sub> (Mixed water) water type. This water type is distributed along calcrete deposits, dolerite intrusions and the lithofeldspathic sandstones of the Teekloof formation and its chemical composition is attributed to a combination of carbonate dissolution, silicate weathering, ion exchange and halite dissolution. The Ca-Cl water type is characterized by calcrete deposits and its chemical composition is attributed to carbonate and halite dissolution followed by ion exchange processes. The mixed Groundwater type, Ca-Na-Cl-HCO<sub>3</sub> is the dominant water type in the study area representing about 67.4% of the total groundwater sample.

Major ion analysis of the groundwater samples using scatter plots revealed further the hydrogeochemical processes that control the groundwater chemistry of the study area. The TDS vs.  $\text{Na}^+ / (\text{Na}^+ + \text{Ca}^{2+})$  and TDS vs.  $\text{Cl}^- / (\text{Cl}^- + \text{HCO}_3^-)$  scatter plots showed that rock-water interaction is the dominant source of the groundwater chemistry with slight influence of evaporation. This is an indication of the weathering of the host rocks being the primary factor that controls the hydrochemistry of the groundwater in the study area.  $\text{Ca}^{2+} + \text{Mg}^{2+}$  vs.  $\text{HCO}_3^- + \text{SO}_4^{2-}$  scatter plot indicated that carbonate, sulphate minerals and silicates with some reverse ion exchange are the main source of these ions. Furthermore,  $\text{Ca}^{2+}$  vs.  $\text{HCO}_3^-$  scatter plot highlighted the dominance of calcite over dolomite in the carbonate dissolution as a source of these ions while  $\text{Ca}^{2+}$  vs.  $\text{SO}_4^{2-}$  indicated the contribution of gypsum for some of the samples. These scatter plots clearly indicate that the dissolution calcite and silicate minerals followed by ion exchange are the dominant geochemical processes that determine the sources of these major ions. The importance of silicate weathering (plagioclase and K-feldspars) and influence of ion exchange in contributing towards the major ion concentrations in the groundwater was analysed and confirmed further using a  $\text{Na}^+ + \text{K}^+$  vs.  $\text{TZ}^+$ ,  $\text{Ca}^{2+}$  vs.  $\text{TZ}^+$  and  $\text{Na}^+ - \text{Cl}^-$  vs.  $\text{Ca}^{2+} + \text{Mg}^{2+} - \text{HCO}_3^- - \text{SO}_4^{2-}$  scatter plots. The strong positive correlation between  $\text{Cl}^-$  and  $\text{SO}_4^{2-}$  is an indication of the effect of surface contamination on the groundwater chemistry of the study area as illustrated by the  $\text{Cl}^-$  vs.  $\text{SO}_4^{2-}$  scatter plot.

The spatial distribution of the major cations and anions with the exception of  $\text{HCO}_3^-$  showed higher concentrations on the calcrete deposits and the lithofeldspathic

sandstones of the Teekloof formation where there is contact with dolerite intrusions around the town of Beaufort West. These high concentrations are attributed to calcite dissolution, silicate weathering, ion exchange processes and evaporation. In addition to the geogenic contribution, the high  $\text{Cl}^-$  and  $\text{SO}_4^{2-}$  concentrations in the catchment J21A's downstream is attributed to possible contamination from domestic wastages and effluents from the sewerage works located in the catchment.

The  $\text{HCO}_3^-$  spatial distribution showed higher concentrations mainly in the lithofeldspathic sandstones of the sedimentary rocks as well as contact zones between these rock and the dolerite intrusions compared to the low-lying calcrete deposits. These high concentrations are ascribed to calcite dissolution and silicate weathering. The J21A quaternary catchment showed highest  $\text{HCO}_3^-$  concentration compared to the other catchments.

The spatial distribution of  $\text{K}^+$  and  $\text{NO}_3^-$  across the six catchments showed higher concentrations in areas with dense urbanization, commercial farms, game farms and sewerage works (quaternary catchments J21A and J21B). These high concentrations are attributed to the effect of domestic effluent and agricultural contaminants while silicate weathering and cation exchange processes in the lithofeldspathic sandstones of the Teekloof formation also contribute to the observed high  $\text{K}^+$  concentrations.

Further multivariate statistical analyses of the groundwater samples of the study area rendered deeper insight in to the hydrogeochemical processes that control the groundwater quality. These techniques supplemented the above discussed conclusion and highlighted the shortcomings of some of the conventional hydrogeochemical analyses techniques.

Factor analysis reduced the multivariate hydrochemical variables in to three factors with Eigenvalues  $\geq 1$  explaining 85.086% of the variance. The total variance explained by these three factors; factor 1, factor 2 and factor 3 are 59.124%, 16.564% and 9.397% respectively. These three factors are characterized by different hydrochemical variables depending on the prevailing hydrogeochemical and anthropogenic processes.

Factor 1 (Hardness) is characterized by  $\text{Ca}^{2+}$ ,  $\text{Mg}^{2+}$ ,  $\text{Na}^+$ ,  $\text{Cl}^-$  and  $\text{SO}_4^{2-}$  and explains the hardness and salinity of the groundwater due to carbonate, silicate, gypsum and halite

dissolution as well as infiltration of concentrated saline surface water resulting from evaporation.

Factor 2 (Alkalinity) is characterized by  $\text{HCO}_3^-$  and TA and explains the alkalinity of the groundwater due to carbonate and silicate weathering processes resulting in alkali carbonates and bicarbonates.

Factor 3 (Anthropogenic) is characterized by  $\text{K}^+$  and  $\text{NO}_3^-$  and explains the effect of human activities on groundwater quality in addition to that of silicate weathering of the lithofeldspathic sandstones. The J21A, J21B and J21C quaternary catchments, especially areas around wastewater treatment and informal settlement show highest distribution of this factor. Catchments L11F and L11G, where both animal and olive farming are practiced show also high anthropogenic factor scores.

Ultimately, the groundwater samples were classified in to specific hydrochemical facies based on the results discussed above using a combination of cluster and discriminant analyses. Comparison of these classification methods with conventional hydrogeochemical classification methods showed the importance and advantages of multiple hydrochemical variables in characterizing the groundwater types. The first classification using the trilinear diagram interpretation variables resulted in three-hydrochemical facies that are similar to the trilinear classification, with one group comprising about 65% of the samples. The second classification using twice the number of the original hydrochemical variables resulted in the classification of the groundwater into six hydrochemical facies. This new classification is attributed to the significant roles of hydrochemical variables such pH and  $\text{NO}_3^-$ , not considered in the trilinear classification method, as well as the use of the raw data values in comparison to percentage meq/L values of the variables.

The six-hydrochemical facies denoted as CB1III, CB2III, CB3III, CB4III, CB5III and CB6III are characterized by different hydrochemical variables depending on the prevailing hydrogeochemical and anthropogenic processes that control the groundwater chemistry.

Cluster CB1III is characterized by high  $\text{NO}_3^-$ , pH, TA and  $\text{HCO}_3^-$ . This characteristic of pH and  $\text{NO}_3^-$  reveals the influence of agricultural activity on the groundwater quality in

addition to the alkalinity effect. Carbonate and silicate weathering and the high  $\text{NO}_3^-$  influence this cluster's groundwater chemistry and the high pH is an indication of the anthropogenic influence. The pH in this group also affects the dissolution and precipitation of carbonates.

Cluster CB2III is characterized by high  $\text{NO}_3^-$ ,  $\text{K}^+$  and pH. The influence of anthropogenic processes is the dominant factor that influences the groundwater chemistry in addition to the rock-water interactions described. The significance of pH is an indication of its effect in the rock water interaction. The distribution of the groundwater sample in this group corresponds to the anthropogenic factor spatial distribution.

Cluster CB3III is characterized by pH alone. This significance of pH indicates its effect on the possible gypsum dissolution, reverse ion exchange, silicate weathering and evaporation processes that showed high  $\text{Na}^+$  and  $\text{SO}_4^{2-}$ . The groundwater in this group is generally used for drinking tends to be slightly hard and its distribution corresponds to the Hardness factor distribution map.

Cluster CB4III is characterized by  $\text{K}^+$  and  $\text{NO}_3^-$ . The significance of  $\text{K}^+$  and  $\text{NO}_3^-$  in this analysis indicates the dominance of silicate weathering and anthropogenic influence in relation to the other rock-water interaction processes while still contributing to the hardness of the water. The distribution of the groundwater samples in this group also correspond to the Hardness factor distribution map

Cluster CB5III is characterized as a Hard and Alkaline water type, which is attributed to groundwater chemistry resulting from carbonate and silicate weathering, halite and gypsum dissolution as well as ion exchange processes. The distribution of the groundwater samples in this group correspond to the Hardness factor distribution.

Cluster CB6III's groundwater chemistry is attributed to the same hydrogeochemical processes that control the hydrochemistry of CB5III with significant anthropogenic influence. The anthropogenic influence is indicated by the higher than WHO  $\text{NO}_3^-$  content ( $>50\text{mg/L}$ ) in the groundwater samples of these group (Nigrini Farm 2 and Steenrotsfontein 1).

Stepwise discriminant analysis of the above six hydrochemical facies revealed that  $\text{NO}_3^-$ ,  $\text{Na}^+$  and pH alone separate the six groups up to 93.9% with  $\text{NO}_3^-$  alone separating the groups up to 42.9%. This highlights the significance of this hydrochemical variable in the classification of the hydrochemical facies, which could not be obtained using conventional methods.

Ultimately, the assessment of the groundwater of the study area explained the important hydrogeochemical processes that control the groundwater chemistry. This assessment classified the groundwater as hard to very hard water with low to medium salinity and useful for irrigation. Multivariate statistical and spatial analyses revealed the complex hydrogeochemical and anthropogenic processes and characterized the groundwater quality based on the influences of these processes. These characterizations of the groundwater in the study area show that many of the groundwater samples are not fit for drinking purpose in the presence of alternative water supply.

## 2. Recommendation

Based on the findings of this assessment, it is recommended that the Local Municipality of Beaufort West needs to treat the groundwater supplied from these boreholes before using it for domestic purposes. Suitable strategies to groundwater recharge, controlled groundwater usage, measures to reduce ground water pollution and awareness of the importance of water quality for private borehole users and owners are recommended.

In light of the small number of boreholes sampled and their uneven distribution, further investigation of the groundwater in the study area and better sampling distribution is recommended for detailed characterization of the aquifers and their water quality.

## List of References

- Adhikary, P., Chandrasekharan, H., Chakraborty, D., Kumar, B., & Yadav, B.R. (2009). Statistical approaches for hydrogeochemical characterization of groundwater in west delhi, india. *Environmental Monitoring and Assessment*, 154(1-4), 41-52. doi: 10.1007/s10661-008-0376-5
- Afifi, A.A., & Clark, V. (1990). *Computer-aided multivariate analysis* (2<sup>nd</sup> ed.). New York: Van Nostrand Reinhold Company.
- Allaby, A., & Allaby, M. (Eds.). (2008). *A dictionary of earth sciences*. Great Clarendon Street, Oxford: Oxford University Press.
- Appelo, C.A.J., & Postma, D. (2010). *Geochemistry, groundwater and pollution* Taylor & Francis.
- Back, W. (1960). Origin of hydrochemical facies of ground water in the Atlantic coastal plain. *Proceedings of 21st International Geological Congress, Copenhagen*, 87-95.
- Back, W. (1961). Techniques for mapping of hydrochemical facies. *US Geol Surv Prof Pap*, 424, 380-382.
- Back, W. (1966). *Hydrochemical facies and ground-water flow patterns in northern part of Atlantic coastal plain* (498A ed.) US Government Printing Office.
- Back, W., & Hanshaw, B.B. (1965). Chemical geohydrology. *Advances in Hydroscience*, 2, 49-109.
- Bartarya, S.K. (1993). Hydrochemistry and rock weathering in a sub-tropical lesser Himalayan river basin in Kumauni, India. *Journal of Hydrology*, 146(0), 149-174. [http://dx.doi.org/10.1016/0022-1694\(93\)90274-D](http://dx.doi.org/10.1016/0022-1694(93)90274-D)
- Beaufort West Municipality. Engineering - sewerage. Retrieved 09/02, 2013, from [http://www.beaufortwestmun.co.za/engineering/eng\\_sewerage.html](http://www.beaufortwestmun.co.za/engineering/eng_sewerage.html)
- Bodin, J., Delay, F., & De Marsily, G. (2003). Solute transport in a single fracture with negligible matrix permeability: 1. fundamental mechanisms. *Hydrogeology Journal*, 11(4), 418-433.
- Botha, J.F., Verwey, J.P., van der Voort, I., Vivier, J.J.P., Buys, J., Colliston, W.P., & Looek, J.C. (1998). *Karoo aquifers: Their geology, geometry and physical properties*. (Standard Research Report No. WRC 487/1/98). Pretoria, South Africa: Water Research Commission.
- Boyacioglu, H., Boyacioglu, H., & Gunduz, O. (2005). Application of factor analysis in the assessment of surface water quality in buyuk menderes river basin.

*European Water*, 9, 10.

Calmbach, L. (1997). *Aquachem* (3.7.42 ed.). Waterloo, Ontario, Canada, N2L 3L3: Waterloo Hydrogeologic.

Cardona, A., Carrillo-Rivera, J., Huizar-Álvarez, R., & Graniel-Castro, E. (2004). Salinization in coastal aquifers of arid zones: An example from Santo Domingo, Baja California Sur, Mexico. *Environmental Geology*, 45(3), 350-366. doi:10.1007/s00254-003-0874-2

Carlyle, H.F., Tellam, J.H., & Parker, K.E. (2004). The use of laboratory-determined ion exchange parameters in the predictive modelling of *Karoo aquifers: Their geology, geometry and physical properties* field-scale major cation migration in groundwater over a 40-year period. *Journal of Contaminant Hydrology*, 68(1-2), 55-81. [http://dx.doi.org/10.1016/S0169-7722\(03\)00125-6](http://dx.doi.org/10.1016/S0169-7722(03)00125-6)

Cattell, R.B. (1978). *The scientific use of factor analysis in behavioral and life sciences* Plenum Press New York.

Catuneanu, Hancox, & Rubidge. (1998). Reciprocal flexural behaviour and contrasting stratigraphies: A new basin development model for the Karoo retroarc foreland system, South Africa. *Basin Research*, 10(4), 417-439. doi:10.1046/j.1365-2117.1998.00078.x

Catuneanu, O., Wopfner, H., Eriksson, P. G., Cairncross, B., Rubidge, B.S., Smith, R.M.H., & Hancox, P.J. (2005). The Karoo basins of south-central Africa. *Journal of African Earth Sciences*, 43(1-3), 211-253. <http://dx.doi.org/10.1016/j.jafrearsci.2005.07.007>

Cederstrom, D.J. (1946). Genesis of ground waters in the coastal plain of Virginia. *Economic Geology*, 41(3), 218-245. doi:10.2113/gsecongeo.41.3.218

Chen, K., Jiao, J.J., Huang, J., & Huang, R. (2007). Multivariate statistical evaluation of trace elements in groundwater in a coastal area in Shenzhen, China. *Environmental Pollution*, 147(3), 771-780. doi:<http://dx.doi.org/10.1016/j.envpol.2006.09.002>

Chevalier, L., Goedhart, M., & Woodford, A.C. (2001). *The influences of dolerite sill and ring complexes on the occurrence of groundwater in Karoo fractured aquifers: A morpho-tectonic approach*. (Standard Research Report No. WRC 937/1/01). Pretoria, South Africa: Water Research Commission.

Chevallier, L., & Woodford, A. (1999). Morpho-tectonics and mechanism of emplacement of the dolerite rings and sills of the western Karoo, South Africa. *South African Journal of Geology*, 102(1), 43-54.

Clausen, F., & Harpøth, O. (1983). On the use of discriminant analysis techniques for classifying chemical data from panned heavy—mineral concentrates—Central

east greenland. *Journal of Geochemical Exploration*, 18(1), 1-24.

Cloutier, V., Lefebvre, R., Therrien, R., & Savard, M.M. (2008). Multivariate statistical analysis of geochemical data as indicative of the hydrogeochemical evolution of groundwater in a sedimentary rock aquifer system. *Journal of Hydrology*, 353(3-4), 294-313. <http://dx.doi.org/10.1016/j.jhydrol.2008.02.015>

Cohen, J., Cohen, P., West, S.G., & Aiken, L.S. (2013). *Applied multiple regression/correlation analysis for the behavioral sciences* Routledge.

Colby, N.D. (1993). The use of 2-way cluster analysis as a tool for delineating trends in hydrogeologic units and development of a conceptual model. *International Ground Water Modeling Center (IGWMC), Proceedings of the 1993 Ground Water Modeling Conference*, 91-100.

Cole, D.I. (1998). In Wilson, M.G.C. & Anhaeusser, C.R. (Ed.), *The mineral resources of south africa. handbook* (pp. 642-652) Council for Geoscience.

Cole, D.I. and Labuschagne, L.S. (1985). Geological environments of uranium deposits in the beaufort group, south africa. In IAEA (Ed.), *Geological environments of sandstone-type uranium deposits: Report of the working group on uranium geology organized by the international atomic energy agency* (IAEA-TECDOC-328 ed., pp. 265). Vienna: International Atomic Energy Agency.

Cook, P.G. (2003). *A guide to regional groundwater flow in fractured rock aquifers*. South Australia: Seaview Press, CSIRO.

Dalton, M.G., & Upchurch, S.B. (1978). Interpretation of hydrochemical facies by factor analysis. *Ground Water*, 16(4), 228-233.

Das, B., & Kaur, P. (2001). Major ion chemistry of renuka lake and weathering processes, sirmaur district, himachal pradesh, india. *Environmental Geology*, 40(7), 908-917. doi:10.1007/s002540100268

Datta, P., & Tyagi, S. (1996). Major ion chemistry of groundwater in delhi area: Chemical weathering processes and groundwater flow regime. *Journal-Geological Society of India*, 47, 179-188.

Davis, J.C. (1973). *Statistics and data analysis in geology*. New York: John Wiley & Sons, Inc.

Davis, S.N., & DeWiest, R.J. (1966). *Hydrogeology*. New York: Wiley.

Department of Water Affairs and Forestry (DWAF). (1996). In Holmes S. (Ed.), *South african water quality guidelines* (2<sup>nd</sup> ed.). Vol. 1: Domestic Use. Pretoria: Department of Water Affairs and Forestry.

Domenico, P.A. (1972). *Concepts and models in groundwater hydrology* McGraw-

Hill New York.

- Durbin, J., & Watson, G.S. (1971). Testing for serial correlation in least squares regression.III. *Biometrika*, 58(1), 1-19. doi:10.1093/biomet/58.1.1
- Durov, S.A. (1948). Natural waters and graphic representation of their composition. *Dokl. Akad. Nauk USSR*, 59(8) 90.
- Department of Water Affairs and Forrestry (DWAf). (2002). 1:500000 *Hydrogeological Map Series 3122 of Beaufort West*. Pretoria: Department of Water Affairs.
- Department of Water Affairs and Forrestry (DWAf). (2005). *Groundwater resources assessment: Phase 2*. Pretoria: Department of Water Affairs.
- Earth Satellite Corporation (EarthSat) (2005). Africa (150m) – EarthSat NaturalVue Global Landsat Mosaic. 2005-04-01, ESRI® Data & Maps, Redlands, California, USA.
- Elango, L., & Kannan, R. (2007). Rock–water interaction and its control on chemical composition of groundwater. In D. Sarkar, R. Datta & R. Hannigan (Eds.), *Developments in environmental science* (Vol 5 ed., pp. 229-243) Elsevier. [http://dx.doi.org/10.1016/S1474-8177\(07\)05011-5](http://dx.doi.org/10.1016/S1474-8177(07)05011-5)
- Farnham, I. M., Singh, A. K., Stetzenbach, K.J., & Johannesson, K.H. (2002). Treatment of nondetects in multivariate analysis of groundwater geochemistry data. *Chemometrics and Intelligent Laboratory Systems*, 60(1–2), 265-281. [http://dx.doi.org/10.1016/S0169-7439\(01\)00201-5](http://dx.doi.org/10.1016/S0169-7439(01)00201-5)
- Fetter, C.W. (2001). *Applied hydrogeology* (4<sup>th</sup> ed.). Upper Saddle River, New Jersey: Prentice Hall Inc.
- Fisher, R.S., & Mullican, I.,W. (1997). Hydrochemical evolution of sodium-sulfate and sodium-chloride groundwater beneath the northern chihuahuan desert, trans-pecos, texas, USA. *Hydrogeology Journal*, 5(2), 4-16. doi:10.1007/s100400050102
- Freez, R.A., & Cherry, J.A. (1979). *Groundwater*. New Jersey: Prentice Hall Inc.
- Garrels, R.M., & Mackenzie, F.T. (1971). *Evolution of sedimentary rocks* Norton New York.
- Gibbs, R.J. (1970). Mechanisms controlling world water chemistry. *Science*, 170(3962), 1088-1090. doi:10.1126/science.170.3962.1088
- GISCOE (2005) 1:250 000 Geological Map Series 3222 of Beaufort West. Council of Geosciences.

- Gomo, M., Tonder, G.J., & Steyl, G. (2013). Investigation of the hydrogeochemical processes in an alluvial channel aquifer located in a typical karoo basin of southern africa. *Environmental Earth Sciences*, 70(1), 227-238.  
doi:10.1007/s12665-012-2118-9
- Gomo, M., & Vermeulen, D. (2013). Investigation of hydrogeochemical processes in groundwater resources located in the vicinity of a mine process water dam. *Journal of African Earth Sciences*, 86(0), 119-128.  
<http://dx.doi.org/10.1016/j.jafrearsci.2013.06.010>
- Guo, H., & Wang, Y. (2004). Hydrogeochemical processes in shallow quaternary aquifers from the northern part of the datong basin, china. *Applied Geochemistry*, 19(1), 19-27.
- Hair, J.F., Anderson, R.E., Tatham, R.L., & Black, W.C. (1998). Multivariate analysis. *Englewood: Prentice Hall International*
- Hanshaw, B.B., Back, W., & Deike, R.G. (1971). A geochemical hypothesis for dolomitization by ground water. *Economic Geology*, 66(5), 710-724.  
doi:10.2113/gsecongeo.66.5.710
- Haran, A.V.L.N.S.H.H. (2002). Evaluation of drinking water quality at jalaripeta village of visakhapatnam district, andhra pradesh. *Nature, Environment and Pollution Technology*, 1(4), 407-410.
- Harman, H.H. (Ed.). (1967). *Modern factor analysis* (2nd ed.). Chicago, Ill.: University of Chicago Press.
- Hem, J.D. (1970). *Study and interpretation of the chemical characteristics of natural water*. U. S. Geology Survey Water-Supply Paper. (pp.263).
- Hem, J.D. (1985). *Study and interpretation of the chemical characteristics of natural water* Department of the Interior, US Geological Survey.
- Hiscock, K.M. (2005). *Hydrogeology : Principles and practice*. Malden, MA: Blackwell Pub.
- Holland, H.D. (1978). *The chemistry of the atmosphere and oceans*. New York: Wiley.
- IBM (2012). *SPSS statistics for windows* (21<sup>st</sup> ed.). Armonk, New York: IBM Corp.
- Jain, C., Kumar, C., & Sharma, M. (2003). Ground water quality in ghataprabha command area, karnataka. *Indian Journal of Environment and Ecoplanning*, 7(2), 251-262.
- Jankowski, J., & Acworth, R.I. (1997). Impact of debris-flow deposits on hydrogeochemical processes and the development of dryland salinity in the yass

river catchment, new south wales, australia. *Hydrogeology Journal*, 5(4), 71-88.  
doi:10.1007/s100400050119

Johnson, M. (1976). Stratigraphy and sedimentology of the cape and karoo sequences in the eastern cape province. Dissertation, Rhodes University

Johnson, M.R., Vuuren, C.J.V., Visser, J.N.J., Cole, D.I., Wickens, H.D.V., Christie, A.D. M., & Roberts, D.L. (1997). Chapter 12 the foreland karoo basin, south africa. *Sedimentary basins of the world* (pp. 269-317) Elsevier.  
doi:10.1016/S1874-5997(97)80015-9

Johnson, M.R., Van Vuuren, C.J., Visser, J.N.J., Cole, D.I., Wickens, H. de V., Christie, A.D.M., Roberts, D.L., Brandl, G. (2006). Sedimentary rocks of the karoo supergroup. In M.R. Johnson, C.R. Anhaeusser & R.J. Thomas (Eds.), *The geology of south africa* (pp. 461-499). Johannesburg/Pretoria: Geological Society of South Africa/Council for Geoscience.

Johnson, R., & Wichern, D. (1992). *Applied multivariate statistical methods*. Englewood Cliffs, N.J.: Prentice-Hall.

Joseph, K., & Jaiprakash, G. (2000). An integrated approach for management of total dissolved solids in hosiery dyeing effluents. *Journal of Indian Association for Environmental Management*, 27(3), 203-207.

Katz, B.G., Coplen, T.B., Bullen, T.D., & Davis, J.H. (1997). Use of chemical and isotopic tracers to characterize the interactions between ground water and surface water in mantled karst. *Ground Water*, 35(6), 1014-1028. doi:10.1111/j.1745-6584.1997.tb00174.x

Kline, P. (1994). *An easy guide to factor analysis*. New York: Routledge.

Kotze, J.C., Pointer, C., & Rosewarne, P.N. (1997). *Beaufort west municipality assessment of the hydrogeological potential of the brandwacht aquifer phase 2 (update of report 227331/1)*. ( No. 227331/2). Cape Town: Steffen Robertson and Kirsten.

Kovalevsky, V.S., Kruseman, G.P., & Rushton, K.R. (2004). *Groundwater studies: An international guide for hydrogeological investigations*. Paris: UNESCO.

Kumar, M., Ramanathan, A., Rao, M., & Kumar, B. (2006). Identification and evaluation of hydrogeochemical processes in the groundwater environment of delhi, india. *Environmental Geology*, 50(7), 1025-1039.

Lakshmanan, E., Kannan, R., & Kumar, M. S. (2003). Major ion chemistry and identification of hydrogeochemical processes of ground water in a part of kancheepuram district, tamil nadu, india. *Environmental Geosciences*, 10(4), 157-166.

- Lambrakis, N., Antonakos, A., & Panagopoulos, G. (2004). The use of multicomponent statistical analysis in hydrogeological environmental research. *Water Research*, 38(7), 1862-1872. doi:<http://dx.doi.org/10.1016/j.watres.2004.01.009>
- Lawrence, F.W., & Upchurch, S.B. (1982). Identification of recharge areas using geochemical factor analysis. *Ground Water*, 20(6), 680-687.
- Levin, M. (1983). *Field manual for geohydrological sampling as applied to the radioactive waste disposal program* Nuclear Development Corporation of South Africa.
- Liu, C., Lin, K., & Kuo, Y. (2003). Application of factor analysis in the assessment of groundwater quality in a blackfoot disease area in taiwan. *Science of the Total Environment*, 313(1-3), 77-89. doi:[http://dx.doi.org/10.1016/S0048-9697\(02\)00683-6](http://dx.doi.org/10.1016/S0048-9697(02)00683-6)
- Love, D., & Hallbauer, D.K. (1998). Characterisation of groundwater contamination in a dolomitic aquifer: A case study from the far west rand. *Geocongress 98, Geological Society of South Africa*, Pretoria, South Africa. 272-275.
- Love, D., Hallbauer, D., Amos, A., & Hranova, R. (2004). Factor analysis as a tool in groundwater quality management: Two southern african case studies. *Physics and Chemistry of the Earth, Parts A/B/C*, 29(15-18), 1135-1143. doi:<http://dx.doi.org/10.1016/j.pce.2004.09.027>
- Manly, B.F.J. (1994). *Multivariate statistical methods: A primer* (2<sup>nd</sup> ed.). New York: Chapman & Hall.
- Martínez, D., & Bocanegra, E. (2002). Hydrogeochemistry and cation-exchange processes in the coastal aquifer of mar del plata, argentina. *Hydrogeology Journal*, 10(3), 393-408. doi:10.1007/s10040-002-0195-7
- Matalas, N.C., & Reihner, B.J. (1967). Some comments on the use of factor analyses. *Water Resources Research*, 3(1), 213-223. doi:10.1029/WR003i001p00213
- Matthess, G. (1982). *Properties of groundwater*. New York: John Wiley, p 498.
- Mayo, A.L., & Loucks, M.D. (1995). Solute and isotopic geochemistry and ground water flow in the central wasatch range, utah. *Journal of Hydrology*, 172(1-4), 31-59. [http://dx.doi.org/10.1016/0022-1694\(95\)02748-E](http://dx.doi.org/10.1016/0022-1694(95)02748-E)
- Melloul, A., & Collin, M. (1992). The 'principal components' statistical method as a complementary approach to geochemical methods in water quality factor identification; application to the coastal plain aquifer of israel. *Journal of Hydrology*, 140(1-4), 49-73. [http://dx.doi.org/10.1016/0022-1694\(92\)90234-M](http://dx.doi.org/10.1016/0022-1694(92)90234-M)
- Meyer, S.L. (1975). *Data analysis for scientists and engineers*. New York: Wiley.

- Middleton, B.J., & Bailey, A.K. (2008). *Water resources of south africa, 2005 study (WR2005)*. (Standard Research Report No. WRC TT381/08). Pretoria: Water Research Commission.
- Nhleko, L., & Dondo, C. (2008). *The hydrogeology of beaufort west*. (Project No. ST-2008-0974 Report No. 2008-0050). South Africa: Council for Geoscience.
- Nordstrom, D.K., & Wilde F.D. (2005). Reduction oxidation potential (electrode method) (ver. 1.2): U.S. Geological Survey Techniques of Water-Resource Investigations, book 9, Chap. A6., sec. 6.5, (July 2013), accessed from [http://water.usgs.gov/owq/FieldManual/Chapter6/6.5\\_\\_contents.html](http://water.usgs.gov/owq/FieldManual/Chapter6/6.5__contents.html) (July 01, 2013).
- Olmez, I., Beal, J.W., & Villaume, J.F. (1994). A new approach to understanding multiple-source groundwater contamination: Factor analysis and chemical mass balances. *Water Research*, 28(5), 1095-1101. [http://dx.doi.org/10.1016/0043-1354\(94\)90195-3](http://dx.doi.org/10.1016/0043-1354(94)90195-3)
- Parsons, A., & Abrahams, A. (1994). Geomorphology of desert environments. In A. Abrahams, & A. Parsons (Eds.), (pp. 13) Springer Netherlands. doi:10.1007/978-94-015-8254-4\_1
- Patrick, M., Almond, J., Atwell, M., Gray, J., & Manhire, T. (2010). Scoping heritage impact assessment mainsteam renewable energy facilities: Land Parcel Beaufort West. Report prepared for Environmental Resource Management.
- Piper, A. M. (1944). A graphic procedure in the geochemical interpretation of water-analyses. *Transactions, American Geophysical Union*, 25, 914-928.
- Ragno, G., Luca, M.D., & Ioele, G. (2007). An application of cluster analysis and multivariate classification methods to spring water monitoring data. *Microchemical Journal*, 87(2), 119-127.
- Raju, N.J. (2006). Seasonal evaluation of hydro-geochemical parameters using correlation and regression analysis. *Current Science-Bangalore-*, 91(6), 820.
- Reghunath, R., Murthy, T.R.S., & Raghavan, B.R. (2002). The utility of multivariate statistical techniques in hydrogeochemical studies: An example from karnataka, india. *Water Research*, 36(10), 2437-2442. [http://dx.doi.org/10.1016/S0043-1354\(01\)00490-0](http://dx.doi.org/10.1016/S0043-1354(01)00490-0)
- Reimann, C., Filzmoser, P., Garrett, R., & Dutter, R. (2008). *Statistical data analysis explained: Applied environmental statistics with R*. John Wiley & Sons.
- Rose, R. (2008). *Aquifer characterisation and groundwater flow regimes of karoo aquifers in beaufort west, western cape province*. (GEOSS Report No.: G2008/07-01).GEOSS.

- Rose, R., & Conrad, J. (2007). *A regional reconnaissance to identify areas for groundwater development in beaufort west*. (GEOSS Report No.: G2007/05-03).GEOSS.
- Rubidge, B.S. (1995). Biostratigraphy of the beaufort group(karoo supergroup). *Biostratigraphic Series*, (1), 46. Council for Geoscience, Pretoria.
- Rummel, R.J. (1988). *Applied factor analysis*. Northwestern University Press.
- SABS. (2001). *Specifications for drinking water* (5<sup>th</sup> ed.). SANS-241. Pretoria: South African Bureau of Standards. pp. 9.
- Saleem, A., Dandigi, M.N., & Kumar, K.V. (2013). Correlation-regression model for physico-chemical quality of groundwater in the south indian city of gulbarga. *African Journal of Environmental Science and Technology*, 6(9), 353-364.
- Sami, K. (1992). Recharge mechanisms and geochemical processes in a semi-arid sedimentary basin, eastern cape, south africa. *Journal of Hydrology*, 139(1-4), 27-48. [http://dx.doi.org/10.1016/0022-1694\(92\)90193-Y](http://dx.doi.org/10.1016/0022-1694(92)90193-Y)
- Sánchez-Martos, F., Jiménez-Espinosa, R., & Pulido-Bosch, A. (2001). Mapping groundwater quality variables using PCA and geostatistics: A case study of bajo andarax, southeastern spain. *Hydrological Sciences Journal*, 46(2), 227-242. doi:10.1080/02626660109492818
- Sawyer, C.N., & McCarty, P.L. (1967). *Chemistry for sanitary engineers* (2<sup>nd</sup> edn.). New York: Education, McGraw-Hill.
- Schoeller, H.J. (1977). *Geochemistry of groundwater studies: An international guide for research and practice*. (Technical Papers: Hydrology). Paris: UNESCO.
- Schot, P.P., & van der Wal, J. (1992). Human impact on regional groundwater composition through intervention in natural flow patterns and changes in land use. *Journal of Hydrology*, 134(1-4), 297-313. [http://dx.doi.org/10.1016/0022-1694\(92\)90040-3](http://dx.doi.org/10.1016/0022-1694(92)90040-3)
- Schuh, W., Klinkebiel, D., Gardner, J., & Meyer, R. (1997). Tracer and nitrate movement to groundwater in the northern great plains. *Journal of Environmental Quality*, 26(5), 1335-1347.
- Siad, A. (1991). Multivariate statistical techniques used to enhance interpretation of geochemical data from West African lateritic soils. Proc. "Eurolat 91 " 5th International meeting", August 23-24, 1991, Berlin, Germany. pp. 164-171.
- Siad, A.M. (1994). *Geomathematical evaluation of trace element patterns in lateritic soils above late proterozoic basement units of nigeria, west africa*. (PhD, Technische Universität Berlin). *Berliner Geowiss. Abh., A*, 159, 122 Pp., Berlin.

- Siad, A.M., Matheis, G., Utke, A., & Burger, H. (1994). Discriminant analysis as a geochemical mapping technique for lateritic covered areas of southwestern and central nigeria. *ITC Journal*, (1), 7-12.
- Smith, P.A., Alexander, W.R., Kickmaier, W., Ota, K., Frieg, B., & McKinley, I.G. (2001). Development and testing of radionuclide transport models for fractured rock: Examples from the Nagra/JNC radionuclide migration programme in the grimsel test site, switzerland. *Journal of Contaminant Hydrology*, 47(2-4), 335-348. doi:[http://dx.doi.org/10.1016/S0169-7722\(00\)00161-3](http://dx.doi.org/10.1016/S0169-7722(00)00161-3)
- Sneath, P.H.A., & Sokal, R.R. (1973). *Numerical taxonomy. the principles and practice of numerical classification*. San Francisco, W.H.: Freeman and Company.
- Soldić-Aleksić, J. Đ. (2001). An application of discriminant analysis and artificial neural networks to classification problems. *Yugoslav Journal of Operations Research*, 11(1), 113-122.
- Spies, J.J., & Du Plessis, D.C. (1976). *Standard encyclopaedia of southern africa*. Elsies River, Cape Town: National Book Printers Ltd.
- Stallard, R.F., & Edmond, J.M. (1983). Geochemistry of the amazon: 2. the influence of geology and weathering environment on the dissolved load. *Journal of Geophysical Research: Oceans*, 88(C14), 9671-9688. doi:10.1029/JC088iC14p09671
- Steinhorst, R.K., & Williams, R.E. (1985). Discrimination of groundwater sources using cluster analysis, MANOVA, canonical analysis and discriminant analysis. *Water Resources Research*, 21(8), 1149-1156. doi:10.1029/WR021i008p01149
- Stiff Jr, H. (1951). The interpretation of chemical water analysis by means of patterns. *Journal of Petroleum Technology*, 3(10)
- Subbarao, C., Subbarao, N.V., & Chandu, S.N. (1996). Characterization of groundwater contamination using factor analysis. *Environmental Geology*, 28(4), 175-180. doi:10.1007/s002540050091
- Suk, H., & Lee, K. (1999). Characterization of a ground water hydrochemical system through multivariate analysis: Clustering into ground water zones. *Ground Water*, 37(3), 358-366. doi:10.1111/j.1745-6584.1999.tb01112.x
- Templ, M., Filzmoser, P., & Reimann, C. (2008). Cluster analysis applied to regional geochemical data: Problems and possibilities. *Applied Geochemistry*, 23(8), 2198-2213. <http://dx.doi.org/10.1016/j.apgeochem.2008.03.004>
- Todd, D.K., & Mays, L.W. (2005). *Groundwater hydrology edition (3<sup>rd</sup> ed.)*. New Jersey: John Wiley & Sons.

- Toth, J. (1985). Role of regional gravity flow in the chemical and thermal evolution of ground water. *First Canadian/American Conference on Hydrogeology: Practical Applications of Ground Water Geochemistry June 22-26, 1984, Banff, Alberta. 1985. p 3-39, 45 Fig, 8 Tab, 68 Ref.*
- Turner, B.R. (1985). Uranium mineralization in the karoo basin, south africa. *Economic Geology, 80(2), 256-269.*
- Tyson, P.D., & Preston-Whyte, R.A. (2000). *The weather and climate of southern africa* (2<sup>nd</sup> ed.). Cape Town, South Africa: Oxford University Press Southern Africa Incorporated.
- UMVOTO. (2010). *Reconciliation Strategy for Beaufort West*. Report prepared for the Western Cape Department of Water Affairs by UMVOTO Africa (Pty) Ltd.
- USGS (a).Index of SRTM Version2.1 documentation. Retrieved, 2013, from [http://dds.cr.usgs.gov/srtm/version2\\_1/Documentation/](http://dds.cr.usgs.gov/srtm/version2_1/Documentation/)
- USGS (b).Index of SRTM Version2.1 SRTM3. Retrieved, 2013, from [http://dds.cr.usgs.gov/srtm/version2\\_1/SRTM3/Africa/](http://dds.cr.usgs.gov/srtm/version2_1/SRTM3/Africa/)
- US Salinity Laboratory Staff (1954) Diagnosis and improvement of saline and alkali soils. USDA, Handbook 60, U.S. Government Printing Office, Washington D. C.
- Usunoff, E.J., & Guzmán-Guzmán, A. (1989). Multivariate analysis in hydrochemistry: An example of the use of factor and correspondence analyses. *Ground Water, 27(1), 27-34.* doi:10.1111/j.1745-6584.1989.tb00004.x
- Van Tonder, G., & Hodgson, F. (1986). Interpretation of hydrogeochemical facies by multivariate statistical methods. *Water SA, 12(1), 1-6.*
- van Wyk, Y., & Witthueser, K. (2011). A forced-gradient tracer test on the hansrivier dyke: Beaufort west, south africa. *Water SA, 37(4), 437-444.*
- Wallick, E., & Toth, J. (1976). Methods of regional groundwater flow analysis with suggestions for the use of environmental isotopes. *Panel Proceedings Series- International Atomic Energy Agency*
- Ward Jr, J.H. (1963). Hierarchical grouping to optimize an objective function. *Journal of the American Statistical Association, 58(301), 236-244.*
- Weaver, J.M.C., Cave, L., & Talma, A.S. (2007). *Groundwater sampling* (2<sup>nd</sup> ed.). Water Research Commission Report No TT 303/07
- World Health Organization (WHO). (1993). *Guidelines for drinking-water quality* (2nd ed.). Geneva: World Health Organization.
- Wilde F.D., Radtke, D.B., Gibs, J., & Iwatsubo, R.T. (1998). Processing of water

samples (ver. 2.2): U.S. Geological Survey Techniques of Water-Resources Investigations, book 9, chap. A5, (July 2013), accessed from <http://pubs.water.usgs.gov/twri9A5/> (July 01, 2013).

Woodford, A.C., & Chevalier, L. (2002). *Hydrogeology of the main karoo basin-current knowledge and future research needs*. (Technical Report No. WRC 179/02). Pretoria, South Africa: Water Research Commission.

Zaporozec, A. (1972). Graphical interpretation of water-quality data. *Ground Water*, 10(2), 32-43. doi:10.1111/j.1745-6584.1972.tb02912.x

Zhang, X.C., & Norton, L.D. (2002). Effect of exchangeable mg on saturated hydraulic conductivity, disaggregation and clay dispersion of disturbed soils. *Journal of Hydrology*, 260(1-4), 194-205. [http://dx.doi.org/10.1016/S0022-1694\(01\)00612-6](http://dx.doi.org/10.1016/S0022-1694(01)00612-6)



# Appendices

## Appendix A: Laboratory chemical analysis results



Director: Dr. W.A.G. Kotzé

AECI Building W21  
De Beers Road  
Somerset West

P O Box 12457  
Die Boord,  
Stellenbosch, 7613

Tel. (021) 851-6401

Fax (021) 851-4379

Sel. 082-804-7489

E-mail akotze@bemlab.co.za

Val Reg. Nr. 4160185577

Report No.: WT1904/2008

### ANALYSES REPORT

Gaathier Mahed  
Universiteit van Weskaapland

Date received: 19/05/2008

Date tested: 21/05/2008

Origin	Lab. No.	pH	EC mS/m	Na	K	Ca	Mg	Fe	Cl	CO <sub>3</sub>	HCO <sub>3</sub>	SO <sub>4</sub>	B	Mn	Cu	Zn	P	NH <sub>4</sub> -N	NO <sub>3</sub> -N
Blydskap 1	1904	7.7	127	152.9	6.7	73.4	24.9	0.08	150.7	108.4	251.1	94	0.55	0.00	0.01	0.03	0.04	1.75	8.16
Blydskap 2	1905	7.6	99	87.9	8.7	80.0	23.6	0.09	88.1		382.8	48	0.34	0.00	0.00	0.02	0.00	1.72	10.95
Brandweg 8	1906	7.7	133	105.6	1.8	114.3	42.1	0.07	130.4	120.5	265.1	174	0.13	0.00	0.00	0.08	0.00	1.74	3.16
Brandweg 9	1907	7.9	241	249.8	2.0	232.7	37.0	0.13	263.5	114.5	125.6	654	0.42	0.22	0.00	0.06	0.00	1.75	0.64
Hansrivier 10	1908	7.7	189	166.2	6.6	158.0	47.7	0.14	264.4	93.4	260.3	232	0.23	0.00	0.00	0.24	0.00	1.73	12.60
Lemoenfontein Noord	1909	7.7	138	126.9	2.5	132.0	31.0	0.09	115.4	135.5	367.5	162	0.22	0.00	0.00	0.11	0.08	1.54	3.88
Lemoenfontein Wes	1910	7.7	155	131.8	2.8	157.8	31.8	0.09	173.6		427.2	197	0.21	0.00	0.00	0.02	0.00	1.43	2.54
Meyerspoort 1	1911	7.4	56	60.6	3.7	45.9	10.5	0.09	35.2		246.5	36	0.10	0.00	0.01	0.01	0.00	1.46	1.81
Mr Basson	1912	7.7	124	135.2	4.3	87.0	32.7	0.10	77.5		627.8	42	0.30	2.59	0.00	0.01	0.05	1.58	0.41
Nigrini Farm 1	1913	2.5	669	132.1	3.6	169.4	51.9	0.08	243.2		0.0	142	0.28	0.02	0.00	0.01	0.00	1.56	280.40
Nigrini Farm 2	1914	7.7	415	285.0	3.1	388.6	135.1	0.16	868.0	90.4	185.3	548	0.30	0.00	0.00	0.03	0.00	1.40	50.60
Schrfont 1	1915	7.6	83	74.5	2.7	96.4	16.5	0.08	52.9		381.2	65	0.12	0.00	0.01	0.01	0.00	1.40	3.66
Schrfont 2	1916	7.6	87	68.5	3.0	94.4	18.9	0.15	65.2	96.4	300.1	52	0.11	0.00	0.01	0.11	0.00	1.27	3.83
Spring	1917	2.3	977	61.3	4.4	70.0	18.4	0.13	33.5		0.0	50	0.18	0.02	0.00	0.01	0.08	1.34	328.40
Steenrotsfontein 1	1918	7.8	262	330.4	3.6	183.7	60.7	0.12	349.8		600.2	357	0.60	0.00	0.00	0.02	0.07	1.47	69.60
Steenrotsfontein 2	1919	7.7	405	390.8	9.8	392.5	78.3	0.13	621.2		583.3	607	0.67	0.05	0.00	0.14	0.03	1.28	3.85
Tweeling	1920	7.8	137	131.4	2.7	141.1	29.1	0.15	107.5		336.8	263	0.23	0.01	0.00	0.03	0.00	1.34	1.11
Windpomp 1	1921	7.8	119	131.4	2.2	126.1	4.8	0.08	111.0		396.6	84	0.26	0.04	0.00	0.05	0.00	1.19	10.44
Methods*		W05	W04	W01	W01	W01	W01	W01	W07	W06	W06	W01	W01	W01	W01	W01		W02	W03

Values in bold is smaller than the lowest quantifiable concentration.

\*Refer to BemLab work instructions - Accredited methods identified by reference number

### Sample conditions

Samples in good condition.

### Statement

The reported results may be applied only to samples received. Any recommendations included with this report are based on the assumption that the samples were representative of the bulk from which they were taken. Opinions and recommendations are not accredited.

Dr. W.A.G. Kotzé (Director)

23-05-2008

for BemLab

Date

Enquiries: Dr. W.A.G. Kotzé  
Arrie van Deventer

Figure A.1 Groundwater sample analysis result: Report WT1904/2008.

Report No.: NR7969/2009

**ANALYSES REPORT**

 Gasthier Mahed  
 Universiteit van Weskaapland  
 Private Bag X12  
 Pretoria  
 0001

Date received: 05/06/2009

Date tested: 12/06/2009

Reference No.	Lab. No.	pH	EC mS/m	Cl mg/l	HCO <sub>3</sub> mg/l	CO <sub>3</sub> mg/l	NO <sub>3</sub> -N mg/l	Na mg/l	K mg/l	Ca mg/l	Mg mg/l	SO <sub>4</sub> mg/l	Fe mg/l	Zn mg/l	Cu mg/l	Mn mg/l	B mg/l
Aardroings	7969	7.0	73	57.27	287.85	15.06	4.98	63.39	0.00	82.65	14.22	50.70	0.048	0.023	0.000	0.000	0.03
Hansrivier 10	7970	6.9	148	202.66	382.77	16.57	7.80	126.11	5.46	143.60	44.31	171.05	0.016	0.000	0.001	0.000	0.13
Hansrivier 12	7971	7.0	110	91.64	575.69	30.12	2.23	96.21	6.47	115.79	30.52	14.89	0.000	0.000	0.000	0.469	0.14
Hansrivier 13	7972	6.9	160	222.04	338.37	22.59	9.93	136.09	7.12	167.67	41.11	184.01	0.017	0.000	0.000	0.000	0.17
Hoenderbok F.	7973	7.0	184	146.27	437.89	30.12	8.28	173.80	1.23	128.62	37.87	232.05	0.000	0.000	0.008	0.000	0.27
Olivegrove 3	7974	7.4	62	39.65	310.81	34.64	5.22	48.79	1.81	93.27	17.12	36.43	0.001	0.003	0.000	0.081	0.07
Saucy's Kuil	7975	7.9	73	52.87	307.75	37.65	8.04	75.42	4.28	81.02	14.47	40.26	0.014	0.111	0.000	0.000	0.14
Steenrotsf. 7	7976	6.6	160	222.92	370.53	24.10	9.38	113.20	3.59	190.49	48.58	186.12	0.003	0.000	0.000	0.000	0.10
Tubleeg. 357	7977	7.4	125	151.55	375.12	30.12	9.46	125.28	2.18	128.47	24.68	93.77	0.057	0.062	0.001	0.000	0.17
Katdoomkuil	7978	7.1	169	236.14	367.46	37.65	21.58	183.38	9.98	126.92	32.84	156.05	0.042	0.027	0.000	0.000	0.34

**Sample conditions**

Samples in good condition.

**Statement**

The reported results may be applied only to samples received. Any recommendations included with this report are based on the assumption that the samples were representative of the bulk from which they were taken. Opinions and recommendations are not accredited.

 Dr. W.A.G. Kotzé (Director)  
 .....  
 for BemLab

 17-06-2009  
 .....  
 Date

 Enquiries: Dr. W.A.G. Kotzé  
 Arie van Deventer

**Figure A.2 Water sample analysis result: Report NR7969/2009**

## Appendix B: Hydrogeochemical data collected from the study area

1	A		B		C		D		E		F		G		H		I		J		K		L		M		N		O		P		Q		R		S		T	
	BOREHOLE	SampleID	SAMPLER	LAB	pH	TEMPERATURE (°C)	EC(mS/cm)	CALCIUM	MAGNESIUM	SODIUM	POTASSIUM	CARBONATE	BICARBONATE	CHLORIDE	SULPHATE	NITRATE	NITRITE	LATITUDE	LONGITUDE	SITEID																				
2	Aardoring	Aa	Hanok	Bemlab: 7969	7	19.3	73	82.65	14.22	63.39	0.01	15.06	287.2	50.7	4.98		-32.64715	22.56148	KaHersfontein-wind pump																					
4	Blydskap 2	BLK2	Hanok	Bemlab: 1905	7.6	20.2	99	80	23.6	87.9	8.7	0	382.8	88.1	48	10.95	-32.60788	23.09525	Blydskap-near dolerite																					
5	Hanurivier 12	HR12	Hanok	Bemlab: 7971	7	22.7	110	115.79	30.52	96.21	6.47	30.12	575.69	91.64	14.89	2.23	-32.39853	22.60189	Hanurivier - west of Pap Dam-near dry water course																					
6	Ladeda	LD	GEOSS	Bemlab: 8302	7.7		90.1	84	23.89	63.52	5.16	9.04	358.28	60.04	58.92	0.37	-32.3933	22.42873	Ladeda-wind pump-north east of rural cluster																					
7	LB11	LB11	GEOSS	Bemlab: 8619	8.2		87.5	87.08	9.81	48.14	9.72	15.06	306.22	43.26	22.03	8.01	-32.43306	22.97283	Lombards Kraal-on hiking trail																					
8	LR03	LR03	GEOSS	Bemlab: 3351	7.4		81.8	78	10.8	47.41	4.14	0	342.28	44.15	48.5	3.463	0.01	-32.4321	22.56151	Lombards Kraal																				
9	Meyerspoort 1	MS1	Hanok	Bemlab: 1911	7.4	19.3	56	45.9	10.3	60.6	3.7	0	246.5	35.2	36	1.81	-32.68124	22.45094	Meyerspoort																					
10	Mr Basson	MrB	Hanok	Bemlab: 1912	7.7	22.5	124	87	32.7	135.2	4.3	0	627.8	77.5	42	0.41	-32.35472	22.586	In Town-Formal Suburb-close to Commercial buildings																					
11	Olivegrove 3	OG3	Hanok	Bemlab: 7974	7.4	21.2	62	93.27	17.12	48.79	1.81	34.64	310.81	39.65	36.43	5.22	-32.50932	22.58652	Lombardskraal-near Olive farm																					
12	Saucy's Kruil	SK	Hanok	Bemlab: 7975	7.8	11.6	73	81.02	14.47	75.42	4.28	37.65	307.75	52.87	40.26	8.04	-32.53846	22.79733	Saucy's Kruil-Teekloof outcrop surrounded by calcrete																					
13	Scharfont 1	SF1	Hanok	Bemlab: 1915	7.6	15	83	96.4	16.5	74.5	2.7	0	381.2	22.9	65	3.66	-32.68577	22.55612	Skaarfontein-near dry water course																					
14	Scharfont 2	SF2	Hanok	Bemlab: 1916	7.6	22.2	87	94.4	18.9	68.5	3	96.4	300.1	65.2	52	3.83	-32.68559	22.57533	Skaarfontein-windpump																					
15	Blydskap 1	BLK1	Hanok	Bemlab: 1904	7.7	19.8	127	73.4	24.9	152.9	6.7	108.4	251.1	150.7	94	8.16	-32.61653	23.13905	Blydskap																					
16	Brandvrag 8	BW8	Hanok	Bemlab: 1906	7.7	17	133	114.3	42.1	105.6	1.8	120.3	265.1	130.4	174	3.16	-32.21398	22.79169	Brandvrag																					
17	Brickfields	BF	GEOSS	Bemlab: 12356	7.1		137.9	138	31.54	119.28	2.43	0	379.71	143.62	175.01	0.1	-32.32475	22.61092	Brickfields-on dry water course																					
18	DLG 1	DLG1	GEOSS	Bemlab: 14767	7.5		226	178.49	61.4	282.36	7.65	0	583.35	309.92	336.73	0.1	-32.38007	22.59244	South East of Formal suburb and East of Sewerage works																					
19	DVR4	DVR4	GEOSS	Bemlab: 1119	7		143.2	133.04	30.47	89.96	3.82	0	344.5	174.46	134.37	8.14	0.01	-32.37755	22.53995	South West of BW Drowerivier																				
20	DVR6	DVR6	GEOSS	Bemlab: 1120	6.9		207	210.52	42.45	133.61	4.08	0	359.81	263.46	278.07	11.25	0.01	-32.37558	22.54483	South West of BW Drowerivier near windpump																				
21	Hanurivier 10	HR10	Hanok	Bemlab: 7970	6.9	22	148	143.6	44.31	126.11	5.46	16.57	382.77	202.66	171.05	7.8	-32.39104	22.64032	Hanurivier - east of Pap Dam-near dry water course and farm																					
22	Hanurivier 13	HR13	Hanok	Bemlab: 7972	6.9	22.3	160	187.87	41.11	136.09	7.12	22.59	338.37	222.04	184.01	8.93	-32.38757	22.64117	Hanurivier - north west of Pap Dam-on dry water course																					
23	Hoenderbok F.	HDF	Hanok	Bemlab: 7973	7	20	184	138.62	37.87	173.8	1.23	30.12	437.89	146.27	232.05	8.28	-32.36228	22.59773	East of Formal suburb near Caravan Park																					
24	HR15	HR15	GEOSS	Bemlab: 14156	7.4		151.9	140.09	33.67	142.33	5.87	0	289.38	224.69	186.96	0.1	-32.385865	22.641121	Hanurivier - north east of Pap Dam-near dry water course																					
25	HR16	HR16	GEOSS	Bemlab: 14157	7.1		149.8	138.31	32.97	132.23	5.62	0	297.03	221.16	172.49	0.1	-32.384835	22.641169	Hanurivier - north east of Pap Dam-near dry water course																					
26	HR18	HR18	GEOSS	Bemlab: 14766	7.5		139.8	138.01	36.85	138.8	15.89	0	352.15	215.88	181.28	0.1	-32.39144	22.59244	Hanurivier - north west of Pap Dam-on dry water course																					
27	Katdoornkruil	KDK	Hanok	Bemlab: 7978	7.1	21.4	169	126.92	32.84	183.38	9.98	37.65	367.46	236.14	156.05	21.58	-32.70107	22.75134	Katdoornkruil-on dry water course																					
28	KH2	KH2	GEOSS	Bemlab: 6261	7.5		209	137.47	43.79	195.67	2.67	0	650.72	300.2	254.8	18.98	0	-32.38868	22.58243	(Kleinhanurivier)-on farm-south of sewerage works and formal township																				
29	KH5	KH5	GEOSS	Bemlab: 17802	7.2		251	178.99	55.21	359.83	2.85	0	950.81	300.2	226.52	0.1	-32.38758	22.585633	(Kleinhanurivier)-south of sewerage works and formal township																					
30	LB18	LB18	GEOSS	Bemlab: 8620	8.3		130.1	108.24	24.13	99.2	9.19	18.07	349.09	135.97	84.55	11.4	-32.5042	22.56768	Lombards Kraal																					
31	LB3	LB3	GEOSS	Bemlab: 8618	8.1		144.6	120.56	25.29	115.94	18.25	12.05	353.68	158.93	91.71	15.4	-32.5054	22.58356	Lombards Kraal																					
32	Lemoenfontein Noord	LFN	Hanok	Bemlab: 1909	7.7	19.4	138	132	31	126.9	2.5	135.5	367.5	115.4	162	3.88	-32.29179	22.64304	Lemoenfontein-on dry water course																					
33	Lemoenfontein Wes	LFW	Hanok	Bemlab: 1910	7.7	18.6	155	157.8	31.8	131.8	2.8	0	427.2	173.6	197	2.54	-32.2984	22.62961	Lemoenfontein-near farm																					
34	QA2	QA2	GEOSS	Bemlab: 6262	7.1		83.1	94.14	13.79	63.14	2.35	0	283.25	101.54	101.76	2.69	0	-32.42632	22.57215	Quagga's Fontein-near farm																				
35	Skierbaan	SB	GEOSS	Bemlab: 12357	7.3		104	85.18	22.07	99.11	0.5	0	321.53	145.39	102.98	0.1	-32.3313	22.5839	north of rural cluster and BW Dam																					
36	SR10	SR10	GEOSS	Bemlab: 1122	7.1		181.8	99.01	37.77	148.01	2.34	0	442.49	189.44	231.01	5.75	0.02	-32.39689	22.56607	Steenrotsfontein																				
37	SR4	SR4	GEOSS	Bemlab: 8301	8.2		179	81.74	40.78	190.36	30.57	18.07	376.65	224.27	215.02	0.35	-32.40495	22.56725	Steenrotsfontein-near farm-on dry water course																					
38	SR5	SR5	GEOSS	Bemlab: 2450	7.9		285	137.45	66.71	274.04	7.32	12.02	673.87	384.08	422.51	1.883	0.01	-32.41258	22.56059	Steenrotsfontein-near farm-on dry water course																				
39	SR7	SR7	GEOSS	Bemlab: 2300	7.9		240	120.96	55.4	227.07	2.79	15.03	589.83	391.15	301.65	2.971	0.01	-32.40715	22.56737	Steenrotsfontein-near farm-near dry water course																				
40	SR8	SR8	GEOSS	Bemlab: 8617	8.3		281	159.21	53.36	350.65	5.18	18.07	600.19	378.79	333.97	3.96	-32.41183	22.56431	Steenrotsfontein-near farm																					
41	SR9	SR9	GEOSS	Bemlab: 4642	8		284	148.35	59.34	345.29	2.77	18.07	625.65	370.1	368.38	2.43	0.01	-32.41726	22.56381	Steenrotsfontein-near farm																				
42	Steenbakkie A	SBA	GEOSS	Bemlab: 17803	7.6		105	71.27	2.6	212.19	1.52	0	312.34	57.39	215.54	0.1	-32.3434	22.6822	Steenbakkie-near dolerite																					
43	Steenrotsf 7	SRF7	Hanok	Bemlab: 7976	6.6	22.2	160	190.49	48.38	113.2	3.59	24.1	370.53	222.92	186.12	9.38	-32.39173	22.53447	Steenrotsfontein																					
44	Steenrotsfontein 1	SRF1	Hanok	Bemlab: 1918	7.8	20	262	183.7	60.7	330.4	3.6	0	600.2	348.8	357	69.6	-32.41827	22.5643	Steenrotsfontein-near farm																					
45	Steenrotsfontein 2	SRF2	Hanok	Bemlab: 1919	7.7	22.8	405	392.5	78.3	390.8	9.8	0	583.3	621.2	607	3.85	-32.41899	22.56389	Steenrotsfontein-near farm-wind pump																					
46	Tulplee 357	TL	Hanok	Bemlab: 7977	7.4	17.1	125	128.47	24.68	125.28	2.18	30.12	575.12	151.55	93.77	9.46	-32.65033	22.65663	Tulp Leeze																					
47	Tweeling	T	Hanok	Bemlab: 1920	7.8	17.7	137	141.1	29.1	131.4	2.7	0	336.8	107.5	263	1.11	-32.22036	22.71901	Tweeling																					
48	Brandvrag 9	BW9	Hanok	Bemlab: 1907	7.9	16	241	232.7	37	249.8	2	114.5	125.6	263.5	654	0.64	-32.21239	22.83581	Brandvrag																					
49	Nigami Farm 2	NF2	Hanok	Bemlab: 1914	7.7	17.7	415	388.6	135.1	286	3.1	90.4	183.3	868	548	50.6	-32.23645	22.80223	Rhanosterkop																					
50	RK1	RK1	GEOSS	Bemlab: 8300	7.8		477	356.55	205.48	264.97	5.29	12.05	248.04	1088.68	954.48	0.9	-32.23644	22.80225	Rhanosterkop																					
51	Steenbakkie B	SBB	GEOSS	Bemlab: 14159	7.3		271	172.31	71.37	307.81	6.67	0	260.29	570.09	390.82	0.1	-32.35	22.6914	Steenbakkie-near calcrete																					

Appendix B continued

	U	V
1		
2	BCOMMENT	Geology
3	Area situated further South of N12 and windpump used for irrigation and livestock.	Teekloof
4	Borehole water utilised for irrigation purposes and growing lucerne.	Teekloof
5	This is also a municipal borehole, with a pungent rotten egg smell (H2S). Could be due to the fact that the borehole has been standing still for a long time	Teekloof
6	old wind pump	Teekloof
7	Near spring, not in use	Teekloof
8	Private borehole	Teekloof
9	Water used for livestock.	Abrahamskraal
10	The water from this borehole has a very pungent smell almost like hydrocarbons. The water from this borehole has a very pungent smell almost like hydrocarbons.	Teekloof
11	This borehole is situated at the olive grove guesthouse and used for drinking water and has extremely low ec values. About 40 meters away there is quite a large dam that could be linked to this borehole.	Teekloof
12	Situated close to the R306 and uranium exploration territory.	Teekloof
13	Irrigation water.	Abrahamskraal
14	Irrigation water.	Abrahamskraal
15	The water from this borehole is mainly utilised for drinking purposes.	Calcrete
16	No DWAF monitoring point nearby.	Calcrete
17		Calcrete
18		Teekloof
19	Newly drilled	Teekloof
20	Newly drilled	Teekloof
21	Borehole situated along dolerite dyke on han rivier farm, and is owned by the municipality.	Teekloof
22	Also municipal borehole earmarked for future water supply. Has been pump tested by GEOSS.	Teekloof
23	A pumping test was attempted by the study team, however, the pumping rate was too low (2l/s) for this borehole. Honderhoek was pump tested by the municipality and gave a yield of 20l/s, which is very strong. This could be due to the borehole intersecting a paleochannel(syncline) as it is close to the spring, however it is very uncharacteristic of the fractured teekloof formation to be this high yielding.	Teekloof
24		Teekloof
25		Teekloof
26		Calcrete
27	Windpump water used for drinking purposes on farm.	Calcrete
28		Calcrete
29	Newly drilled. Fractures 35m and 54m. Blow yield 20 l/s. High yielding. No dolerite intersected	Calcrete
30	low yielding borehole, solar pump	Teekloof
31	irrigation of olive trees	Teekloof
32	Used for town supply, this sampling point was about 20m away from DWAF's monitoring borehole : G29879B	Calcrete
33	Used for town supply, however there was no DWAF monitoring borehole visible.	Calcrete
34		Teekloof
35		Calcrete
36		Teekloof
37	Private borehole - irrigation	Calcrete
38	Private borehole, high yielding	Calcrete
39	private borehole, not in use	Calcrete
40	drinking and irrigation borehole, private	Teekloof
41	2 l/s borehole, not currently in use	Teekloof
42	Sand flowing into hole. Borehole cleaned out by Jan du Plessis. pH 7.3	Teekloof
43	This borehole is located next to the N12 and is on Natie Nel's private farm. The Droerivier bed is approximately 2m below the surface. It is also located close to a DWAF borehole SRFOO02H.	Teekloof
44	This particular borehole is used for drinking purposes although it has a rather high TDS and high calcrete content.	Teekloof
45	The water from this borehole is not used for drinking purposes as it has a high TDS content.	Teekloof
46	Windpump situated on farm and water used for livestock.	Teekloof
47	Two DWAF monitoring boreholes a few km away namely: G29867A (elevation: 984m) and G29855F(981).	Calcrete
48		Calcrete
49	Water has a high TDS and Fe content, therefore not used for consumption.	Calcrete
50	Private borehole, high yielding	Calcrete
51		Teekloof

## Appendix C: Calculated hydrogeochemical data of the study area

BORENUM	SampleID	Ion Balance	SAR	TDS (mg/l)	TA (mg/l)	TH (mg/l)	lnEC	lnSAR	CATIONS (Natural logs)				ANIONS (Natural logs)				lnTDS	lnTA
									CALCIUM	MAGNESIUM	SODIUM	POTASSIUM	BICARBONATE	CHLORIDE	SULPHATE	NITRATE		
Aardoring	Aa	3.762021154	1.7113	567.45	236.037	264.927	4.2904594	0.5372583	4.4146148	2.654649424	4.1493061	-4.61	5.662439511	4.047776926	3.925925911	1.60542989	6.3411562	5.4639886
Blydskap 2	BLK2	0.237883656	2.2407	732.7	313.896	296.76	4.5951199	0.8067732	4.3820266	3.161246712	4.4761998	2.163323026	5.94751266	4.478472533	3.871201011	2.39333946	6.5967363	5.7490617
Hansrivier 12	HR12	1.093120412	2.0752	807.99	472.0658	414.607	4.7004804	0.7300503	4.7517782	3.418382206	4.5665333	1.867176109	6.355569321	4.517867858	2.700689847	0.80200159	6.6945484	6.1571184
Ladeda	LD	1.01096026	1.5993	566	293.7896	304.259	4.5009202	0.4695492	4.4308168	3.135059339	4.1513548	1.640936579	5.881314804	4.095011007	4.076180592	-0.9942523	6.3385941	5.6828639
LB1	LB11	-2.232917579	1.4672	424	251.1004	207.921	4.2121276	-0.184441	4.2058859	2.283402274	3.8741134	2.274185618	5.724303798	3.767228421	3.093312602	1.79342475	6.0497335	5.5258529
LK03	LK03	-7.251878745	1.3613	624.66	280.6696	234.28	4.4042772	0.308443	4.3307333	2.379546134	3.8588332	1.420695788	5.835629116	3.787592927	3.881563798	1.24213527	6.4372088	5.6371782
Meyerspoort 1	MS1	0.628643699	2.1191	442.3	202.13	157.8	4.0235517	0.7508984	3.8264651	2.351375257	4.1042949	1.30833282	5.507361993	3.561046083	3.583518938	0.59332685	6.0919884	5.3089111
Mr Basson	MrB	-1.267376316	3.1653	1011.9	514.796	351.57	4.8202816	1.1522503	4.4659081	3.487375078	4.9067552	1.458615023	6.442221644	4.350277936	3.737669618	-0.8915981	6.919585	6.2437707
Olivegrove 3	OG3	7.702387757	1.2308	495.94	254.8642	303.367	4.1271344	0.2076643	4.5354985	2.840247371	3.8875254	0.59326845	5.739181793	3.680090948	3.595392611	1.6524974	6.206457	5.5407309
Saucy's Kuil	SK	6.959890156	2.0478	567.45	252.355	261.877	4.2904594	0.716775	4.394696	2.672077541	4.3230725	1.45395301	5.729287765	3.96783607	3.69535842	2.08442908	6.3411562	5.5308368
Schfont 1	SF1	1.750203983	1.8634	694.9	312.584	308.65	4.4188406	0.6223799	4.5685062	2.803360381	4.3107991	0.993251773	5.943324172	3.968403339	4.17438727	1.29746315	6.543768	5.7448732
Schfont 2	SF2	8.248997472	1.6997	704.2	246.082	313.49	4.4659081	0.5304645	4.5475411	2.939161922	4.2268337	1.098612289	5.704115752	4.177459469	3.951243719	1.3428468	6.5570624	5.5056648
Blydskap 1	BLK1	9.051953622	3.9723	873.1	205.902	285.59	4.8441871	1.37935	4.2959239	3.214867803	5.0297841	1.902107526	5.525851266	5.015291106	4.543294782	2.09924417	6.7720501	5.3274003
Brandwag 8	BW8	8.27831286	2.1653	959.4	217.382	458.36	4.8903491	0.7725594	4.7388266	3.740047741	4.6596584	0.587786665	5.580107113	4.870606649	5.159055299	1.15057203	6.8663081	5.3816562
Brckfields	BF	2.834618829	2.4058	1030	311.3622	474.314	4.9265288	0.8778987	4.9272537	3.451256582	4.7814737	0.887891257	5.939407803	4.967170923	5.16483115	-2.3025851	6.9373141	5.7409569
DLG 1	DLG1	2.165663537	4.6923	1699	478.347	697.965	5.420535	1.5459234	5.1845326	4.117409835	5.6431829	2.032087845	6.368787349	5.7363142	5.819281432	-2.3025851	6.1703364	6.1703364
DVR4	DVR4	-1.262660841	1.8479	1071	282.49	457.527	4.9642423	0.6140268	4.8906498	3.416742593	4.4995874	1.340250423	5.84209409	5.161695489	4.900597189	2.09679018	6.9763481	5.6436432
DVR6	DVR6	1.575351936	2.2181	1561	295.0442	700.345	5.3327128	0.796645	5.3495807	3.748326913	4.8949251	1.406096988	5.885576114	5.573901554	5.627872881	2.42036813	7.3530819	5.6871252
Hansrivier 10	HR10	2.37232912	2.3815	1055	313.8714	540.671	4.9972123	0.8677239	4.9670713	3.791210385	4.8371545	1.69744879	5.947434287	5.311529698	5.141955911	2.05412373	6.9613216	5.7489833
Hansrivier 13	HR13	6.103287974	2.4657	1133	277.4634	587.726	5.0751738	0.9024598	5.1219978	3.716251401	4.9133164	1.962907725	5.824139971	5.402857546	5.214990104	2.29556048	7.0326587	5.625689
Hoenderbok F.	HDF	2.575516985	3.4952	1289.1	359.0698	476.817	5.2149358	1.2513766	4.8568623	3.634159242	5.1579052	0.207014169	6.081967737	4.985454229	5.446952866	-2.3025851	7.1616709	8.8851358
HR15	HR15	3.628035538	2.8292	1130	237.2916	488.272	5.0232224	0.0532401	4.9422851	3.516607233	4.9581283	1.769854634	5.667740703	5.414721674	5.23089469	-2.3025851	7.0299729	5.4692898
HR16	HR16	2.683835813	2.6484	1119	243.5646	480.952	5.0093011	0.0507185	4.9294973	3.495598057	4.8845428	1.726331664	5.698833144	5.398886421	5.150339264	-2.3025851	7.021907	5.4953822
HR18	HR18	2.269978922	2.7368	1068	288.763	496.11	4.9402128	0.0637531	4.9273261	3.606855619	4.933034	2.765689981	5.864057221	5.374722698	5.199932465	2.11384297	6.973543	5.665603
Katdoomkuil	KDK	2.958953556	3.7886	1191.5	301.3172	451.944	5.1298987	1.3319875	4.843557	3.491647285	5.2115605	2.30058309	5.906614469	5.464424849	5.050176469	3.07176696	7.0830086	5.7081635
KH2	KH2	-13.01187633	3.756	1271	533.5904	523.214	5.3423343	1.3233657	4.9234057	3.779405481	5.2764296	0.982078472	6.478079442	5.704448919	5.540478924	2.94338579	7.1475593	6.2796285
KH5	KH5	0.740626844	6.0867	1898	785.63	673.836	5.5254529	-0.002882	5.1873299	4.011144096	5.8856317	1.047318994	6.857314253	5.704448919	5.422833241	-2.3025851	7.548556	6.6664859
LB18	LB18	1.871091028	2.2669	449	286.2538	369.533	4.8683034	0.8184076	4.684351	3.18345588	4.597138	2.218115936	5.855329769	4.912434273	4.437343075	2.43361336	6.1070229	5.6698788
LB3	LB3	4.505259472	2.5307	903	290.0176	405.089	4.9739713	0.9284805	4.7921476	3.230409061	4.7530728	2.90416508	5.86839255	5.068463854	5.18631425	2.73436751	6.8057226	6.659416
Lemoenfontein Noord	LFN	7.321241459	2.6072	1079	301.35	457.1	4.9272537	0.9582751	4.8828019	3.433987204	4.8433994	0.916290732	5.906723319	4.748404354	5.087596335	1.35583515	6.98379	5.7082724
Lemoenfontein Wes	LFW	0.78890178	2.5274	1126.7	330.304	524.88	5.0434251	0.9272079	5.0613284	3.45946629	4.8812856	1.029619417	6.057252288	5.156753802	5.283203729	0.93216408	7.0270483	5.8588013
QA2	QA2	-5.621515931	1.6242	505	232.265	291.889	4.4200447	0.4850074	4.544783	2.623943692	4.1453545	0.854415328	5.6463299	4.62045281	4.6226171	0.98954119	6.2245584	5.4447879
Skaerbaan	SB	-5.141026333	2.4989	782	263.6546	303.437	4.6443909	0.9158478	4.4447667	3.09421922	4.5962303	-0.693147181	5.773090852	4.979419787	4.634534795	-2.3025851	6.6618547	5.5746399
SR10	SR10	-9.207676828	3.239	1376	362.8418	402.382	5.2029072	1.1752572	4.5952209	3.631515137	4.9972798	0.850150929	6.092417865	5.244072352	5.442461	1.74919985	7.226936	5.8939669
SR4	SR4	-1.449035241	4.3334	1122	308.853	371.548	5.1873858	1.466361	4.4035435	3.708191765	5.248917	3.420019136	5.931316374	5.412850683	5.370731047	-1.0498221	7.0228681	5.7328654
SR5	SR5	-11.33010242	4.8407	2130	444.27	617.136	5.6524892	1.5770537	4.9232602	4.200354867	5.6132741	1.990610328	6.513037214	5.950850864	6.046213115	0.63286625	7.6668773	6.0964325
SR7	SR7	-13.63254889	4.3304	1803	466.358	529.54	5.4806389	1.4656648	4.7954599	4.014579594	5.4252583	1.026041596	6.37983436	5.969091118	5.709267405	1.0888986	7.4972072	6.1449536
SR8	SR8	-7.808500521	4.4017	1769	492.1558	625.001	5.6383547	1.4819909	5.0702241	4.013857311	5.5240575	1.644805056	6.397246272	5.936981962	5.811051169	1.08518927	7.4781697	6.1987959
SR9	SR9	4.289036371	6.1157	2130	341.36	614.169	5.6489742	1.8108594	4.9995743	4.083283615	5.8443846	1.01884732	6.053617412	5.913773239	5.909115014	0.88789126	7.6638773	5.8329376
Steenbokkie_A	SBA	7.46542246	6.7918	792	213.35	188.835	4.6339604	1.9157206	4.2664755	0.955511445	5.3574821	4.018710335	5.744092338	4.049870072	5.373146507	-2.3025851	6.6745614	5.362394
Steenrots 7	SRF7	6.114090113	1.9131	1133	303.8346	675.403	5.0751738	0.6487259	5.2495997	3.883211924	4.7291562	1.278152203	5.914934413	5.406812963	5.226391627	2.23857976	7.0326587	5.7164835
Steenrotsfontein 1	SRF1	0.674713334	5.4514	1957.6	492.164	708.12	5.5683445	1.6958783	5.213304	4.105943698	5.800304	1.280993845	6.397262933	5.857361563	5.877735782	4.24276457	7.5794745	6.198812
Steenrotsfontein 2	SRF2	4.211075939	4.7578	2689.2	478.306	1302.28	6.0038871	1.5597786	5.9725365	4.360547603	5.9681959	2.282382386	6.368701634	6.431653091	1.3480791	7.896999	6.1702507	5.7287589
Tulpheeg 357	TL	5.3682																

Appendix C continued

lnTH	FACTOR SCORES			CATIONS (meq/l)				ANIONS (meq/l)				TOTAL CATIONS (meq/l)	TOTAL ANIONS (meq/l)	SATURATION INDICES		WATER_TYPE (PIPER, 1944)	Group
	HARDNESS	ALKALINITY	LAND_USE	SODIUM	POTASSIUM	CALCIUM	MAGNESIUM	BICARBONATE	NITRATE	SULPHATE	CHLORIDE			CALCITE	DOLOMITE		
5.5794543	-1.25626861	-0.62040457	0.387326778	2.7573134	0.002255766	4.1244573	1.170129603	4.717550106	0.3555278	1.05556169	1.61537811	8.052156038	7.744017735	1.58125465	2.7448541	Ca-HCO3	1
5.6929237	-0.94760627	0.232133831	1.241143478	3.8234397	0.222516068	3.9922152	1.941987245	6.27367789	0.7817329	0.99934834	2.48498011	9.980158224	10.53973924	2.28926953	4.3950491	Ca-HCO3	1
6.0273311	-0.87510157	1.397103276	0.830734364	4.1849049	0.165480341	5.7782324	2.511417404	9.434936322	0.1592022	0.31000618	2.58483062	12.64003504	12.48897535	2.02870539	3.8250123	Ca-HCO3	1
5.7178793	-1.0760605	0.071683215	-0.3711478	2.7629681	0.131975048	4.1918259	1.891791812	5.871821615	0.0264147	1.22670009	1.69350972	8.97856085	8.81844614	2.38114446	4.5462367	Ca-HCO3	1
5.3371582	-1.82409854	-0.3286421	1.121896879	2.0939748	0.248604159	3.3474724	0.807241308	5.018614533	0.4290607	0.45907564	1.22020703	6.497292738	7.126957916	2.70937325	4.9305105	Ca-HCO3	1
5.456517	-1.46103591	-0.126311549	0.204396067	2.0622216	0.105886957	3.7926044	0.888706028	5.609598924	0.2472275	1.00975822	1.24531069	6.849418994	8.111895327	2.01920918	3.5377166	Ca-HCO3	1
5.0613284	-1.88432412	-0.332484943	-0.31371468	2.635955	0.094633271	2.2905335	0.864019749	4.039868338	0.1292179	0.74951126	0.99286379	5.885141515	5.911461335	1.65764352	3.0213517	Ca-HCO3	1
5.8624088	-0.70010529	1.743443372	-0.53444786	5.8808766	0.109979206	4.341534	2.690804361	10.28896285	0.0292704	0.8744298	2.18599272	13.02319416	13.37865574	2.54542737	5.0216681	Ca-HCO3	1
5.7149433	-1.40873474	-0.515768639	0.090928052	2.1222483	0.046293573	4.6544239	1.408763629	5.093839668	0.3726617	0.75846375	1.11838208	8.231729362	7.343347212	2.06625098	3.7429518	Ca-HCO3	1
5.5678749	-1.29852751	-0.404415509	0.586686608	3.2805896	0.109467675	4.0431159	1.190701502	5.043689578	0.5739847	0.83820342	1.49127013	8.623874685	7.947147833	2.49783007	4.5942245	Ca-HCO3	1
5.7322079	-1.04872445	0.107723144	-0.04299743	3.2405718	0.069056711	4.8106193	1.35774532	6.24745562	0.2612915	1.35328421	1.49211632	9.477993108	9.354147699	2.36843753	4.3169701	Ca-HCO3	1
5.7477675	-0.97030268	-0.305218655	0.144380728	2.9795861	0.076729679	4.7108139	1.55235548	4.918314354	0.273428	1.08262737	1.83905452	9.322365278	8.113424282	2.25544545	4.1590688	Ca-HCO3	1
5.6545572	-0.43306669	-0.869565732	0.630294423	6.6507842	0.171362949	3.6628574	2.048691119	4.115257362	0.5825516	1.95705717	4.25069811	12.53396574	10.90556428	2.16818507	4.2135615	Ca-Na-Cl-HCO3	2
6.1276549	-0.01944857	-0.992365094	-0.34030289	4.5933474	0.046037807	5.7038774	3.464307756	4.344702217	0.225596	3.62263774	3.67810905	13.80757039	11.87104498	2.28954219	4.5011051	Ca-Na-Cl-HCO3	2
6.1618695	0.015236763	0.121217962	-1.55787896	5.1883947	0.06215104	6.8865712	2.595350751	6.223036132	0.0071391	3.64366569	4.05099709	14.75246764	13.92483803	1.92979139	3.5743502	Ca-Na-Cl-HCO3	2
6.548169	0.892443148	1.367597252	-0.89478477	12.281985	0.19514915	8.9071311	5.052458342	9.560475436	0.0071391	7.01063681	8.74171438	26.43672314	25.31996575	6.26279802	5.1459354	Ca-Na-Cl-HCO3	2
6.1258359	-0.80541901	-0.305218655	0.599582588	3.9139148	0.097702458	6.6390538	2.507303024	5.645982322	0.5811238	2.79755076	4.2088117	13.15797408	13.94553807	3.259267	3.259267	Ca-Na-Cl-HCO3	2
6.5515731	0.700304106	-0.311535783	0.748888035	5.8117154	0.104352363	10.505514	3.493108414	5.89869666	0.8031502	5.78934986	7.431247	19.91469041	19.92064376	1.89012161	3.4406124	Ca-Na-Cl-HCO3	2
6.292811	0.161456793	-0.001572601	0.829528057	5.4854833	0.139648015	7.1660262	3.646163341	6.273186222	0.5568508	3.56121945	5.71630045	16.43732093	16.10755696	1.75084736	3.3468269	Ca-Na-Cl-HCO3	2
6.3762609	0.33173241	-0.363425376	1.089472222	5.9195895	0.182105104	8.367184	3.382843036	5.545518254	0.7089139	3.83104351	6.26293967	17.85172158	16.34841537	1.76460223	3.2744814	Ca-Na-Cl-HCO3	2
6.1671328	0.273393634	-0.556018201	-1.00893763	7.5598842	0.031459168	6.418484	3.116231228	7.176543394	0.5911186	4.83122464	4.12574394	17.1260586	16.72463055	1.86129806	3.5473678	Ca-Na-Cl-HCO3	2
6.1908726	-0.217745601	-0.488072426	-1.01018831	6.1910145	0.150134405	6.9908678	2.770623329	4.742625151	0.0071391	3.89262179	6.33768651	16.10264007	14.97991257	2.11754186	3.9717046	Ca-Na-Cl-HCO3	2
6.1757675	0.171850884	0.034414576	-0.29568978	5.7516887	0.143740265	6.902041	2.713022012	4.868000375	0.0071391	3.59119991	6.23811807	15.51049198	14.70445747	1.82411411	3.3812785	Ca-Na-Cl-HCO3	2
6.2067977	0.221708656	0.359927012	-0.42127736	6.037468	0.046411532	6.8870702	3.032297881	5.771357547	0.0071391	3.77378917	6.0891885	16.3632476	15.64147434	2.29589299	4.3740978	Ca-Na-Cl-HCO3	2
6.1135583	0.171883555	-0.005752062	1.400893612	7.9765913	0.255254065	6.3336494	2.703234625	6.022271884	1.5406206	3.2489231	6.66064931	17.2678194	17.47246492	1.87920039	3.5270587	Ca-Na-Cl-HCO3	2
6.2599906	0.372718621	1.421517701	0.494584821	8.5111769	0.068289414	8.6601228	3.603373791	10.66459668	1.3550037	5.30487411	8.46754859	19.04296289	25.79202324	2.56085705	4.980666	Ca-Na-Cl-HCO3	2
6.5129868	0.796037065	2.732382768	-1.57501585	15.651744	0.072893195	8.9320824	4.543098128	15.58274732	0.0071391	4.71609138	8.46754859	29.19981799	28.7735264	2.54448668	4.9339472	Ca-Na-Cl-HCO3	2
5.91224	-0.62999048	-0.170151963	1.359988321	4.3149627	0.235048583	5.4014671	1.98599671	5.721207457	0.8138589	1.76031046	3.83521846	11.93707809	12.13059528	2.97608799	5.6561304	Ca-Na-Cl-HCO3	2
6.0041068	-0.28339265	-0.074955508	1.832487407	5.0431127	0.466772213	6.0162683	2.081053281	5.796432591	1.0994234	1.90937993	4.48283643	13.60720642	13.28807238	2.83314662	3.3438237	Ca-Na-Cl-HCO3	2
6.1249022	-0.06570075	-0.076751968	-0.13115712	5.5198464	0.063941399	6.587155	2.550915449	6.022927441	0.2769976	3.37280065	3.25501368	14.72185833	12.92773937	2.49391778	4.7144082	Ca-Na-Cl-HCO3	2
6.2631697	0.154188068	0.290314	-0.17922764	5.7329847	0.071614367	7.8746444	2.616745526	7.001345858	0.1813335	4.10149215	4.8966237	16.29598905	16.18079518	2.63682485	4.9337547	Ca-Na-Cl-HCO3	2
5.6763736	-0.96219989	-0.788709442	-0.28804361	2.746439	0.060104915	4.6978392	1.134745937	4.642161082	0.1920421	2.11861848	2.86407356	8.639129025	9.816895274	1.73064714	2.9737724	Ca-Na-Cl-HCO3	2
5.715174	-0.54198912	-0.292216855	-2.70524783	4.3110479	0.01278828	4.2507111	1.816087225	5.269528871	0.0071391	2.14401859	4.10092235	10.39063453	11.52160892	1.94185714	3.643867	Ca-Na-Cl-HCO3	2
5.9974019	0.105970687	0.487715961	-0.17819513	6.4380809	0.059849149	4.9408653	3.108002469	7.251932417	0.410499	4.80957209	5.34341241	14.54679787	17.81541592	1.85204281	3.6413384	Ca-Na-Cl-HCO3	2
5.9176781	0.082300409	0.386594201	0.364853844	8.2802046	0.781875427	4.0790459	3.35568813	6.172886043	0.0249869	4.47666418	6.32583984	16.49681405	17.00037696	2.7896766	5.6331506	Ca-Na-Cl-HCO3	2
6.4250894	0.942155649	1.40185231	0.114559747	11.920084	0.187220416	6.8591247	5.489405472	11.04400031	0.1344295	8.79655558	10.8334979	24.45583505	30.80848326	2.87821961	5.7982703	Ca-Na-Cl-HCO3	2
6.2720087	0.660078088	1.236189308	-0.30203741	9.8770018	0.071358601	6.0362294	4.558732771	9.666675626	0.2121031	6.28027973	11.0329168	20.54332254	27.19197523	2.84378912	5.7042311	Ca-Na-Cl-HCO3	2
6.4377532	0.848723268	1.306291641	0.161648109	10.902675	0.132486579	7.9450072	4.555441267	9.836464819	0.2113178	6.95317428	10.6842862	23.53561049	27.68524309	3.37902316	6.6550569	Ca-Na-Cl-HCO3	2
6.4202701	1.064254035	0.378511226	-0.49320594	15.019289	0.07084707	4.7403064	4.882945896	6.975943035	0.1734805	7.66982133	10.439173	27.37614601	25.2581786	2.89563794	5.7491207	Ca-Na-Cl-HCO3	2
5.2408736	-0.96041231	-0.40395664	-3.027187	9.2297574	0.038876371	3.5565647	0.213947747	5.118914713	0.0071391	4.48749045	1.61876287	13.03914623	11.23307014	1.97692252	2.8716965	Ca-Na-Cl-HCO3	2
6.5153095	0.391286387	-0.222411777	0.759416043	4.9239292	0.091819849	9.5059634	3.997531372	6.072585863	0.669488	3.87497319	6.28776126	18.5192438	16.90496914	1.55970212	2.8817744	Ca-Na-Cl-HCO3	2
6.5626136	0.98270308	1.156102489	1.135362603	14.37161	0.092075165	9.1671241	4.994857025	9.9688228	4.9688228	7.43265329	9.86658393	28.62566638	32.10468871	2.94967421	5.7742128	Ca-Na-Cl-HCO3	2
7.1718719	1.894195299	1.033727122	0.838721118	16.998865	0.250650284	19.586806	6.4431187	9.55965599	0.2748559	12.6375926	17.5217894	43.27943986	39.99389383	3.16781841	5.9913438	Ca-Na-Cl-HCO3	2
6.0458651	-0.2606592	-0.03255568	0.205735026	5.4493803	0.0557569	6.4109986	2.030857848	6.147810998	0.6753601	1.95226862	4.27647351	13.94699361	13.05011324	2.19263826	4.0246048	Ca-Na-Cl-HCO3	2
6.1571061	0.040905519	-0.313352421	-0.6729106	5.7155857	0.069056711	7.0412695	2.394569019	5.519787652	0.0792442	5.47559612	3.03218345	15.22048093	14.10681138	2.58416773	4.8384863	Ca-Na-Cl-HCO3	2
6.5977594	1.353281932	-3.103444553	-1.26386127	10.865702	0.051153119	11.612356	3.04464102	2.058448127	0.0456903	13.6161212	7.43237526						